

Syracuse University

SURFACE

Biomedical and Chemical Engineering – Theses College of Engineering and Computer Science

8-2012

An Experimental Study on Thermal Stability of Biodiesel Fuel

Yiyang Zhu

Syracuse University

Follow this and additional works at: https://surface.syr.edu/bce_thesis



Part of the [Chemical Engineering Commons](#)

Recommended Citation

Zhu, Yiyang, "An Experimental Study on Thermal Stability of Biodiesel Fuel" (2012). *Biomedical and Chemical Engineering – Theses*. 1.

https://surface.syr.edu/bce_thesis/1

This Thesis is brought to you for free and open access by the College of Engineering and Computer Science at SURFACE. It has been accepted for inclusion in Biomedical and Chemical Engineering – Theses by an authorized administrator of SURFACE. For more information, please contact surface@syr.edu.

Abstract

Biodiesel fuel, as renewable energy, has been used in conventional diesel engines in pure form or as biodiesel/diesel blends for many years. However, thermal stability of biodiesel and biodiesel/diesel blends has been minimally explored. Aimed to shorten this gap, thermal stability of biodiesel is investigated at high temperatures.

In this study, batch thermal stressing experiments of biodiesel fuel were performed in stainless steel coils at specific temperature and residence time range from 250 to 425 °C and 3 to 63 minutes, respectively.

Evidence of different pathways of biodiesel fuel degradation is demonstrated chromatographically. It was found that biodiesel was stable at 275 °C for a residence time of 8 minutes or below, but the cis-trans isomerization reaction was observed at 28 minutes. Along with isomerization, polymerization also took place at 300 °C at 63 minutes. Small molecular weight products were detected at 350 °C at 33 minutes resulting from pyrolysis reactions and at 360 °C for 33 minutes or above, gaseous products were produced. The formed isomers and dimers were not stable, further decomposition of these compounds was observed at high temperatures.

These three main reactions and the temperature ranges in which they occurred are: isomerization, 275-400 °C; polymerization (Diels-Alder reaction), 300-425 °C; pyrolysis reaction, ≥ 350 °C.

The longer residence time and higher temperature resulted in greater decomposition. As the temperature increased to 425 °C, the colorless biodiesel became brownish. After 8 minutes,

almost 84% of the original fatty acid methyl esters (FAMES) disappeared, indicating significant fuel decomposition.

A kinetic study was also carried out subsequently to gain better insight into the biodiesel thermal decomposition. A three-lump model was proposed to describe the decomposition mechanism. Based on this mechanism, a reversible first-order reaction kinetic model for the global biodiesel decomposition was shown to adequately describe the experimental data points of the concentrations or the decomposition percentage as a function of time. The forward and reverse rate constants were determined at each temperature for the model. The Arrhenius pre-exponential factors A for k_1 and k_2 obtained were 1.50×10^9 and 257 min^{-1} , and the energies of activation E_a were 126.0 and 46.0 KJ/mol, respective. The high linearity of the Arrhenius plots ($R^2 > 98\%$) further validated the rationality of the assumed reversible first-order kinetics to represent the overall biodiesel decomposition.

Moreover, a Van't Hoff plot was established, the reaction enthalpy ΔH° for biodiesel thermal decomposition is 80.0 KJ/mol, indicating the overall decomposition is an endothermic reaction.

**AN EXPERIMENTAL STUDY ON THERMAL STABILITY OF
BIODIESEL FUEL**

By

Yiying Zhu

B.Eng., Hebei polytechnic University, Tangshan, China, 2009

THESIS

Submitted in partial fulfillment of the requirements for the degree of Master of Science in

Chemical Engineering in the Graduate School of Syracuse University

August 2012

Copyright © Yiying Zhu 2012

All Rights Reserved

Acknowledgements

I am immensely grateful to my esteemed advisor, Prof. Lawrence L. Tavlarides, for his consistent guidance, encouragement, support and patience throughout my precious graduate career at Syracuse University. I have learned a lot from him, not only a rigorous attitude toward work, but also the passion for the chemical engineering domain. Without his expert direction and instruction, this thesis would not have reached its present form.

I am thankful to all the members of the Department of Biomedical and Chemical Engineering for providing me this opportunity to receive the higher education.

I would like to express my heartfelt thanks to Dr. Ronghong Lin who has instructed and helped me through all the stages of this thesis. Then, I would like to extend my sincere thanks to Dr. George Anitescu for sharing his valuable experience with biodiesel degradation and GC-FID analysis, and thanks to Prof. Philip A. Rice for giving me some valuable advices. I am also grateful to all other colleagues in Tavlarides research lab, and especially thank Mr. Jiuxu Liu, for his constant assistance and sincere friendship.

Special thanks is given to Prof. Jesse Bond for allowing me access to the GC-MS in his laboratory for biodiesel analysis, without his help, this work would not have progressed as well.

I am greatly indebted to Professors Benjamin Akih-Kumgeh, Dacheng Ren, and Jesse Bond for serving on my examination committee and for their valuable comments and suggestions.

Finally, my deepest appreciation goes to my parents, the rest of my family and my dearest friend Mr. Shijing Lu. During my two years abroad, they have been there always giving me continuous support and endless love.

*Dedicated to my beloved parents, respectful teachers and all
my dear friends...*

Table Of Contents

Acknowledgements	v
List Of Figures.....	x
List Of Tables	xvi
Chapter I Introduction	1
Chapter II Literature review	6
2.1 Introduction	6
2.2 Biodiesel production technology	6
2.3 Supercritical fuel combustion	7
2.4 Thermal stability of biodiesel fuels	8
2.4.1 Definition of thermal stability	8
2.4.2 A comprehensive summary of the work on thermal stability of biodiesel	8
2.4.3 A breakthrough in the thermal stability study on biodiesel	9
2.4.4 Analogous research related to thermal stability of biodiesel.....	10
2.5 Mechanism of thermal decomposition of biodiesel fuel.....	12
2.6 Kinetic models of thermal decomposition of biodiesel fuel	15
Chapter III Experiments.....	19
3.1 Materials	19
3.2 Experimental setup	22
3.3 Experimental conditions and procedure	24

3.3.1 Selection of thermal stressing temperature range	24
3.3.2 Definition of thermal stressing time.....	27
3.3.3 Thermal stressing experimental conditions	28
3.3.4 Thermal stressing experimental procedure	31
3.4 Analytical methods.....	33
3.4.1 GC-FID analysis	33
3.4.2 GC-MSD analysis	36
3.4.3 Sample preparation for GC analysis	36
3.4.4 Definition of biodiesel fuel thermal decomposition percentage.....	39
Chapter IV Results and discussion.....	41
4.1 Calibration curves of FAMES	41
4.2 Compositions of fresh biodiesel.....	43
4.2.1 Identification of BD-100 biodiesel (Peter Cremer) compositions.....	43
4.2.2 Mass fraction of BD-100 biodiesel fuel compositions	46
4.3 Thermal stability of biodiesel fuel.....	46
4.3.1 Visual observation of thermal decomposition of biodiesel fuel	46
4.3.2 Gas-chromatographic observation of thermal behaviors of biodiesel.....	52
4.3.3 Effect of temperature on thermal stability of biodiesel.....	69
4.3.4 Effect of thermal stressing time on thermal stability of biodiesel.....	71
4.4 Quantitative analysis of the extent of thermal decomposition of biodiesel.....	71

4.5 Discussion on the impact of thermal decomposition on biodiesel fuel properties and synthesis.....	77
4.6 Kinetic model for thermal decomposition of biodiesel	78
4.6.1 Biodiesel decomposition mechanism.....	78
4.6.2 Proposed kinetic model	81
4.6.3 Simulation results	82
4.6.4 Determination of Arrhenius parameters.....	86
Chapter V Conclusions.....	91
Chapter VI Future work	93
Appendix A Supplementary information	94
Appendix B Permission to reuse copyright material.....	135
References	137
Vita	143

List Of Figures

- Fig. 1 GC chromatograms of the product of the reaction performed at different conditions. Chromatographic peaks. 1 = diglycerides; 2 = possible thermal decomposition products; 3 = glycerin; 4 = 1, 2, 4-butanetriol (internal standard no. 1); 5 = monoglycerides, 6 = glyceryl tridecanoate (internal standard no.2); 7 = triglycerides (Quesada-Medina & Olivares-Carrillo, 2011). Reused with Elsevier's permission (attached in Appendix A)..... 11**
- Fig. 2 Yield of methyl linoleate (18:2) at different reaction conditions: ♦, 250 °C/12 Mpa; ○, 275 °C/18 Mpa; ▲, 300 °C/26 Mpa, □, 325/35 Mpa; ●, 350 °C /43 Mpa (Quesada-Medina & Olivares-Carrillo, 2011). Reused with Elsevier's permission (attached in Appendix A). 13**
- Fig. 3 Different possible ways for the decomposition of methyl stearate (18:0) (A) and methyl oleate (18:1) (B) via the supercritical methanol synthesis (Shin et al., 2011). Reused with Elsevier's permission (attached in Appendix A)..... 16**
- Fig. 4 Heating time required for biodiesel to rise from room temperature to different setting points 29**
- Fig. 5 An overall schematic diagram of the experimental setup (A) and stainless steel reactors (B)..... 32**
- Fig. 6 An illustration of selected two ramps oven temperature program in HP 5890 GC-FID. 35**
- Fig. 7 GC-FID calibration curves for standard analytes of FAMEs (C16:0-C22:0 and C18:1-3). 42**

Fig. 8 GC/FID chromatograms for fresh biodiesel (A), GLC-10 and GLC-100 mixture (B), GLC-10 FAME mix (C), GLC-100 FAME mix (D). Labeled peaks are C16:0 (1), C18:1-3 (2), C18:0 (3), C19:4 (4), C20:0 (5), C21:0 (6), C22:0 (7)..... 45

Fig. 9 Photographs of biodiesel samples collected after different heat treatment. Numbers below samples indicate the thermal stressing temperature and time. Note that the thermal stressing time also includes the 3 minute heat up time. The time value on the bottles does not include the heat up time. 49

Fig. 10 GC/FID chromatograms of biodiesel fuel subjected to heat treatment at 250 °C.... 56

Fig. 11 GC/FID chromatograms of biodiesel fuel subjected to heat treatment at 275 °C. The red arrows indicate the formation of trans-type C18:2 isomers. 57

Fig. 12 GC/FID chromatograms of biodiesel fuel subjected to heat treatment at 300 °C. The red arrows indicate the formation of trans-type C18:2 isomers and dimers. 58

Fig. 13 GC/FID chromatograms of biodiesel fuel subjected to heat treatment at 325 °C. The red arrows indicate the formation of trans-type C18:2 isomers and dimers. 59

Fig. 14 GC/FID chromatograms of biodiesel fuel subjected to heat treatment at 350 °C. The red arrows indicate the formation of smaller molecular weight compounds, trans-type C18:2 isomers and dimers..... 60

Fig. 15 GC/FID chromatograms of biodiesel fuel subjected to heat treatment at 360 °C. The red arrows indicate the formation of smaller molecular weight compounds, trans-type C18:2 isomers and dimers..... 61

Fig. 16 GC/FID chromatograms of biodiesel fuel subjected to heat treatment at 375 °C. The red arrows indicate the formation of small molecular weight compounds, trans-type C18:2 isomers and dimers..... 62

Fig. 17 GC/FID chromatograms of biodiesel fuel subjected to heat treatment at 400 °C, indicating the dynamic behavior of biodiesel decomposition and the formation of smaller molecular weight FAMES and hydrocarbons. 63

Fig. 18 GC/FID chromatograms of biodiesel fuel subjected to heat treatment at 425 °C, demonstrating the formation of significant amounts of smaller molecular weight FAMES and hydrocarbons owing to pyrolysis of FAMES. 64

Fig. 19 GC/MS chromatogram of biodiesel fuel subjected to heat treatment at 425 °C for 23 min, demonstrating the distribution of decomposition productions. FAMES C16:0, C18:0 and C20:0 are present in the fresh biodiesel. 65

Fig. 20 Plot of concentration of biodiesel sample as a function of thermal stressing time at different temperatures. 75

Fig. 21 Thermal decomposition percentage of biodiesel fuel variation as a function of time at different temperatures. 76

Fig. 22 A mechanism of biodiesel thermal decomposition. \Leftrightarrow reversible reaction; \rightarrow irreversible reaction; A: biodiesel; B: isomers, dimers, etc.; C: smaller FAMES, hydrocarbons, gases, etc.; k_{AB} , k_{BA} , k_{AC} and k_{BC} are reaction rate constants. 80

Fig. 23 Modeling of biodiesel concentration as a function of time for various stressing temperatures using the reversible first-order kinetics fitted with experimental data. . 84

Fig. 24 Plot of predictions of biodiesel thermal decomposition as a function of time under different stressing conditions using the reversible first-order kinetic model fitted with experimental data. 85

Fig. 25 Arrhenius plot for the first-order forward decomposition of biodiesel. The Arrhenius parameters determined from the fit to the data are $A = 1.50 \times 10^9 \text{ min}^{-1}$ and $E_a = 126.0 \text{ KJ/mol}$ 87

Fig. 26 Arrhenius plot for the first-order reverse decomposition of biodiesel. The Arrhenius parameters determined from the fit to the data are $A = 257 \text{ min}^{-1}$ and $E_a = 46.0 \text{ KJ/mol}$ 88

Fig. 27 Van't Hoff plot for the reversible first order decomposition of biodiesel. The determination of the reaction enthalpy ΔH° for biodiesel thermal decomposition is 80.0 KJ/mol , indicating an overall endothermic reaction. 89

Fig.A- 1 GC-FID calibration curves for supplementary FAME analytes and mixtures (C19:0, C21:0 and analytical standard mixtures)..... 96

Fig.A- 2 Chromatograms of fresh biodiesel (A), fresh biodiesel and GLC-10 FAME mix (B), fresh biodiesel and GLC-100 FAME mix (C). Peaks shown in the chromatograms are C 16:0 (1), C 18:1-3 (2), C 18:0 (3), C 19:4 (4), C 20:0 (5), C 21:0 (6), C 22:0 (7)..... 97

Fig.A- 3 Chromatograms of biodiesel samples thermal stressed at 250°C for 3 and 8 minutes..... 98

Fig.A- 4 Chromatograms of biodiesel samples thermal stressed at 250°C for 18 and 33 minutes..... 99

Fig.A- 5 Chromatogram of biodiesel sample thermal stressed at 250°C for 63 minutes. . 100

Fig.A- 6 Chromatograms of biodiesel samples thermal stressed at 275°C for 3 and 8 minutes..... 101

Fig.A- 7 Chromatograms of biodiesel samples thermal stressed at 275°C for 28 and 38 minutes..... 102

Fig.A- 8 Chromatogram of biodiesel samples thermal stressed at 275 °C for 63 minutes.	103
Fig.A- 9 Chromatograms of biodiesel samples thermal stressed at 300 °C for 3 and 8	
minutes.....	104
Fig.A- 10 Chromatograms of biodiesel samples thermal stressed at 300 °C for 18 and 33	
minutes.....	105
Fig.A- 11 Chromatogram of biodiesel sample thermal stressed at 300 °C for 63 minutes.	106
Fig.A- 12 Chromatograms of biodiesel samples thermal stressed at 325 °C for 3 and 8	
minutes.....	107
Fig.A- 13 Chromatograms of biodiesel samples thermal stressed at 325 °C for 18 and 33	
minutes.....	108
Fig.A- 14 Chromatogram of biodiesel sample thermal stressed at 325 °C for 63 minutes.	109
Fig.A- 15 Chromatograms of biodiesel samples thermal stressed at 350 °C for 3 and 8	
minutes.....	110
Fig.A- 16 Chromatograms of biodiesel samples thermal stressed at 350 °C for 18 and 33	
minutes.....	111
Fig.A- 17 Chromatograms of biodiesel samples thermal stressed at 360 °C for 3 and 8	
minutes.....	112
Fig.A- 18 Chromatograms of biodiesel samples thermal stressed at 360 °C for 18 and 33	
minutes.....	113
Fig.A- 19 Chromatogram of biodiesel sample thermal stressed at 360 °C for 43 minutes.	114
Fig.A- 20 Chromatograms of biodiesel samples thermal stressed at 375 °C for 3 and 8	
minutes.....	115

Fig.A- 21 Chromatograms of biodiesel samples thermal stressed at 375 °C for 18 and 33 minutes..... 116

Fig.A- 22 Chromatogram of biodiesel sample thermal stressed at 375 °C for 43 minutes. 117

Fig.A- 23 Chromatograms of biodiesel samples thermal stressed at 400 °C for 3 and 8 minutes..... 118

Fig.A- 24 Chromatograms of biodiesel samples thermal stressed at 400 °C for 18 and 28 minutes..... 119

Fig.A- 25 Chromatogram of biodiesel sample thermal stressed at 400 °C for 33 minutes. 120

Fig.A- 26 Chromatograms of biodiesel samples thermal stressed at 425 °C for 3 and 8 minutes..... 121

Fig.A- 27 Chromatograms of biodiesel samples thermal stressed at 425 °C for 13 and 18 minutes..... 122

Fig.A- 28 Chromatogram of biodiesel samples thermal stressed at 425 °C for 23 minutes. 123

List Of Tables

Table 1: Analytes of 1891-1AMP GLC-10 FAME mix (100 mg).....	20
Table 2: Analytes of 1899-1AMP GLC-100 FAME mix (100 mg).....	21
Table 3 Settings of Techne SBL-2 for frequently used temperatures	25
Table 4 Values of critical properties of common used alcohols in supercritical transesterification method.	26
Table 5 Conditions for thermal stressing experiments of biodiesel	30
Table 6 GC-FID Chromatographic conditions	34
Table 7 Selected gas chromatographic conditions for GC-MSD.....	37
Table 8 Constants and coefficient of determination (R^2) for FAMES calibration curves ...	44
Table 9 Mass fractions of BD-100 biodiesel compositions*	47
Table 10 Observations of thermal stressed biodiesel samples	53
Table 11 GC-FID data for fresh biodiesel	73
Table 12 Concentrations of fresh biodiesel samples	74
Table 13 Rate constants and equilibration constant for biodiesel thermal decomposition reactions.....	83
Table A- 1 GC-FID data for analytical standard GLC-10 FAME mix	124
Table A- 2 GC-FID data for analytical standard GLC-100 FAME mix	125
Table A- 3 GC-FID data for thermally-stressed biodiesel samples.....	126
Table A- 4 Concentrations of thermal stressed biodiesel samples	129
Table A- 5 Data of Ink_1, Ink_2, and InK for each temperature.....	132
Table A- 6 Comparison of modeling data and experimental data of biodiesel concentration and thermal decomposition percentage.....	133

Chapter I

Introduction

Biodiesel is a mixture of long-chain fatty acid mono-alkyl esters obtained by transesterification reaction of vegetable oil or animal fats and short chain alcohol (Jain & Sharma, 2011). Biodiesel compositions vary among samples from different feed stocks. Saturated methyl palmitate (C16:0), methyl stearate (C18:0) along with unsaturated methyl oleate (C18:1), methyl linoleate (C18:2) and methyl linolenate (C18:3) are common compounds present in biodiesel fuel (Imahara, Minami, Hari, & Saka, 2008).

Biodiesel fuel, as a renewable energy source, is becoming increasingly popular nowadays, since it is an ideal substitute for fossil fuels in diesel engines without modification on account of the highly similar properties (Bunyakiat, Makmee, Sawangkeaw, & Ngamprasertsith, 2006). It can be used pure directly or blended with diesel in different proportions according to different requirements (Jain & Sharma, 2010; Ragonese, Tranchida, Sciarrone, & Mondello, 2009). Usually the abbreviation BX is used to define the mixing proportion where X represents the biodiesel percentage (v/v). For instance, 80% biodiesel plus 20% petro-diesel is referred as B80 while 20% biodiesel and 80% petro-diesel is labeled B20. The current work focuses on B100 biodiesel which is petro-diesel free.

Even though fossil fuel is the main contemporary worldwide consumed energy source, the limited storage amount of fossil fuel and long formation time reveal the inevitable short supply in the near future. In addition, there is no denying the fact that our world is facing another serious problem of environment deterioration as well as energy shortage. It was found that using

biodiesel to replace diesel fuel can reduce the greenhouse gas emission and other air pollutants drastically (Shay, 1993). Under such conditions, biodiesel stands out since it is reproducible, environmentally friendly, compatible with conventional diesel engines and easy to be manufactured from diverse feasible raw materials, such as animal fat (Marulanda, Anitescu, & Tavlarides, 2010b), vegetable oils (Demirbas, 2005; Ma & Hanna, 1999), algal oils (Chisti, 2007) and waste cooking oils (Kulkarni & Dalai, 2006).

Alkali-catalyzed transesterification (ester exchange) reaction is a conventional method to produce biodiesel fuel. However, this method has a number of disadvantages. Catalyst should be removed after use which means extra work. Additionally, to achieve ideal conversion to the esters, the raw materials have some limitations. Only those with content of free fatty acids lower than 0.5% (Freedman, Pryde, & Mounts, 1984) and water lower than 0.06% can meet the requirement (Ma, Clements, & Hanna, 1998). The catalyst may be consumed and lose effectiveness to some extent which results in saponification reaction caused by free fatty acids. Water has a worse influence than that of the free fatty acids, because it might reduce the yield more significantly (Freedman et al., 1984).

Taking into account these non-negligible drawbacks, the biodiesel production technologies turn to non-catalyst methods aimed to address such issues. The latest well known approach is catalyst-free supercritical transesterification between long-chain triglycerides in oils/fats and alcohol, which has made great progress. This technology is characterized by producing biodiesel without restrictions in the amount of the free fatty acids and water. It is stated that a certain amount of water can even advance the conversion (Kusdiana & Saka, 2004). In this advanced process, the reaction rate is substantially accelerated since animal fats/vegetable oil and methanol become a well mixed homogenous phase which means there is no need of interphase mass

transfer (Quesada-Medina & Olivares-Carrillo, 2011).

About this novel method, while ethanol and some other alcohols have come into use for biodiesel research (Knothe, 2005), previous research focuses on methanol to produce methanol-based biodiesel of fatty acid methyl esters (FAMEs) (Demirbas, 2007a; He, Wang, & Zhu, 2007)

Apparently this supercritical transesterification process is in need of high temperatures, being above the alcohol critical point. The critical temperatures for the most commonly used methanol and ethanol are 239 °C and 241°C, respectively (Gude & Teja, 1995). Owing to this severe condition, the thermal stability of biodiesel is a major challenge. Excessive reaction temperature and exposure time might lead to fuel degradation and impaired fuel quality. The Saka group (Kusdiana & Saka, 2001; Saka & Kusdiana, 2001) first detected decomposition of unsaturated FAMEs at 350-500 °C. Similar observations were published later on which further confirmed the thermal instability of biodiesel at high temperatures (Imahara et al., 2008; Marulanda, Anitescu, & Tavlarides, 2010a; Vieitez et al., 2008). In order to achieve maximum output of high quality biodiesel, the effect of temperature and residence time on thermal stability of biodiesel should be investigated in greater depth.

Another reason to place importance on thermal stability of biodiesel is an innovational, clean diesel combustion technology. This approach was recently proposed by our group at Syracuse University to simultaneously increase energy efficiency substantially and reduce harmful emissions by injecting and combusting fuels under the supercritical conditions (up to 450 °C) (Anitescu, Tavlarides, & Geana, 2009). The traditional way is to inject biodiesel in the liquid state. Even though a clean and high efficient combustion can be achieved by making this change, this breakthrough brings about some obstacles at the same time. The high temperature is

more likely to cause unexpected fuel degradation when the engines operate under such severe thermal conditions. The problem of instability of biodiesel will lead to poor engine performance, low efficiency, engine failure, and engine malfunction (Batts & Fathoni, 1991). As a result, the engine will become less reliable and more vulnerable, maintenance costs will increase, and the lifetime of the engines can be shorted. To implement and improve this novel method, thermal stability restrictions of the supercritical fluid on engines need to be explored.

Although there were some researches on the thermal stability of biodiesel recently, the work in this area is still inadequate. To guarantee the biodiesel fuel quality, this subject still requires a further understanding. With the knowledge of the reactivity of biodiesel under supercritical conditions, it is more desirable to find an optimization of the production and combustion process.

By extension, there is a quantity of literature available on the models describing biodiesel formation kinetics, but few works have been published so far about the kinetics for thermal decomposition of biodiesel (Gunvachai, Hassan, Shama, & Hellgardt, 2007). This shortage makes the kinetic study very meaningful and valuable. A proper model is useful for inferring the behaviors of biodiesel at high temperatures.

The importance of this work is to develop a deep understanding of the principal effects of some main factors on the thermal stability of biodiesel fuel, particularly the temperature and thermal stressing time. Another primary objective is to propose a model which can represent the kinetics of thermal decomposition of biodiesel fuel. With this model, the behaviors of biodiesel caused by exposure to high temperatures can be predicted. All in all, these tasks are worthwhile because there is a huge demand in the market currently for stable fuel to meet reliability requirements.

In this study, thermal stressing experiments of BD-100 biodiesel samples were executed in stainless steel batch reactors at 250-425 °C for residence times up to 63 minutes. A fluidized bath served as the heat source for thermal stressing the reactors. Collected samples were investigated using gas chromatography (GC) equipped with a flame ionization detector (FID) and a mass selective detector (MSD). A three-lump model is proposed to denote the thermal decomposition mechanism. And, lastly, a reversible first-order reaction model with validation was established for the overall decomposition kinetics.

Chapter II

Literature review

2.1 Introduction

In this chapter, previous works intimately associated with this study are reviewed. Existing knowledge and key findings on thermal stability at high temperatures is summarized. In the meantime, some flaws and disagreements of precedent statements are also concluded in this part. A review relating to a kinetic model for the aviation turbine fuel is also outlined, and this model merits attention because it proposes logical assumptions and ideas and forms a basis which led to the model for biodiesel fuel in this study.

2.2 Biodiesel production technology

The biodiesel production technology has developed over scores of years. Works by Demirbas, Leung, Pinnarat et al. indicate that this technology can be classified into two prime categories: catalytic processes and non-catalytic supercritical processes (Anitescu & Bruno, 2012; Demirbas, 2005; Leung, Wu, & Leung, 2010; Pinnarat & Savage, 2008).

In the traditional catalytic process, biodiesel is made from vegetable oil or animal fat through alkaline or acid catalysts. The supercritical method is a rising and promising technology. In this process, biodiesel is produced via exposure to supercritical alcohol of animal fat or oil, usually methanol in industry (Bunyakiat et al., 2006).

At present, the non-catalytic supercritical process is usually preferred as it performs better and has much superiority over the catalytic process. First of all, the catalytic process demands

pretreatment of the feedstocks because of the presence of free fatty acids (FFAs) and water, or else it cannot produce in an efficient way (Glisic & Skala, 2009; Glisic & Skala, 2009; Marulanda, Anitescu, & Tavlarides, 2010b; Pinnarat & Savage, 2008). What is more, since alkaline or acid catalysts are used, extra work relating to the removal of the catalysts and the generated wastes such as saponified products is required for the purification of the final products (Quesada-Medina & Olivares-Carrillo, 2011; Saka & Kusdiana, 2001). These additional steps virtually increase the cost. By contrast, the profitable and environmentally friendly supercritical method not only dispenses with these redundant stages but also is able to approach the complete conversion (Kusdiana & Saka, 2004; Lee, Posarac, & Ellis, 2011; Lim, Lee, Lee, & Han, 2009; West, Posarac, & Ellis, 2008).

However, supercritical transesterification method has its drawbacks. The most significant one is related to thermal instability of biodiesel at high temperature which is the focus of this thesis. This method will be much more competitive if this issue is addressed.

2.3 Supercritical fuel combustion

Recently, our group proposed an innovative, clean diesel combustion technology that would largely improve the performance of diesel fuel engine (Anitescu, 2008; Lin, 2011). Conventional diesel fuel combustion method is to inject liquid fuel in diesel engines, yet the engine efficiency is limited by poor fuel air mixing upon injection. In this proposed new technology, diesel fuel is mixed with and heated by recycled exhaust gas (EGR) up to supercritical fluid status. Fuel at supercritical state has many prominent physical and chemical properties, for example, it has very short ignition delay; it mixes rapidly with intake air and combusts quickly before the fuel hits the cylinder walls, which means less heat loss by heat conduction (Demirbas, 2007b). By utilizing

these features of supercritical state fuel, supercritical fuel combustion can boost the fuel efficiency and reduce the pollutants substantially.

However the promising side of the supercritical fuel combustion, it has an evident drawback: the fuel must be compressed and heated before it is injected into combustion chamber. It is likely to decompose in the meantime due to its thermal instability at supercritical temperature. Therefore, the behavior of biodiesel near the critical region should be examined to improve the development of this technology.

2.4 Thermal stability of biodiesel fuels

2.4.1 Definition of thermal stability

The term “thermal stability” is defined as the thermal-stressing resistant ability of a fuel for a short exposure time without appreciable deterioration (Batts & Fathoni, 1991). Color changes and formation of solid deposits and gas phase are some indicators of instability. It also includes physical and chemical properties change, fuel composition transformation, and combustion property variation, etc. A fuel with good thermal stability means having the great capability to remain unchanged by thermal treating. Color change is an apparent indicator of fuel degradation. B100 biodiesel is totally colorless, but it will darken or deepen gradually over the course of decomposition. Even though the color change is not directly relevant to fuel quality, the market always tends to lightly colored fuel products without doubt.

2.4.2 A comprehensive summary of the work on thermal stability of biodiesel

Up to now, work has been done by other researchers on thermal stability of biodiesel mainly via the synthesis of biodiesel with supercritical methanol. Generally, after close scrutiny of the

yields and products at different reaction temperatures and time, the behavior of biodiesel was analyzed and deduced.

The members from Saka group were the pioneers in affirming the decomposition of unsaturated FAMES at temperatures above 350 °C (Kusdiana & Saka, 2001; Saka & Kusdiana, 2001). The following will concentrate on the representative papers chosen.

2.4.3 A breakthrough in the thermal stability study on biodiesel

Imahara et al. (Imahara et al., 2008) studied the thermal stability of biodiesel resources derived from a variety of plant oils via the supercritical methanol method over the temperature and pressure range from 270 °C/17 MPa to 380 °C/56 MPa. The result illustrated that all fatty acid methyl esters possessed stability at 270 °C/17 MPa, but at 350 °C/43 MPa, they partially degraded. The authors claim that both methyl linoleate (C18:2) and methyl linolenate (C18:3) underwent a great decrease in concentration at 300 °C and above. FT-IR analyses were performed and showed that this decomposition was caused by isomerization from cis-type to trans-type. As the peaks of naturally existing cis-type C=C bond decreased, the distinguishable peaks of trans-type C=C was observed and increased along with thermal-stressing expose time.

The investigators also confirmed that the unsaturated fatty acid methyl esters (FAMES) are rather more reactive and unstable than saturated ones. Especially, the poly-unsaturated ones were extremely vulnerable to the unwanted thermal breakdown. This characteristic completely coincides with oxidation stability. It is well known that poly-unsaturated biodiesel has much less ability to withdraw oxidation denaturation. Also, it was pointed out that the FAMES with shorter chain length have higher thermal stability. In the paper, the researchers concluded that the thermal stability of the main biodiesel constituents is in the order: methyl palmitate (C16:0)>

methyl stearate (C18:0)>methyl oleate (C18:1)>methyl linoleate (C18:2)>methyl linolenate (C18:3).

Based on the results of the experiments, the investigators bring out the statement that the reaction temperature should be controlled below 300 °C, preferred at 270 °C when it comes to this supercritical methanol technique.

Imahara et al. (Imahara et al., 2008) made a breakthrough in the topic of thermal stability of biodiesel, but their conclusions still have some weaknesses and limitations. Isomerization is not the only reason that results in the low recovery of biodiesel. Shin et al. (Shin, Lim, Bae, & Oh, 2011) put forward other supplementary degradation behaviors based on their findings. These observations will be discussed more concretely in the “**Mechanism of thermal decomposition of biodiesel fuel**” section. Moreover, there is a disagreement with the production temperature. Higher temperatures can also be considered if a reasonable short residence time is chosen, or adjustments can be made of other related parameters. All in all, temperature is not the only key factor.

2.4.4 Analogous research related to thermal stability of biodiesel

Similarly, Quesada and Olivares (Quesada-Medina & Olivares-Carrillo, 2011) implemented another set of experiments on this topic. Gas chromatography was used to determine the decomposition products. An unexpected broad peak (peak 2 in **Fig. 1**) was observed chromatographically of reaction samples produced at higher temperature. The investigators suggested that it might be thermal decomposition compounds.

Then they conducted another experiment to verify this assumption. They studied diverse kinds of biodiesel compounds generated during the synthesis of refined soybean oil with

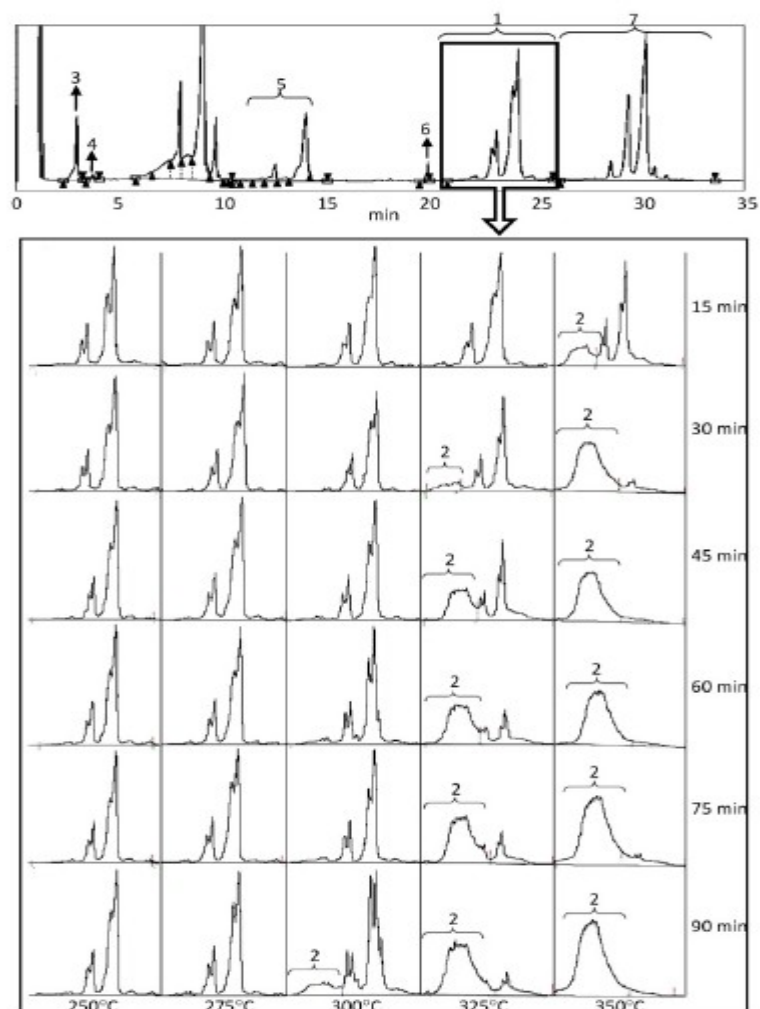


Fig. 1 GC chromatograms of the product of the reaction performed at different conditions. Chromatographic peaks. 1 = diglycerides; 2 = possible thermal decomposition products; 3 = glycerin; 4 = 1, 2, 4-butanetriol (internal standard no. 1); 5 = monoglycerides, 6 = glyceryl tridecanoate (internal standard no.2); 7 = triglycerides (Quesada-Medina & Olivares-Carrillo, 2011). Reused with Elsevier's permission (attached in Appendix A).

supercritical methanol, especially methyl linoleate (C18:2), as shown in **Fig. 2**. The authors placed an emphasis on this ester in that linoleic acid (C18:2) is most abundant in the feedstock. **Fig. 2** showed that the yield of methyl linoleate continues increasing at a practically constant rate when temperatures were lower than 300 °C. It displayed that this product was not thermally decomposed, even when the reaction times surpassed 90 minutes. This result neatly dovetailed with that from Imahara et al. As the same, peak 2 did not appear below 300 °C from the chromatograms in **Fig. 1**. Besides, productivities peaked at 300 °C and above, along with that, they started falling off in **Fig. 2**. This can well explain the detected peak 2 in **Fig. 1**, which should represent decomposition compounds. Combining these experiments focused on the behavior of these fatty acid methyl esters, the evidence well revealed that biodiesel started thermal decomposition at 300 °C and above.

Moreover, Quesada and Olivares (Quesada-Medina & Olivares-Carrillo, 2011) pointed out that even though a certain degree of thermal decomposition exists in the supercritical methanol process, the highest yield of biodiesel was achieved at 325 °C, which can be seen in **Fig. 2**. This original viewpoint helps develop a better understanding of the relationship between highest yield and decomposition as well as finding an optimization of non-catalyst supercritical reaction.

Although Imahara, Quesada et al. (Imahara et al., 2008; Quesada-Medina & Olivares-Carrillo, 2011) confirmed the occurrence of thermal decomposition and isomerization at high temperatures, they did not explore further the mechanism and other possible reactions.

2.5 Mechanism of thermal decomposition of biodiesel fuel

Since thermal instability becomes a big issue in biodiesel production and combustion under supercritical conditions, some efforts are made to study the thermal decomposition mechanism of

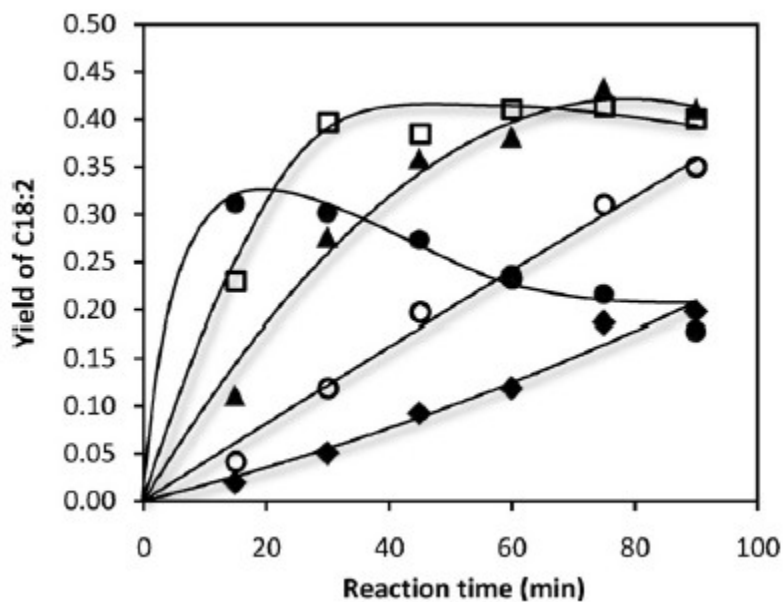
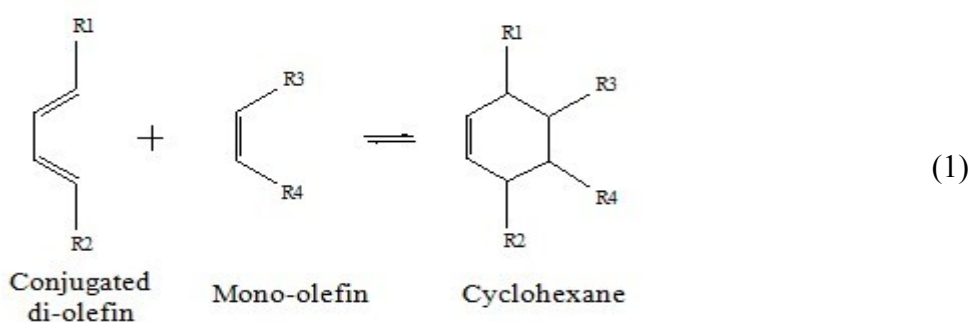


Fig. 2 Yield of methyl linoleate (18:2) at different reaction conditions: ◆, 250 °C/12 Mpa; ○, 275 °C/18 Mpa; ▲, 300 °C/26 Mpa, □, 325/35 Mpa; ●, 350 °C /43 Mpa (Quesada-Medina & Olivares-Carrillo, 2011). Reused with Elsevier's permission (attached in Appendix A).

biodiesel in the hope that methods can be found to block the pathway of biodiesel decomposition (Bridgwater, 2003; Imahara et al., 2008). The primary proposed reactions during the thermal decomposition of biodiesel at high temperatures will be reviewed in brief in the following text.

Generally speaking, two unsaturated fatty acid chains can be linked together through the thermal polymerization reaction at high temperature (≥ 250 °C). As shown in Eq. (1), the thermal polymerization reaction is usually preceded by Diels-Alder reaction (Jain & Sharma, 2011) in which conjugated diene reacts with single olefin to form a substituted cyclohexene product.

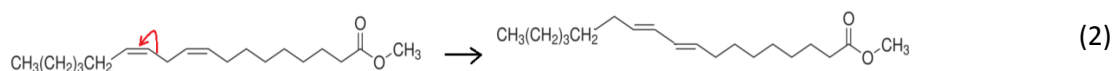
The following is the well-known Diels-Alder reaction:



To form conjugated di-olefin structure, an isomerization reaction (as shown in Eq. (2)) is needed. When the temperature is high enough, the polyunsaturated di-olefin group from the fatty acid chain may commence to isomerize to more stable conjugated group. Isomerization is important in understanding the chemistry of thermal degradation of unsaturated chemicals because of the fact that most isomerization reactions happen only when temperature is higher than 250 °C which is also the temperature range of thermal polymerization of fatty oils. This fact implies that isomerization is one of the determinative reactions in the kinetics of thermal degradation of FAMES.

A possible isomerization reaction of methyl linoleate prior to the Diels-Alder reaction can be

written as:



In addition to polymerization and isomerization, thermal pyrolysis also plays an important role in thermal degradation of biodiesel. Hee-Yong Shin *et al.* (Shin et al., 2011), did a series of thermal decomposition experiments of FAMES via the supercritical methanol synthesis at temperature in the range from 325 °C to 420 °C and kept the pressure at 23MPa.

The author claims that a kind of pyrolysis pathway, as shown in **Fig. 3**, is analogous to the commonly recognized radical chain scission processes through the polymer pyrolysis. From **Fig. 3**, we can see that the dominating chemical reactions in thermal degradation of unsaturated FAMES are isomerization and hydrogenation of carbon-carbon double bond; and the analogous radical chain scission such as β -scission and H-abstraction are the main elementary reactions for saturated FAMES. The main pyrolyzed products of methyl oleate are small molecular weight FAMES, alkenes and alkanes.

Besides, some other types of side reactions might also be involved. For instance, the dehydrogenation reaction was also cited for the loss of the material (He et al., 2007).

In summary, the thermal decomposition of biodiesel is very complicated. Diverse kinds of reactions might happen. Hence, to grasp a global perception of the mechanism of biodiesel decomposition, it is best to pay attention on the primary reactions.

2.6 Kinetic models of thermal decomposition of biodiesel fuel

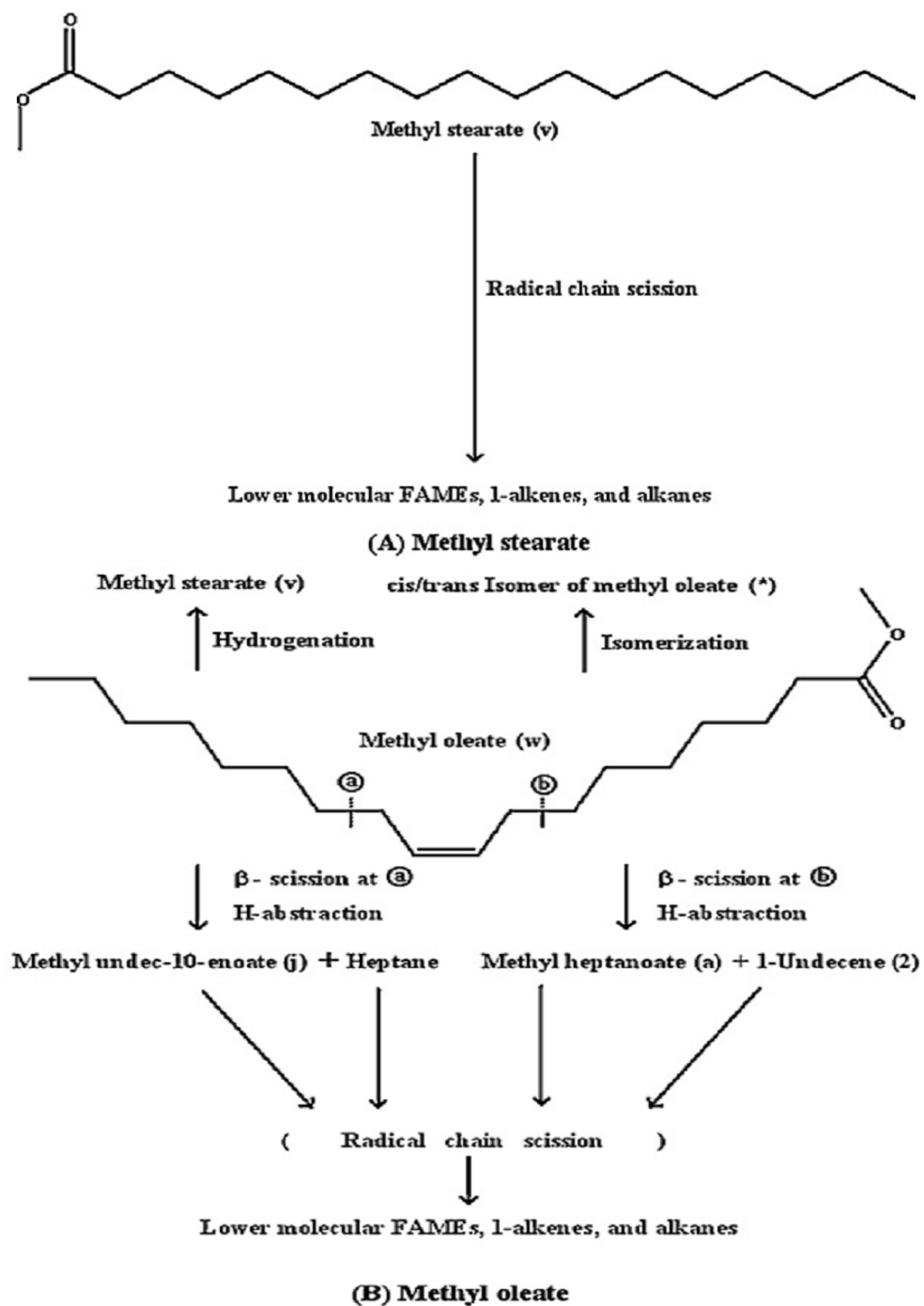


Fig. 3 Different possible ways for the decomposition of methyl stearate (18:0) (A) and methyl oleate (18:1) (B) via the supercritical methanol synthesis (Shin et al., 2011). Reused with Elsevier's permission (attached in Appendix A).

As mentioned in the previous text, in the real world, thermal decomposition of FAMES is a complex chemical process that involves many reactions. Other than the three major types of reactions found in thermal degradation of FAMES of isomerization, polymerization and thermal pyrolysis, there are a number of decomposition reactions such as hydrogenation, dehydrogenation, etc. Moreover, more than one product (disproportionation) may be produced through one reaction pathway. Also, the degradation rate of a single component can be altered by the occurrence of the other ones.

Therefore, it is not easy to find a kinetic model to describe decomposition showing the complex reactions. But on the other hand, the whole thermal decomposition can sometimes be described by a global kinetic reaction model. For instance, Jason A. Widegren *et. al.* (Widegren & Bruno, 2008) investigated the thermal decomposition process of Aviation Turbine Fuel Jet A and it turned out that the thermal decomposition reactions at 375, 400, 425, and 450°C can be well described by a pseudo-first-order kinetic reaction model and the temperature dependent rate constant was given by Arrhenius expression. The constant pre-exponential factor A ($4.1 \times 10^{-12} \text{ s}^{-1}$) and activation energy E_a ($220 \text{ kJ} \cdot \text{mol}^{-1}$) were determined experimentally.

This method of modeling kinetics of thermal degradation of biodiesel fuel is also straightforward and useful. For example, it can be used to estimate the resident time of biodiesel fuel in a stainless steel container at high temperature. But the method also has some drawbacks, and one chief defect is that the computed rate constant is also known to have dependence on many other factors beside temperature. For instance, it may depend on the material of container in the experiments. Strictly speaking the aforementioned values for A and E_a are valid only when the container is constructed from 300 series stainless steels in that Jet A fuel experiment. Also this modeling method does not distinguish one reaction from other reactions.

That means it changes with constituents of the fuel. However, there is no denying the fact that the advantages of this method far outweigh the disadvantages and it will play a significant role in modeling the decomposition of fuels.

In this thesis, the kinetics study of the global thermal decomposition of biodiesel fuel was done in a similar manner as that of the Jet A fuel. For example, use the simplified first order idea and assumption, and the method of obtaining Arrhenius parameters.

Chapter III

Experiments

3.1 Materials

In the marketplace, pure biodiesel fuel is usually blended with petroleum diesel fuel in order to improve their combustion efficiency and to reduce visible emissions. When it comes to the thermal decomposition of the blend, it is hard to tell which is to blame since diesel fuel is also not stable at high temperatures. Hence our experimental studies focus on the pure (100%) biodiesel so that its properties would not be obscuring or interfering with petroleum diesel fuel. The biodiesel fuel (Nexsol BD-100, where BD refers to biodiesel and 100 means 100% purity) was supplied by Peter Cremer North America Company. This raw material is made from vegetable oils. However, the detailed information relating to the compositions and content present in this BD-100 biodiesel is not provided by this company.

Two analytical standards for GC analysis, namely 1891-1AMP GLC-10 FAME mix (100 mg) and 1899-1AMP GLC-100 FAME mix (100 mg) were purchased from Sigma-Aldrich, Inc. **Table 1** and **Table 2** show the composition of the analytes of these standards. Notice that GLC-10 FAME mix and Nexsol BD-100 have the same constituents only that the weight percentages of components are different. Since the analytical standards have known concentration of analytes, GLC-10 is therefore an ideal collator for Nexsol BD-100 biodiesel.

As to GLC-100 FAME MIX, one of its constituent, methyl stearate (C18:0), is also contained in Nexsol BD-100 biodiesel. In chromatogram output, peak of methyl stearate can be used as an anchor point to calibrate chromatogram curve. In addition, we expect that

Table 1: Analytes of 1891-1AMP GLC-10 FAME mix (100 mg)

Chemicals	Chemical formula abbreviation*	Weight percentage (%)
Methyl palmitate	C16:0	20
Methyl stearate	C18:0	20
Methyl oleate	C18:1	20
Methyl linoleate	C18:2	20
Methyl linolenate	C18:3	20

*About the chemical formula abbreviation such as C16:0, the first number denotes that of carbons in the alkyl chain, while the second number shows the number of carbon double bonds.

Table 2: Analytes of 1899-1AMP GLC-100 FAME mix (100 mg)

Chemicals	Chemical formula abbreviation	Weight percentage (%)
Methyl stearate	C18:0	20
Methyl nonadecanoate	C19:0	20
Methyl arachidate	C20:0	20
Methyl heneicosanoate	C21:0	20
Methyl behenate	C22:0	20

polymerization reactions occur during the thermal degradation process which means long carbon chains are formed by short chains linking together. Meanwhile GLC-100 has long chain constituents such as methyl behenate (C22:0). Thus we expect that some polymerization products can be identified from GLC-100. In fact, Methyl behenate like chemicals were indeed identified by this method. In results and analysis chapter, we will show the details.

Hexane ($\geq 99\%$) was supplied by Fisher Scientific, Inc. This chemical was used to clean the reactors and also served as solvent for GC analysis of both biodiesel and analytical standards as well. Hexane is an ideal solvent for GC analysis since it ensures that no distracting peaks greater than 2 minutes are shown on final chromatogram. GC-FID makeup gas (Ultra high purity Nitrogen), carrier gas (Helium), flame gases Ultra zero Air, and hydrogen were purchased from Airgas, Inc.

3.2 Experimental setup

Roughly speaking, there were two components to consider in thermal decomposition experiment: (i) The thermal stressing experiments in which biodiesel fuel was heated in a thermal bath and decomposed products were collected. (ii) GC-FID experiments where post-decomposition products were analyzed. In this subsection, setup of the thermal stressing experiments will be sketched. The batch thermal stressing experimental setup is divided into the following parts:

The first part is the installation of the heating source. In our experiments, industry standard Fluidized Temperature Sand bath (Techne SBL-2) was used. Techne SBL-2 is an ideal fluidized sand bath for organic material heat treatment experiments. It is able to maintain high temperatures up to 600 °C with fluctuation of ± 1 °C. During the high temperature reaction

experiments, the biodiesel fuel was immersed in the sand bath that provides excellent heat transfer and temperature uniformity.

The bath was connected to clean and dry air whose pressure was 3psi and maximum flow was 57L/min (2ft³/min) via a control valve and a porous plate that ensures a uniform flow of air across the section of the container. The low pressure air stream then fluidizes the “sand particles”, *i.e.* small aluminum oxide particles.

Second, five stainless steel coils (Small parts, Inc., I.D. = 1.524 mm×200 mm, $V=\pi D^2/4 \times L=0.365$ ml) were made as batch thermal stressing reactors. Biodiesel was filled in coils manually and enclosed by hex head caps. The K-type thermocouple (Omega) was set up to monitor the temperatures of the fluidized bath. The thermocouple is set up to be at the same horizontal position with stainless steel coils so that the temperature of environment is the same as the temperature of biodiesel within the coils.

The sand bath was heated to required temperatures before samples were put in. Temperature control of the sand bath was achieved by manually adjusting two units, the heater switches and the energy regulation knob. The heater switches have only three options, namely low, medium and high. These options represent selections of either 1kW or 2kW or 3kW heat input. The energy regulation knob is a vernier regulator that provides more precise control of energy input. For instance, to elevate sand bath temperature to 400 °C from room temperature, the heater switches were set to medium status, and the energy regulator knob was set to high value, say 8 or 9. When temperature was elevated to approximately 400 °C, the energy regulator knob was then turned anti-clockwise to lower down energy input. Empirically we found that the energy regulator must be set between 2 and 3 to maintain 400 °C sand bath temperature. The

temperature should be controlled carefully so that the required temperature can be achieved quickly and safely. Settings for several commonly seen temperatures are listed in **Table 3**.

3.3 Experimental conditions and procedure

3.3.1 Selection of thermal stressing temperature range

As mentioned in the chapter of literature review, thermal instability is one of the most critical problems in biodiesel production, especially when the high temperature non-catalytic transesterification in supercritical alcohol conditions has proved to be the most promising process for future biodiesel fabrication.

Methanol, ethanol, propanol and butanol can be used in this supercritical alcohol method (Warabi, Kusdiana, & Saka, 2004). The values of their critical properties are listed in **Table 4** (Gude & Teja, 1995). Methanol and ethanol are the most commonly used alcohols in supercritical transesterification method and their critical temperatures are around 240°C. It means that Non-catalytic synthesis of biodiesel in supercritical methanol or ethanol should be carried out above 240 °C. The production of biodiesel in this method can cover a wide temperature range from 250 °C up to around 425 °C (Anitescu, Deshpande, & Tavlarides, 2008; Saka & Kusdiana, 2001).

Considering the facts that thermal degradation during supercritical transesterification is a big problem of the decrease of yield. In order to learn more about it to address this issue, we regard temperatures that are lower than the critical points of the commonly used alcohols are unimportant, and thermal stressing experiments of biodiesel fuel in this research were selected at nine different temperatures from 250 °C to 425 °C (roughly 25 °C every data point).

Table 3 Settings of Techne SBL-2 for frequently used temperatures

Bath temperature	Heater Switches Settings	Energy Reg. Knob Settings
200°C (392°F)	LOW	7 ~ 8
300°C (572°F)	LOW	9 ~ 10
400°C (752°F)	MEDIUM	2 ~ 3
500°C (932°F)	MEDIIUM	8 ~ 9
600°C (1112°F)	HIGH	4 ~ 5

Table 4 Values of critical properties of common used alcohols in supercritical transesterification method.

Alcohol	Critical Temperature $T_c/^\circ\text{C}$	Critical Pressure P_c/MPa
Methanol	239	8.1
Ethanol	241	6.1
1-Propanol	264	5.2
1-Butanol	290	4.4

3.3.2 Definition of thermal stressing time

In this study, compared to temperature, exposure time was considered to be no less important for contributing to biodiesel degradation. The residence time (or thermal stressing time) was defined as the duration of coils being placed in the heated fluidized bath including the quick heating period.

Due to the significance of determination thermal stressing time, it is of great importance to figure out the heat up time and cool down time as well.

I. Heat up time determination

During the thermal stressing period, the temperature of the fluidized sand bath was kept constant at setting point. When the coils filled with biodiesel were immersed into the constant temperature fluidized sand bath, the first stage was the heat up period from room temperature to the same setting point. After the initial warm up course, the samples and bath maintained at a uniform temperature within a very small variation.

The temperature of biodiesel in the initial heat up period was elevated from room temperature to sand bath temperature and thusly was not constant. Therefore, the thermal decomposition reaction time was not precise to some extent. In order to determine the degree to which errors were introduced, we did a series of experiments to study the initial heat up behavior of biodiesel in the stainless steel reactors.

Similar to set ups of thermal stressing experiments, the biodiesel samples were enclosed in stainless steel coils. Instead of being sealed off with hex head cap as was described previously, the coil was enclosed with a cap that had a thermometer penetrate through the cap. The

thermometer could measure the temperature inside the coil.

The times were recorded for biodiesel warm up to different desired point. It was found that within the temperature range from 250 to 425 °C, the heating time was approximately 3 minutes.

Fig. 4 demonstrated the heating time change over various temperatures.

II. Cool down time determination

After biodiesel samples were thermal stressed in the sand bath. They were quenched to room temperature (or a little lower) in water. Similarly to quick heat up phase, we expect that time taken for quenching is also linear dependent on the experimental temperatures. However, during our analysis, we regarded this process is negligible for some reasons:

First the cool down of samples proceeded quickly, at least quicker than quick heat phase. In real operation, it has been recorded by thermocouple that the temperatures of biodiesel samples dropped from experimental temperatures (i.e. 250 ~ 425 °C) to below 50 °C in about 2 minutes. It should be pointed out that biodiesel cooled down to below 250 °C within ~ 30 seconds to quench the reactions.

3.3.3 Thermal stressing experimental conditions

Table 5 was the summing-up table of all the experimental conditions, each cross in the table represents an experiment that a certain amount of biodiesel sample was thermal stressed under a specific temperature T for a period of time t_r . It is noted that the heat up time is approximately 3 minutes for the stainless steel coils to be heated from room temperature to reach the fluidized bath temperature which ranges from 250 °C to 425 °C depending on the experiment. The time shown on the sample bottles (**Fig. 9**) represents the time of the coil at the fluidized bath

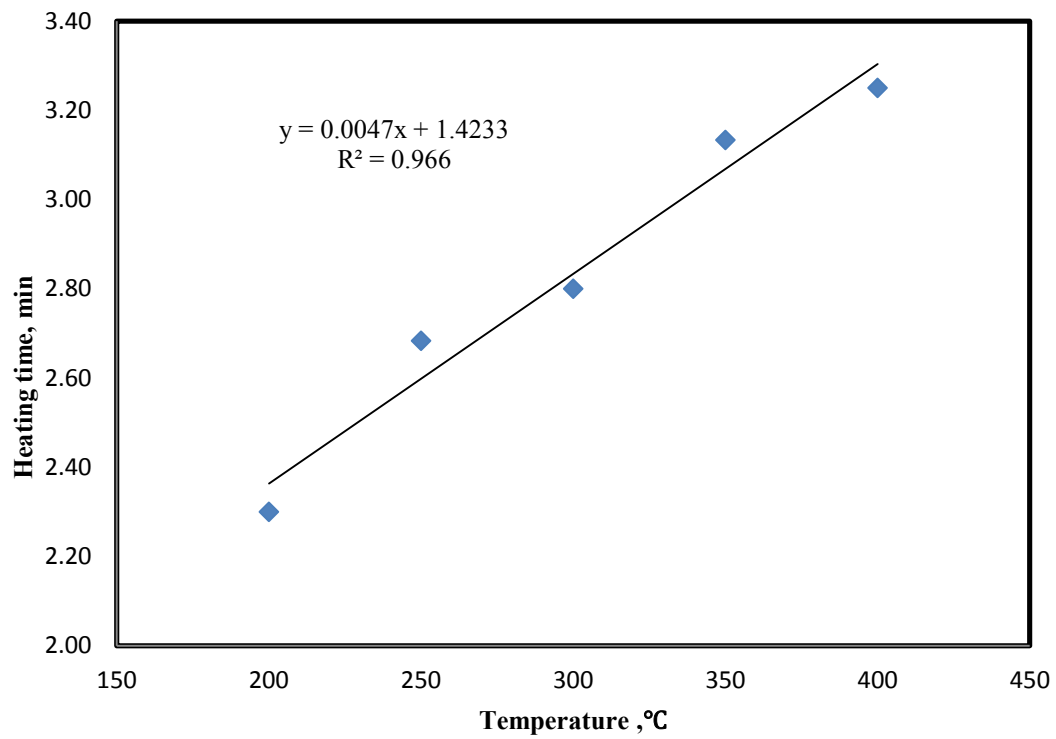


Fig. 4 Heating time required for biodiesel to rise from room temperature to different setting points

Table 5 Conditions for thermal stressing experiments of biodiesel

T, °C	250	275*	300	325*	350	360	375*	400	425*
<i>t_r</i> , residence time, min									
3	×	×	×	×	×	×	×	×	×
8	×	×	×	×	×	×	×	×	×
13									×
18	×		×	×	×	×	×	×	×
23									×
28		×						×	
33	×		×	×	×	×	×	×	
38		×							
43						×	×		
63	×	×	×	×					

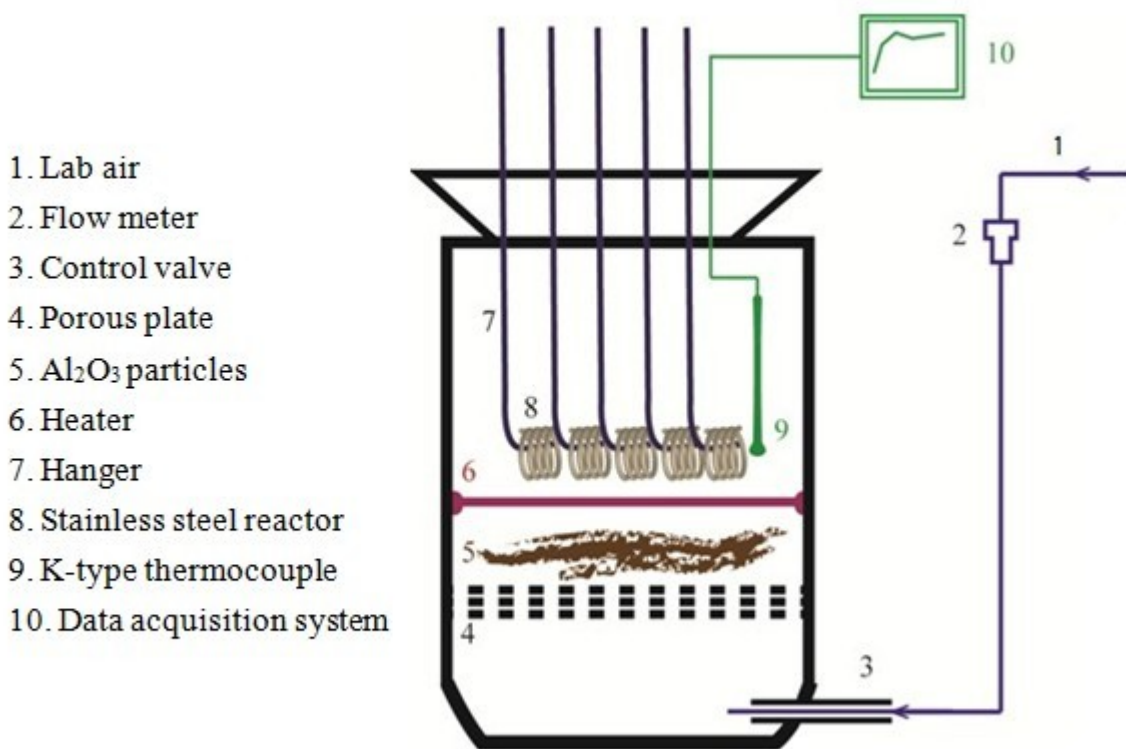
* Experiments were duplicated in these conditions

temperature. In addressing unavoidable experimental errors and uncertainty, experiments at 275 °C, 325 °C, 375 °C and 425 °C were conducted twice to improve accuracy.

3.3.4 Thermal stressing experimental procedure

Based on all the discussions above, thermal stressing research was carried out with the aim to find out how biodiesel evolve with various residence times at different temperatures. In this experiment, when the temperature of the sand bath was elevated to a higher temperature and maintained stably (± 1 °C), five coils were then placed into the bath simultaneously. Before removing them, each coil was heated for a specific period of time which also known as the residence time. The residence time was chosen from 3 to 63 minutes which included the quick heating time (around 3 minutes) of the biodiesel from room temperature to the experimental temperatures that range from 250 °C to 425 °C. After 3 minutes exposure to the vigorously thermostatic boiling sand, biodiesel within the coils would reach the same temperature as their environments. It must be noted that the air flow was manually adjusted after thermal stressing reactors were put in to avoid violent fluidization.

The coils were taken out of the bath one after another and cooled in the water bath when the predetermined residence time of each was achieved. The thermal stressed samples were unloaded from the reactors and collected separately in vials for the GC analysis. **Fig. 5 (A)** is the overall schematic diagram of the Experimental setup, and coils are shown in **Fig. 5 (B)**. Hexane was used to clean the reactors and removed in a GC oven (HP 5890). Then used air supply to blow away hexane and took at least 1 hour at 150 °C to dry the reactors completely in the oven for every run. The data were collected by a data acquisition system (Lab VIEW, National Instrument).



(A)



(B)

Fig. 5 An overall schematic diagram of the experimental setup (A) and stainless steel reactors (B)

3.4 Analytical methods

Two types of gas chromatography were used to analyze post-thermal-stressing samples: gas chromatograph with flame ionization detector (GC-FID) and gas chromatography with 5975C mass Spectrometer Detector (GC-MSD) respectively. Both chromatographs have their own unique advantages: GC-FID is commonly used analytic equipment in laboratories for determination of 70 fatty acids of bio-lipids due to the fact that flame ionization detector (FID) is sensitive to hydrocarbons. GC-MSD is beneficial for identification of FAMES when standards are not available.

3.4.1 GC-FID analysis

A Hewlett-packard Model HP 5890 series II GC-FID was used for quantitative analysis of fresh and thermal stressed biodiesel. This GC-FID was equipped with a Restek Rtx-Biodiesel TG column with dimensions of 10 meter \times 0.32 mm ID \times 0.10 μ m film thickness.

In order to achieve good separation of peaks in chromatograms, the gas chromatographic conditions should be investigated and selected. In this study, different conditions were tried and the optimal gas chromatographic conditions were determined for biodiesel analysis as shown in **Table 6**, and **Fig. 6** is an illustration of this two ramps oven temperature program. In this operation, oven temperature was held at 60 °C for 2 minutes and then elevated from 60 °C to 150 °C at a rate of 6 °C/min for the first ramp. The oven temperature was held at 150 °C for 10 minutes during which, those fatty acids with high volatility will be separated. The oven temperature was then elevated quickly from 150 °C to 350 °C at a rate of 10 °C/min for the second ramp, also known as ramp A. After that the oven temperature was held at 350 °C for 1 minute before the oven temperature was cooled down to its initial value, i.e. 60 °C. During the

Table 6 GC-FID Chromatographic conditions

Detector temperature	350 °C
Injector temperature	350 °C
Injection volume	1 µL
Equilibrium time	1 minute
Initial temperature	60 °C
Initial time	2 minutes
Injector mode	Splitless
Oven temperature program	60 - 150 °C at 6 °C/min, hold 10 minutes 150 - 350 °C at 10 °C/min, hold 1 minute

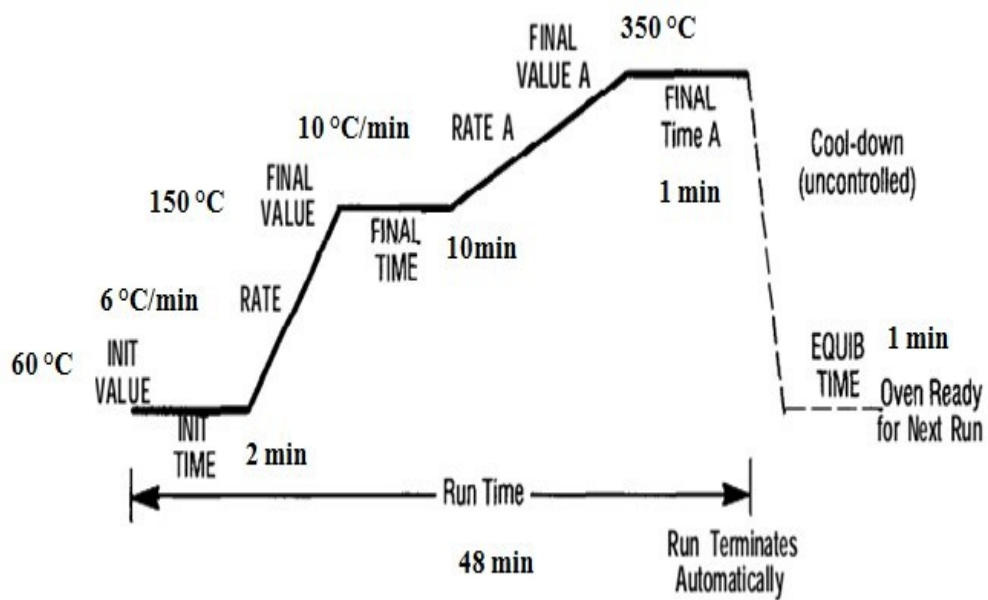


Fig. 6 An illustration of selected two ramps oven temperature program in HP 5890 GC-FID.

stage of ramp A, low volatility fatty acids, which usually are long chain fatty acids, will be separated.

Although some peaks lapped over each other in the chromatograms, the setting listed in **Table 6** separated them to the most extent and well spaced other peaks. Since the column used is 10 meter length instead of 30 meter, overlapped peaks exist inevitably.

3.4.2 GC-MSD analysis

Agilent Technologies 7890A Gas Chromatography with 5975C Mass Spectrometer Detector (GC-MSD) was also used to identify the fresh components and degradation compounds of biodiesel samples. It was equipped with an HP-5MS capillary column with dimensions of 30 m × 0.25 mm I.D. × 0.25 μm film thickness. Compared to HP 5890 GC-FID, HP-5MS GC-MSD has a much longer and thinner column which allows GC-MSD to generate higher resolution chromatogram. However it also took a longer time to complete a run. In most cases GC-FID is sufficient for analysis. In actual operation, we used GC-MSD identify the decomposition products that cannot be determined by GC-FID.

Settings of GC-MSD were mostly similar to aforementioned GC-FID settings. The same as GC-FID, two ramps temperature program was also used in GC-MSD. The detailed gas chromatographic conditions are shown in **Table 7**.

3.4.3 Sample preparation for GC analysis

When it comes to the significant stages in GC-analysis, sample preparation is equally important as choosing a good chromatographic condition and Data analysis. Each stage carried out incorrectly will result in inaccurate or imprecise results. For instance, the concentrations of

Table 7 Selected gas chromatographic conditions for GC-MSD

Injector temperature	285 °C
Interface line temperature	320 °C
Injection volume	1 µL
Initial temperature	60 °C
Initial time	3 minutes
Split ratio	40:1
Oven temperature program	60 - 315 °C at 20 °C/min, hold 1 minute 315 - 300 °C at 20 °C/min, hold 42.5 minutes

samples to be analyzed were carefully planned. If the concentration of a sample was too low, many constituents of the sample would not be quantified because the signals captured by FID were too weak and the peaks in the chromatogram were too small to be integrated. On the other hand if the concentration was too high, the peaks would overlap and be indistinguishable. Generally, samples preparation for GC analysis can be divided into the following branches:

I. Prepare experimental samples

In our experiments, the concentrations of samples were determined empirically and were closely related to concentrations of calibration analytical standards. For instance, six concentrations were used in constructing a calibration curve. In unit of volume fraction, they were 500, 750, 1000, 1250, 1500, and 2000 ppm respectively. And the concentrations of thermal stressed samples were consistently chosen as the median of the six values, i.e. 1000 ppm by volume.

Concentrations of calibration standards were determined empirically so that corresponding output chromatogram showed distinctive peaks of all components of calibration standards. Figures of calibration chromatograms and calibration curves are shown in the later sections.

To make a volume fraction of 1,000 ppm solution of analytical samples, they were prepared by diluting 1 μ l biodiesel fuel into 1 ml hexane.

Preparations of thermal stressed biodiesel samples for GC-MSE were very similar. Only that 10 μ l instead of 1 μ l of thermal stressed biodiesel samples were added into 1 ml hexane. The biodiesel concentration is 10,000 ppm by volume. Notice that the sample concentration here is 10 times higher than that used in GC-FID. This is because the GC-MSD took split-mode as inlet option. The detailed explanation has been stated in the previous text.

II. Prepare analytical standard samples

In order to construct calibration curves of biodiesel components, two kinds of analytical standards of 100 mg (ca.0.118 ml) mixture were prepared. The mixture of 1899-1AMP standard was in powder state shipped in dry ice, the dissolved liquid phase had a large viscosity. For the sake of loss and inaccurate calibration curve, solvent should be added into the analytical standard bottle. Taking into account of this factor, the samples were designed to be prepared in the following procedures.

- a) Added 3.8 ml hexane into the reagent bottle (ca.5 ml) containing the analytical standards mixture. Since the density of solid 1899-1 AMP analytical standards is 850 g/l. The total volume of 100 mg 1891-1 AMP is $V_{sd} = 100/850 = 0.1176$ ml. The volume fraction of the calibration standard solution is then equal to $V_{sd} / (3.8+V_{sd}) = 30,000$ ppm.
- b) Shake the bottle to make sure the solid powders of 1899-1AMP standard or liquid 1891-1AMP standards dissolve in hexane completely in room temperature.
- c) Took 16.67, 25, 33.33, 41.66, 50, 66.66 μ L of this standard solution and diluted each into 1ml of hexane respectively to make 500, 750, 1000, 1250, 1500, and 2000 ppm (by volume) solutions for GC analysis.
- d) In order to avoid the evaporation of volatile hexane, solutions were kept in the refrigerator whose temperature was below 0 °C.

3.4.4 Definition of biodiesel fuel thermal decomposition percentage

Palmitic acid methyl ester (C16:0) is present in fresh BD-100 biodiesel. This constituent has been proven to possess fairly higher stability compared to other FAMES (Imahara et al., 2008). By the same token, in this study, it was found that very little of C16:0 was decomposed at 360 °C

and below. To make good use of this, C16:0 was treated as an ideal internal standard in the data analysis portion. Because the relative content of a constituent can be calculated from the chromatogram of GC-FID, the change in content of palmitic acid methyl ester in biodiesel can therefore be employed to estimate the progress of thermal decomposition of biodiesel.

Thermal decomposition percentage of biodiesel can be calculated by

$$Dec\% \equiv \frac{\sum C_{i,fresh} - \sum C_{i,TS}}{\sum C_{i,fresh}} \times 100 \quad (3)$$

where the subscript i stands for a type of fatty acid such as C16:0, C18:0, C18:1-3, C20:0 and C22:0 which are the original components present in fresh biodiesel. $C_{i,fresh}$ is the FAME concentration of component i in fresh biodiesel fuel. The FAME concentration is derived from the calibration curve equation using the peak area manually integrated from GC/FID chromatogram. $C_{i,fresh}$ is showed in **Table 9** (Mass fractions of BD-100 biodiesel compositions*). In order to minimize experimental uncertainties due to sample preparation $C_{i,TS}$ was corrected by the factor of $C_{16:0,fresh}/C_{16:0,TS}$. However, C16:0 is not stable at 375 °C and above, as shown in this study; this correction was made only for samples thermally stressed at 250 °C to 360 °C.

Chapter IV

Results and discussion

4.1 Calibration curves of FAMES

A Chromatography separates analytes of a mixture, a detector such as FID measures the abundance of analytes and generates chromatogram in which strength of signals from the detector is plotted along y-axis while retention time were plotted along x-axis.

Good calibration curves were able to well delineate the linear relationship between the concentration of target analyte and instrument (computer) response. Once the curves have been created, other samples can be analyzed. Unknown volume concentrations of analytes in samples can be determined by making use of these relevant curves created by a series of known analytes.

In our experiments, calibration curves were conducted by comparing concentrations of FAMES to peak areas from chromatograms. Each peak in a chromatogram represents one of analytes in the mixture, and the peak areas are the detector responses for the analytes. The peak areas were manually integrated by GC-FID supporting software. **Fig. 7** shows the derived calibration curves for the analytes containing in experimental used biodiesel. Figure A-1 in Appendix A is the supplementary calibration curves for other FAME analytes.

In these calibration curves, the straight lines are the linear regression of experimental data points. They show the fact that the instrument response was a linear function of the concentration of each analyte. Linear calibration was characterized by its relatively constant slope, and a benefit of this was that it could simplify the calculations and data interpretation. The shape of these calibrations can be modeled by the following linear equation:

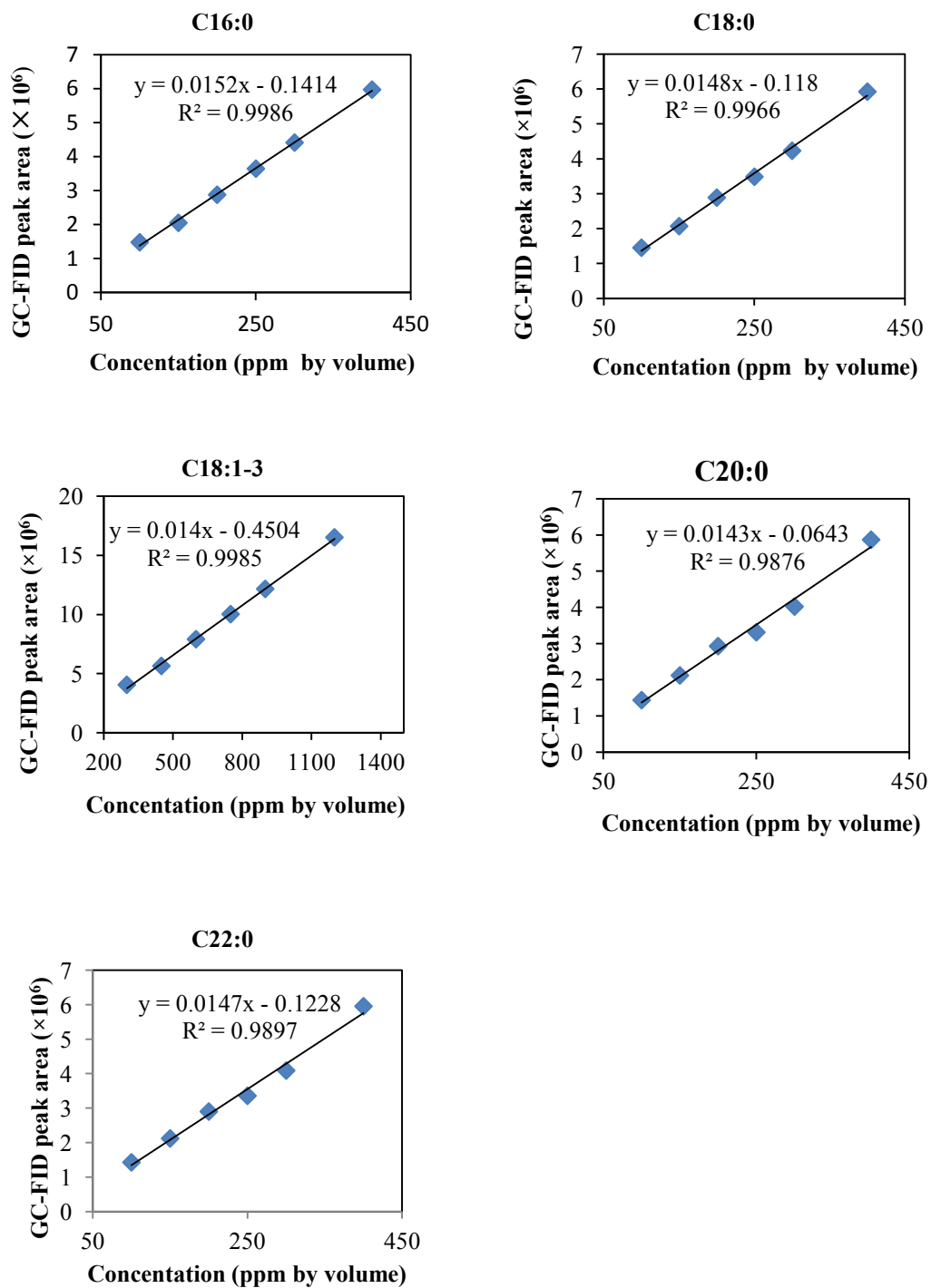


Fig. 7 GC-FID calibration curves for standard analytes of FAMEs (C16:0-C22:0 and C18:1-3).

$$A_i = a_i C_i + b_i \quad (4)$$

where A is the GC peak area (instrument response), C represents the concentration of the analyte, a and b are constants gained after fitting the experimental point data, and subscript i acts on behalf of the substance of individual FAME or FAME mixtures. R^2 is also showed to indicate the goodness-of-fit of linear regression. C18:1-3 represents that a mixture of C18:1, C18:2 and C18:3. The reason was that both columns of GC-FID and GC-MSD used in this research cannot isolate them. **Table 8** collected a, b and R^2 values for different FAME analyte. **Table A- 1** and **Table A- 2** in **Appendix A** recorded the GC-FID data for these analytical standards.

4.2 Compositions of fresh biodiesel

4.2.1 Identification of BD-100 biodiesel (Peter Cremer) compositions

By making comparisons of the GC/FID chromatograms of analytical standards GLC-10 FAME (1891-1AMP SUPELCO) mix, GLC-100 FAME (1899-1AMP SUPELCO) mix and fresh biodiesel, it was found that fresh biodiesel purchased from Peter Cremer not only contained methyl palmitate (C16:0-Me), methyl stearate (C18:0-Me), large amounts of methyl oleate (C18:1-Me), methyl linoleate (C18:2-Me) and methyl linolenate (C18:3-Me), but also had very small quantities of methyl arachidate (C20:0-Me) and methyl behenate (C22:0-Me) as well. The chromatograms were revealed in **Fig. 8**.

According to **Table 1**, calibration standard GLC-10 FAME mix has five analytes: C16:0, C18:0, C18:1, C18:2 and C18:3. However, the chromatogram of it showed only three peaks, as shown in **Fig. 8 (C)**. Further, it was found that peak 2 had much larger integrated peak areas than that of peak 1 or peak 3. This indicates that peak 2 contains signals of more than one analyte. In addition, integrated area of peak 2 in the chromatogram of the mixture of GLC-10 and GLC-100

Table 8 Constants and coefficient of determination (R^2) for FAMES calibration curves

FAME	a	b	R^2
C16:0	0.0152	-0.1414	0.9986
C18:0	0.0148	-0.118	0.9966
C18:1-3	0.0140	-0.4504	0.9985
C20:0	0.0143	-0.0643	0.9876
C22:0	0.0147	-0.1228	0.9897

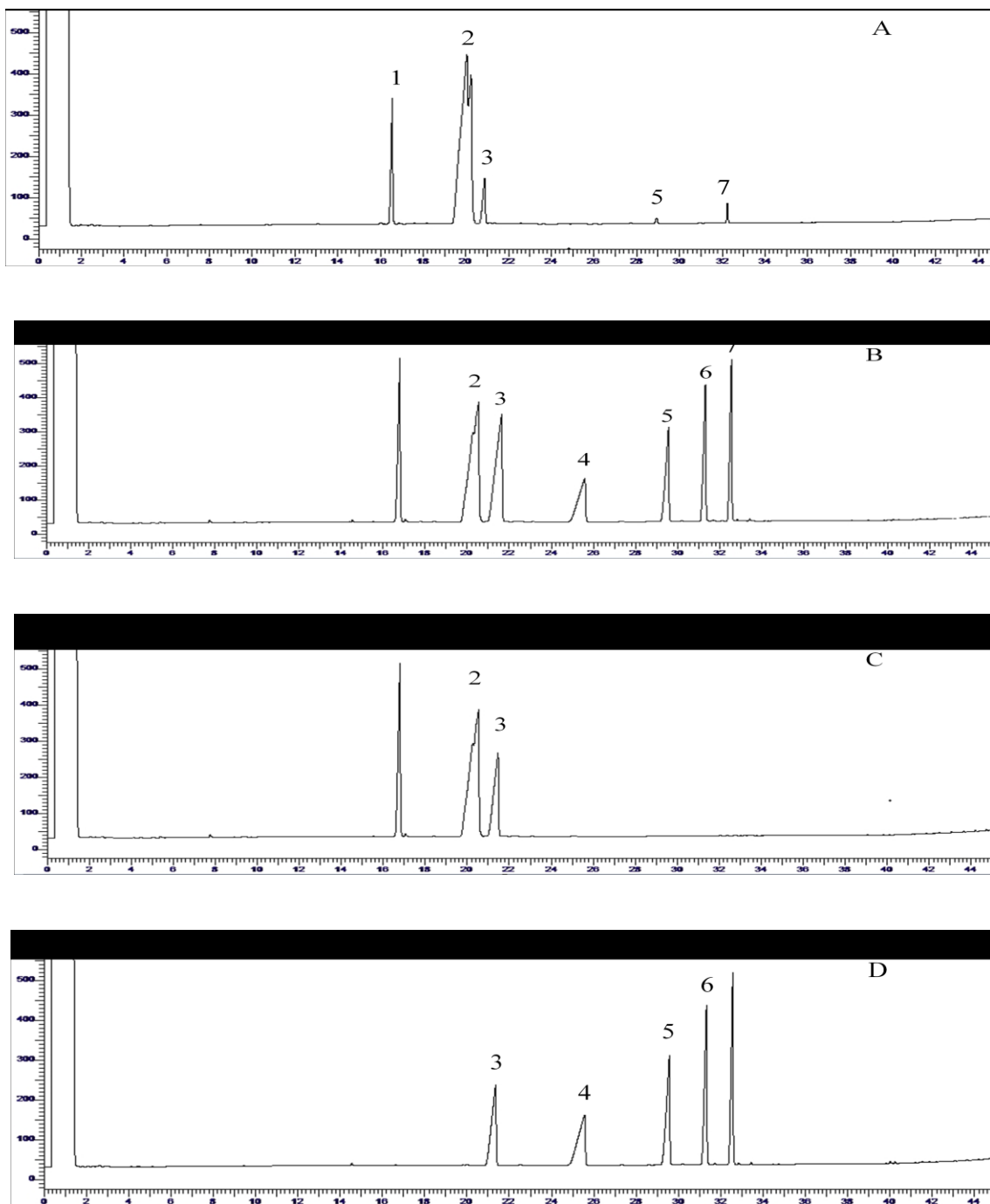


Fig. 8 GC/FID chromatograms for fresh biodiesel (A), GLC-10 and GLC-100 mixture (B), GLC-10 FAME mix (C), GLC-100 FAME mix (D). Labeled peaks are C16:0 (1), C18:1-3 (2), C18:0 (3), C19:4 (4), C20:0 (5), C21:0 (6), C22:0 (7).

had almost the same value as that in the chromatogram of GCL-10. This fact indicates that the peak 2 represents the concentration of C18:1, C18:2 and C18:3 combined.

4.2.2 Mass fraction of BD-100 biodiesel fuel compositions

By analysis of peaks areas of the compositions existing in BD-100 biodiesel fuels and combined with the constructed calibration curves, mass fractions were calculated and indicated in **Table 9**. They were determined using the equation:

$$W_i = C_j / \sum_{j=1}^n C_j \times 100 \quad (5)$$

where W_i is the mass fraction (wt%) of the FAME i . The FAME concentrations adjusted in **Table 9** will be treated as the initial FAME concentration values for the later biodiesel degradation calculations. From **Table 9**, we can know that the mass fraction of unsaturated FAMES (80.9%) far outweighs than that of saturated FAMES (19.1%).

4.3 Thermal stability of biodiesel fuel

4.3.1 Visual observation of thermal decomposition of biodiesel fuel

It is well known in the diesel industry that diesel fuel generally darkens in colors as it degrades. This phenomenon was also observed in our thermal stressing experiments. The undegraded biodiesel sample is colorless or in very light amber brown color while the post-degradation samples showed darkened color at high temperatures.

Thermal stressing experiments of BD-100 biodiesel were performed at 250 to 425 °C for a residence time from 3 to 63 minutes (**Table 5**). The Photos of collected samples are arranged in

Table 9 Mass fractions of BD-100 biodiesel compositions*

FAME		C16:0	C18:1-3	C18:0	C20:0	C22:0	Total
Peak Area ($\times 10^6$)	Average	1.603	11.849	0.847	0.073	0.151	14.524
	Std Dev	0.082	0.581	0.050	0.013	0.010	0.718
Concentration (ppm by volume)	Average	114.8	878.5	65.2	9.6	18.6	1086.8
	Std Dev	5.4	41.5	3.4	0.9	0.7	50.7
Mass concentration (wt %)	Average	10.6	80.8	6.0	0.9	1.7	100
	Std Dev	0.06	0.06	0.15	0.08	0.05	n/a

* The average and standard deviation were obtained from five replicates (See **Table 11** and **Table 12**).

Fig. 9 (a), Fig. 9 (b) and Fig. 9 (c).

In the process of collecting heat treated biodiesel samples, there were two primary phenomena as below:

a) Observed color changed responsible for thermal degradation of biodiesel fuel

From the photographs, it is clear that there was no pronounced variation of color at temperatures up to 350 °C. The color retained colorless as fresh biodiesel at 250 °C and a little bit changed to light yellow when the temperature increased. Once the temperature reached 360 °C for a residence time of 8 minutes and longer, obvious color change was observed from colorless to yellowish. At this temperature, what deserves special mention is that the color of 8 minutes sample was more pigmented than 18 minutes one. One possible explanation is that the reactor touched the heating elements of the sand bath leading to a higher thermal stressing temperature.

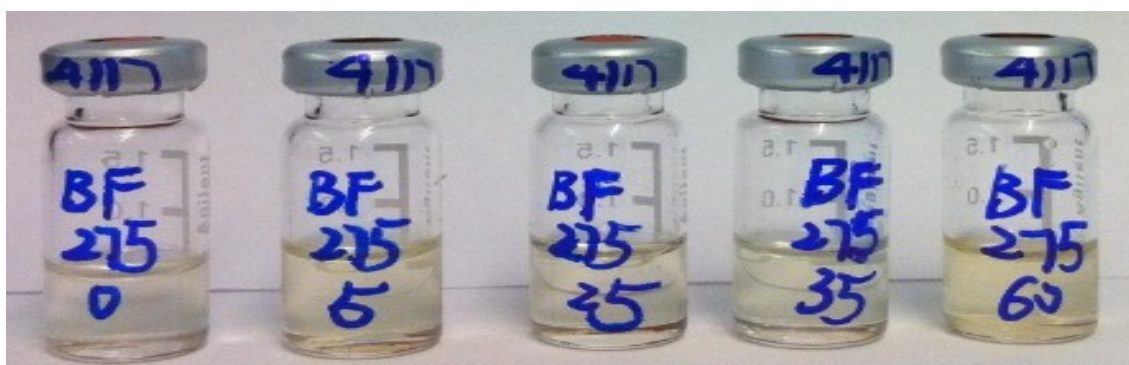
With a further increase in thermal stressing temperature, the color change of biodiesel was more significant. It became dark yellow at 400 °C after 3 minutes, and turned to brown at 425°C and 23 minutes. Color change is a good apparent indicator of fuel degradation. From these contrasting photographs in **Fig. 9**, whether samples decomposed or not can be distinguished.

b) Visual detection of gas products

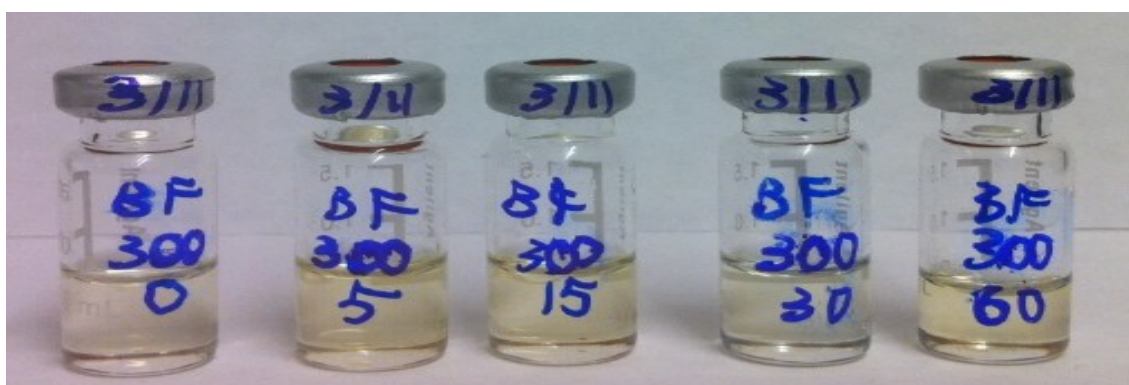
According with color changes, gases were produced during the following thermal stressing conditions: 360 °C for 33 minutes or above, 375 °C for 8 minutes or above, 400 °C and 425 °C for all residence times. Gas products were detected visually by observing the small bubbles displayed in the biodiesel when fuel samples were taken out from the sealed reactor. It was found



(i). Temperature: 250°C; Times: 3, 8, 18, 33 and 63 minutes (from left to right)



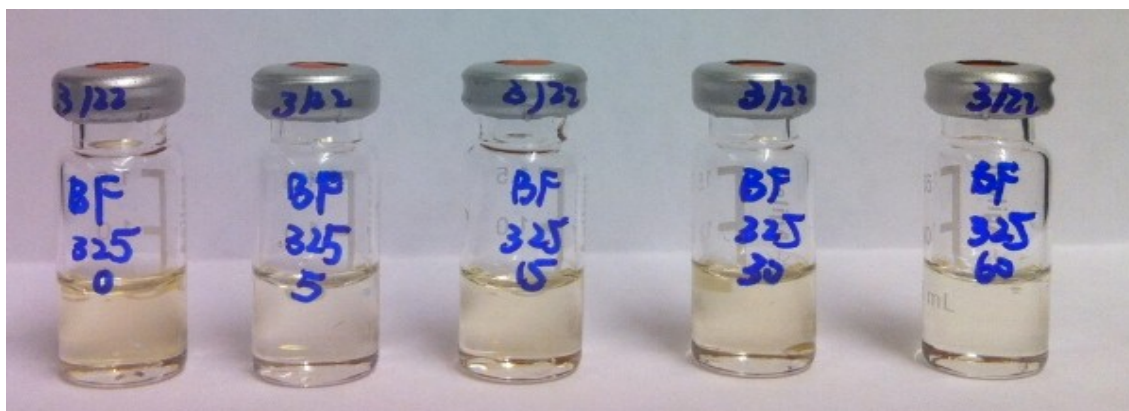
(ii). Temperature: 275°C; Times: 3, 8, 28, 38 and 63 minutes (from left to right)



(iii). Temperature: 300°C; Times: 3, 8, 18, 33 and 63 minutes (from left to right)

Fig. 9 (a) Photographs of biodiesel samples collected after different heat treatment.

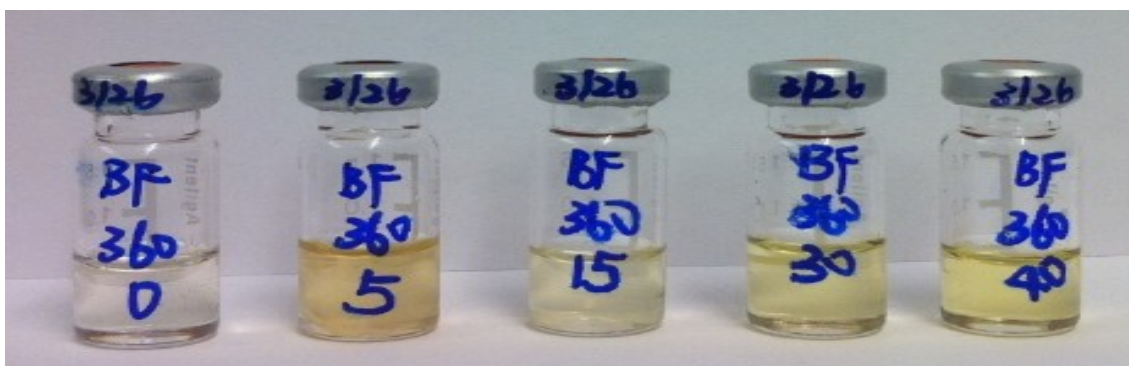
Numbers below samples indicate the thermal stressing temperature and time. Note that the thermal stressing time also includes the 3 minute heat up time. The time value on the bottles does not include the heat up time.



(i). Temperature: 325°C; Times: 3, 8, 18, 33 and 63 minutes (from left to right)



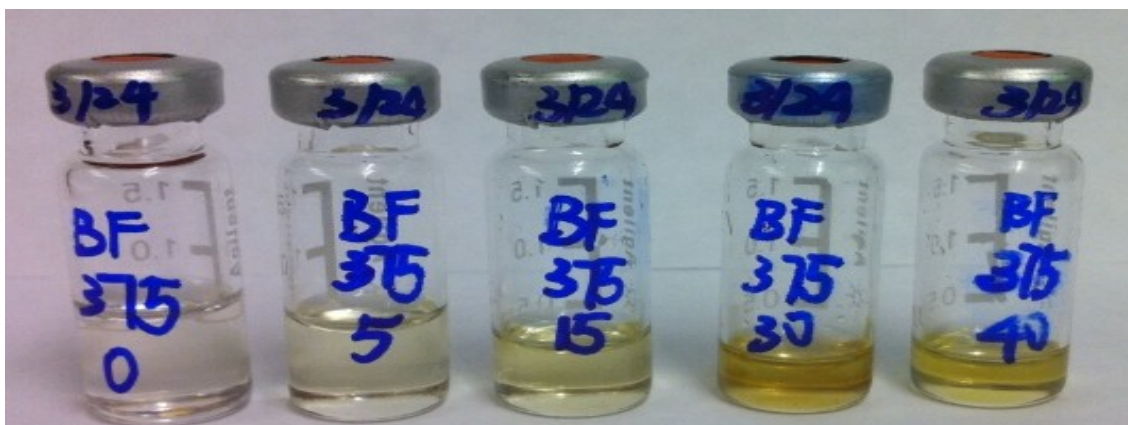
(ii). Temperature: 350°C; Times: 3, 8, 18 and 33 minutes (from left to right)



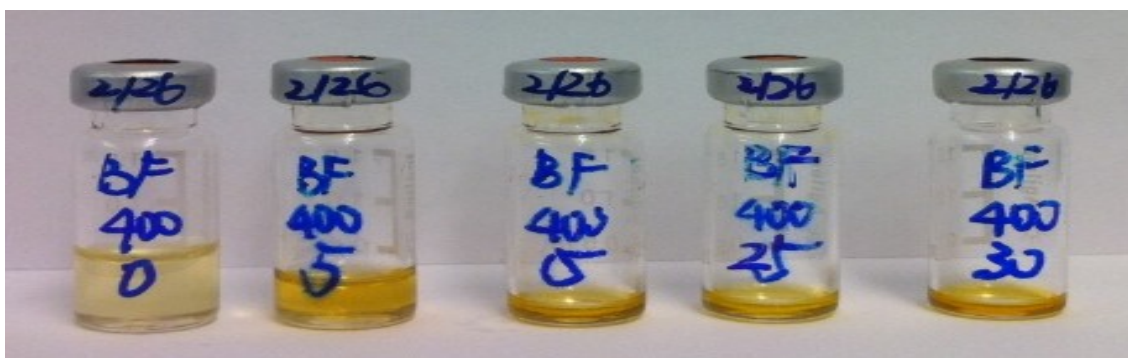
(iii). Temperature: 360°C; Times: 3, 8, 18, 33 and 43 minutes (from left to right)

Fig. 9 (b) Photographs of biodiesel samples collected after different heat treatment.

Numbers below samples indicate the thermal stressing temperature and time. Note that the thermal stressing time also includes the 3 minute heat up time. The time value on the bottles does not include the heat up time.



(i). Temperature: 375°C; Times: 3, 8, 18, 33 and 43 minutes (from left to right)



(ii). Temperature: 400°C; Times: 3, 8, 18, 28 and 33 minutes (from left to right)



(iii). Temperature: 425°C; Times: 3, 8, 13, 18 and 23 minutes (from left to right)

Fig. 9 (C) Photographs of biodiesel samples collected after different heat treatment.

Numbers below samples indicate the thermal stressing temperature and time. Note that the thermal stressing time also includes the 3 minute heat up time. The time value on the bottles does not include the heat up time.

that the amount of gas products increased with increasing temperature.

Gas products not only directly resulted in the undesirable weight loss of the liquid biodiesel fuel, but also increased the difficulty of collecting samples from the coils, which explained less amounts of biodiesel collected under these particular conditions, as displayed in **Fig. 9 (b) and Fig. 9 (c)**.

From the visual observation of thermal treated biodiesel samples summed up in **Table 10**, it can be perceived overtly that higher temperature and longer residence resulted in greater degradation. The visual observation suggests that biodiesel is quite stable at temperatures up to 350 °C. It also suggests that thermal stability generally reduced under these more severe situations. The respective influence of these two determinant factors in relation to the thermal stability quality of biodiesel will be discussed more in detailed as below.

4.3.2 Gas-chromatographic observation of thermal behaviors of biodiesel

For the goal of qualitative and quantitative analysis, collected biodiesel samples were analyzed chromatographically. The GC/FID chromatograms are presented in **Fig. 10** to **Fig. 18**. Another GC/MS chromatogram is showed in **Fig. 19**. After analysis of these chromatograms, three major types of reactions, isomerization, polymerization and pyrolysis reaction respectively, were detected.

I. Isomerization reactions of FAMES

As shown in **Fig. 10**, biodiesel remained stable by exposure to 250 °C even for 63 minutes. When temperature was elevated to 275 °C for 28 minutes, biodiesel began to lose stability. New peaks were observed at that point or longer, as demonstrated by red arrows in **Fig. 11**. With the

Table 10 Observations of thermal stressed biodiesel samples

Run#	Temperature, °C	Residence time, min	Color	Gas product
1	250	3	colorless	No
2	250	8	colorless	No
3	250	18	colorless	No
4	250	33	colorless	No
5	250	63	colorless	No
6	275	3	colorless	No
7	275	8	colorless	No
8	275	28	Light yellow	No
9	275	38	Light yellow	No
10	275	63	Light yellow	No
11	300	3	colorless	No
12	300	8	Light yellow	No
13	300	18	Light yellow	No
14	300	33	Light yellow	No

15	300	63	Light yellow	No
16	325	3	colorless	No
17	325	8	Light yellow	No
18	325	18	Light yellow	No
19	325	33	Light yellow	No
20	325	63	Light yellow	No
21	350	3	Colorless	No
22	350	8	Light yellow	No
23	350	18	Light yellow	No
24	350	33	Light yellow	No
25	360	3	Colorless	No
26	360	8	Yellow	No
27	360	18	Yellow	No
28	360	33	Yellow	Yes, little
29	360	43	Yellow	Yes, little
30	375	3	Colorless	No
31	375	8	Yellow	Yes, little

32	375	18	Yellow	Yes, little
33	375	33	Yellow	Yes, large
34	375	43	Yellow	Yes, large
35	400	3	Yellow	Yes, little
36	400	8	Dark yellow	Yes, large
37	400	18	Dark yellow	Yes, large
38	400	28	Dark yellow	Yes, large
39	400	33	Dark yellow	Yes, large
40	425	3	Yellow	Yes, large
41	425	8	Dark yellow	Yes, large
42	425	13	Dark yellow	Yes, large
43	425	18	Dark yellow	Yes, large
44	425	23	Brown	Yes, large

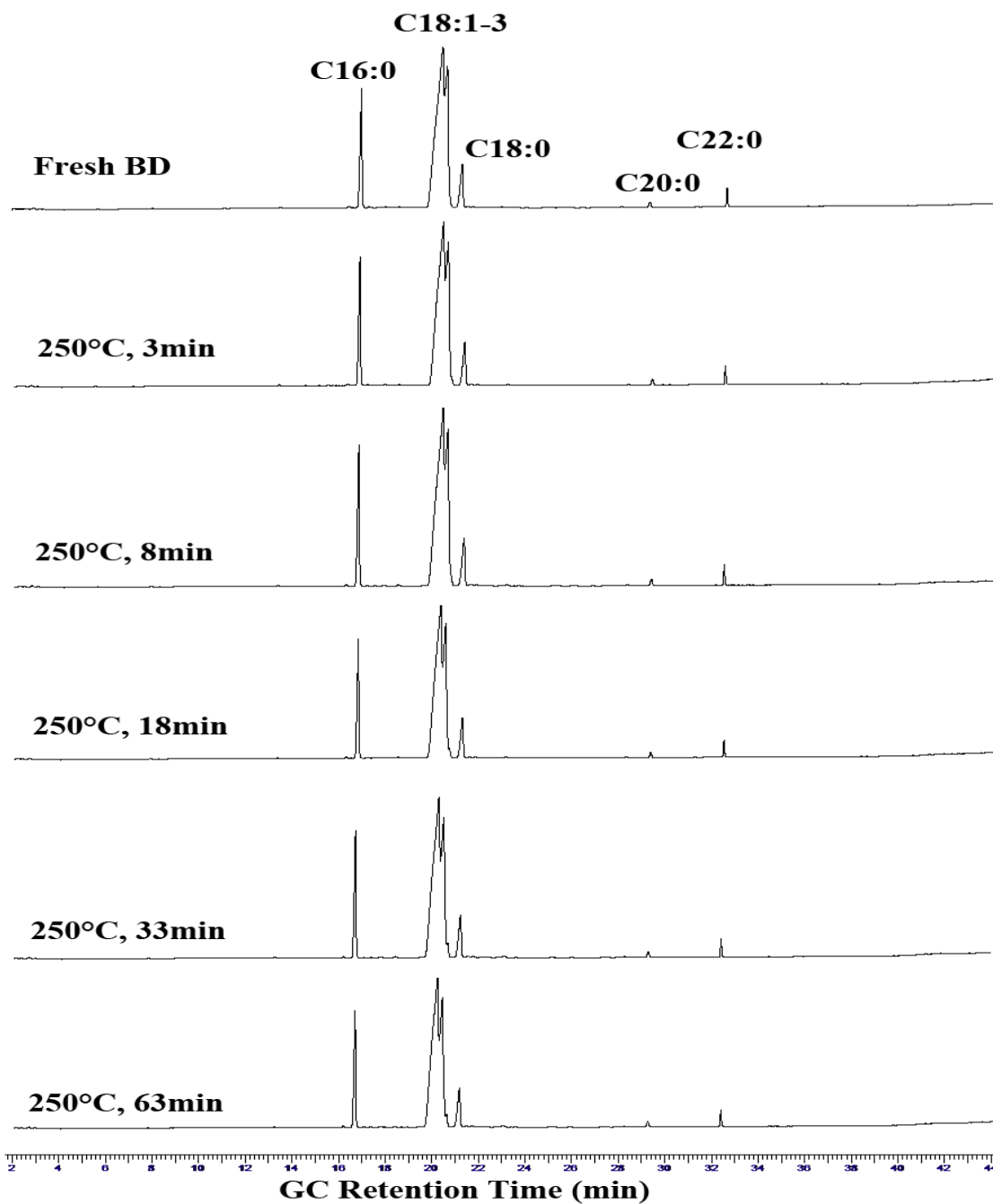


Fig. 10 GC/FID chromatograms of biodiesel fuel subjected to heat treatment at 250 °C.

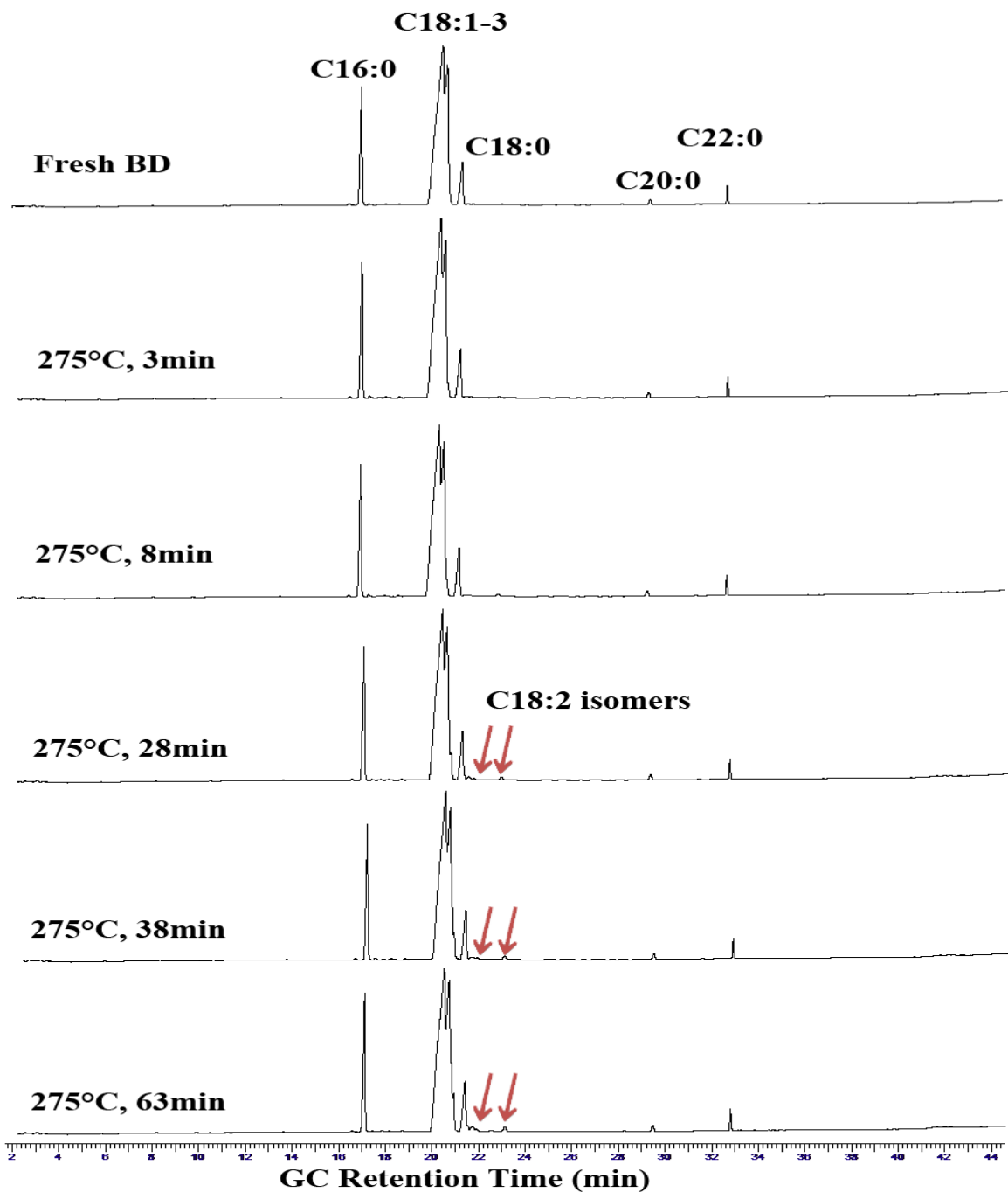


Fig. 11 GC/FID chromatograms of biodiesel fuel subjected to heat treatment at 275 °C. The red arrows indicate the formation of trans-type C18:2 isomers.

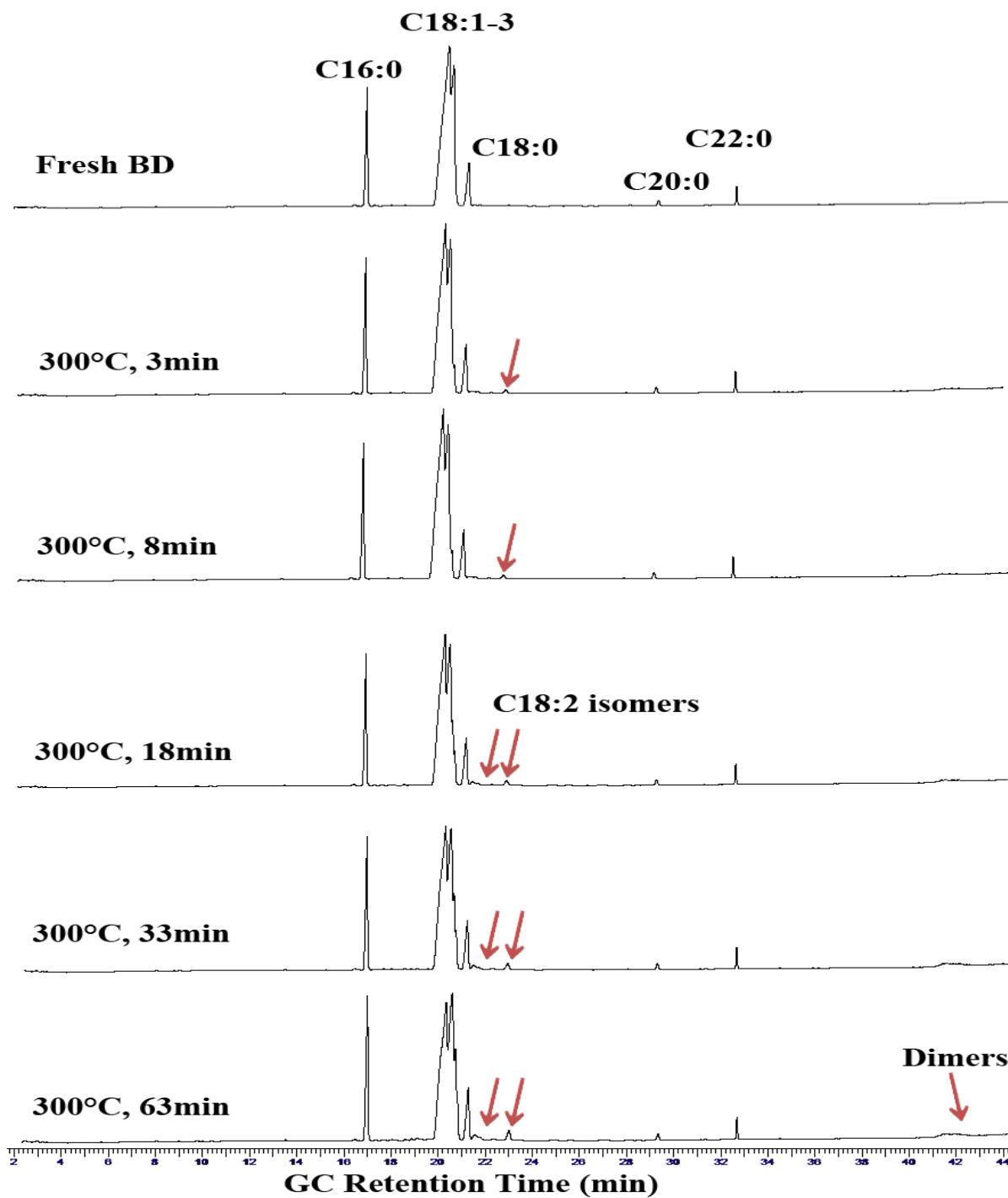


Fig. 12 GC/FID chromatograms of biodiesel fuel subjected to heat treatment at 300 °C. The red arrows indicate the formation of trans-type C18:2 isomers and dimers.

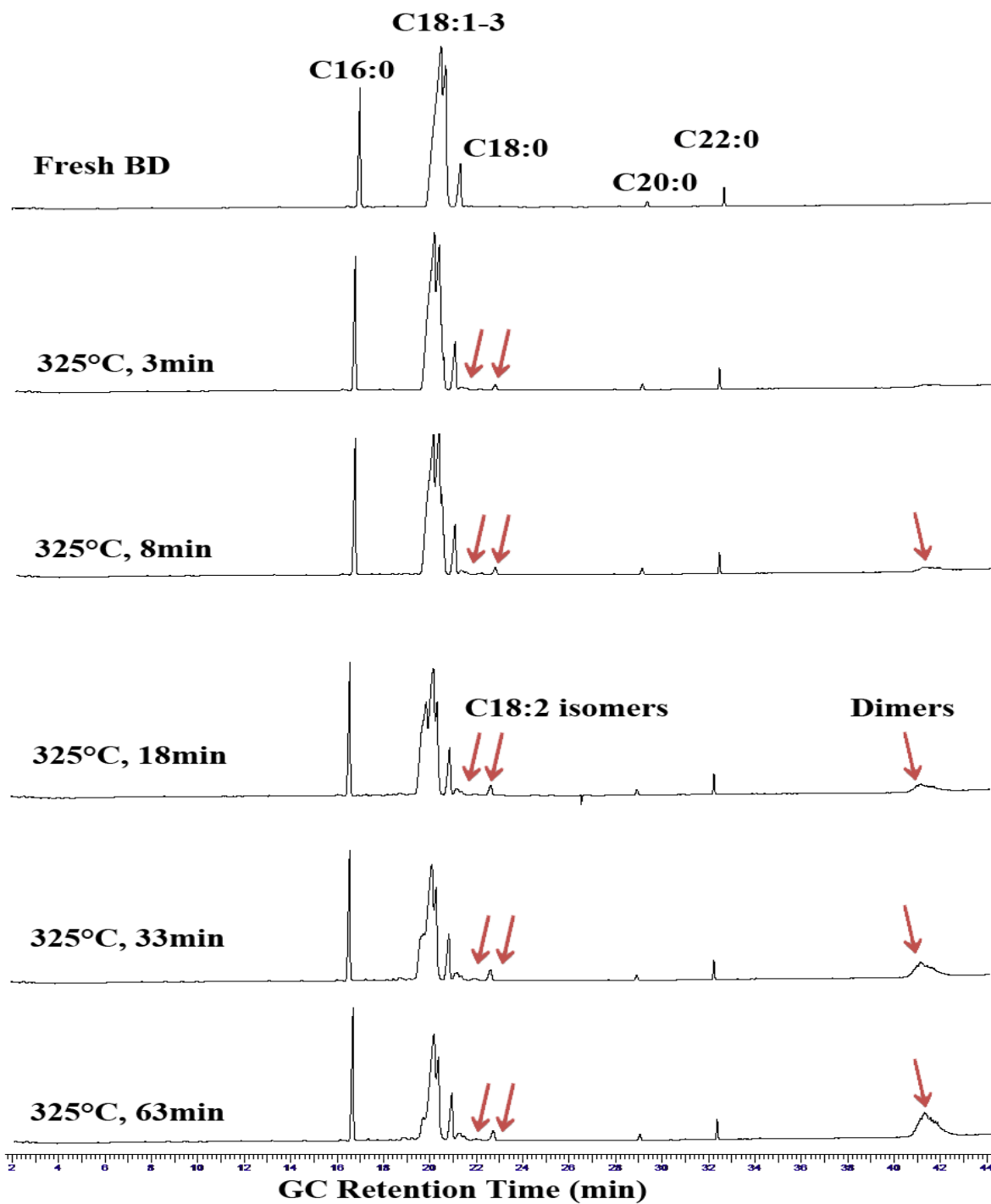


Fig. 13 GC/FID chromatograms of biodiesel fuel subjected to heat treatment at 325 °C. The red arrows indicate the formation of trans-type C18:2 isomers and dimers.

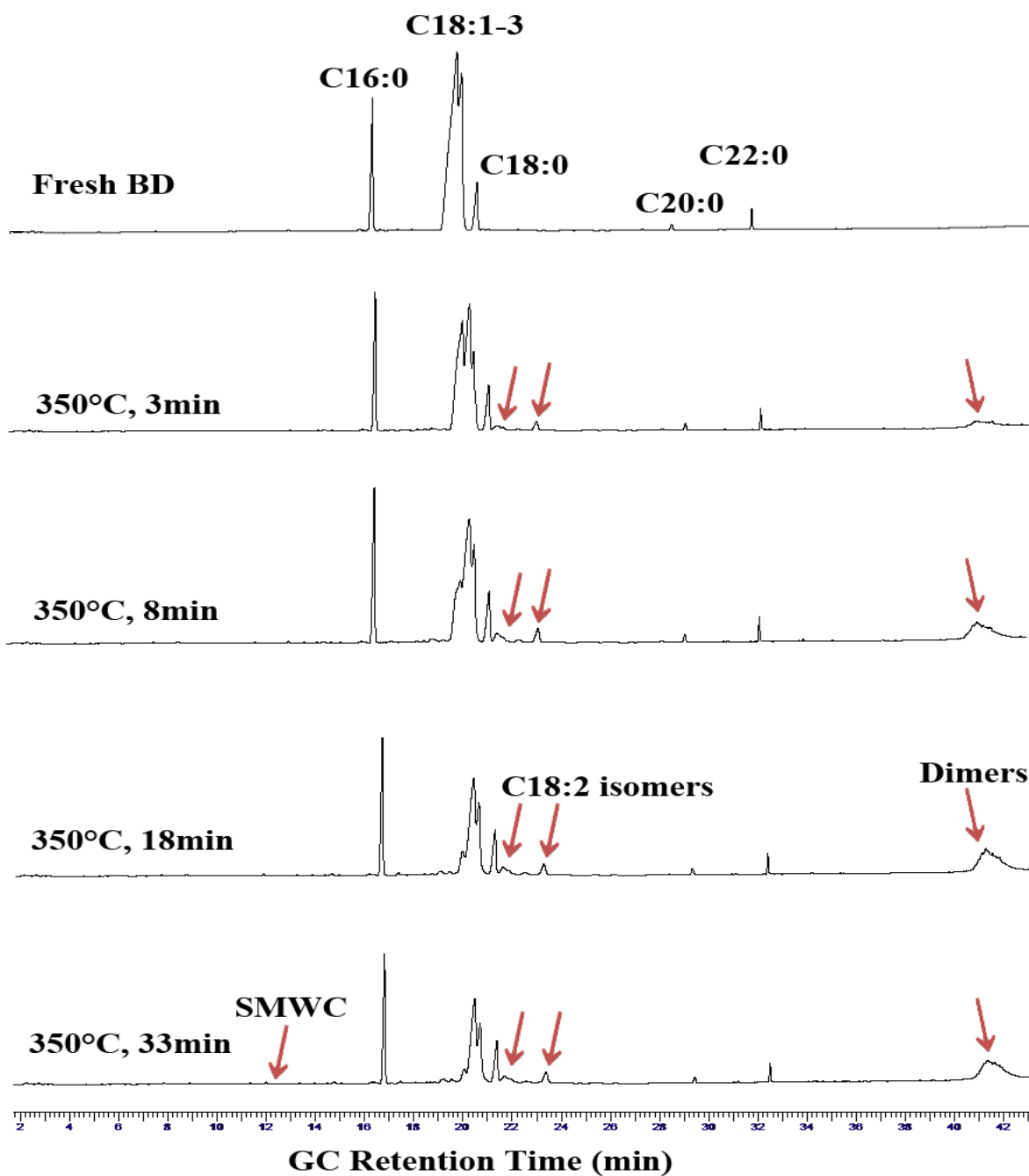


Fig. 14 GC/FID chromatograms of biodiesel fuel subjected to heat treatment at 350 °C. The red arrows indicate the formation of smaller molecular weight compounds, trans-type C18:2 isomers and dimers.

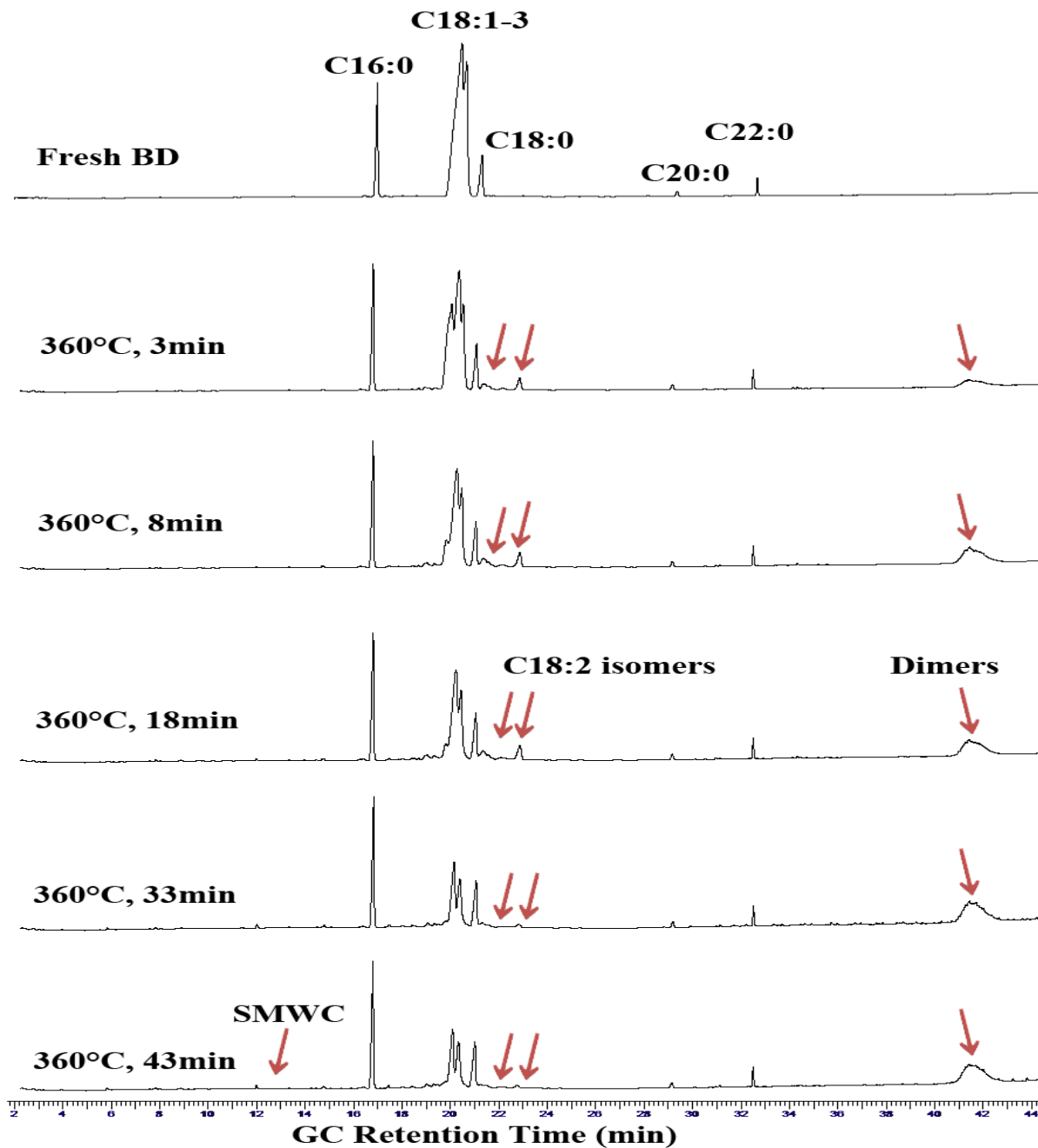


Fig. 15 GC/FID chromatograms of biodiesel fuel subjected to heat treatment at 360 °C. The red arrows indicate the formation of smaller molecular weight compounds, trans-type C18:2 isomers and dimers.

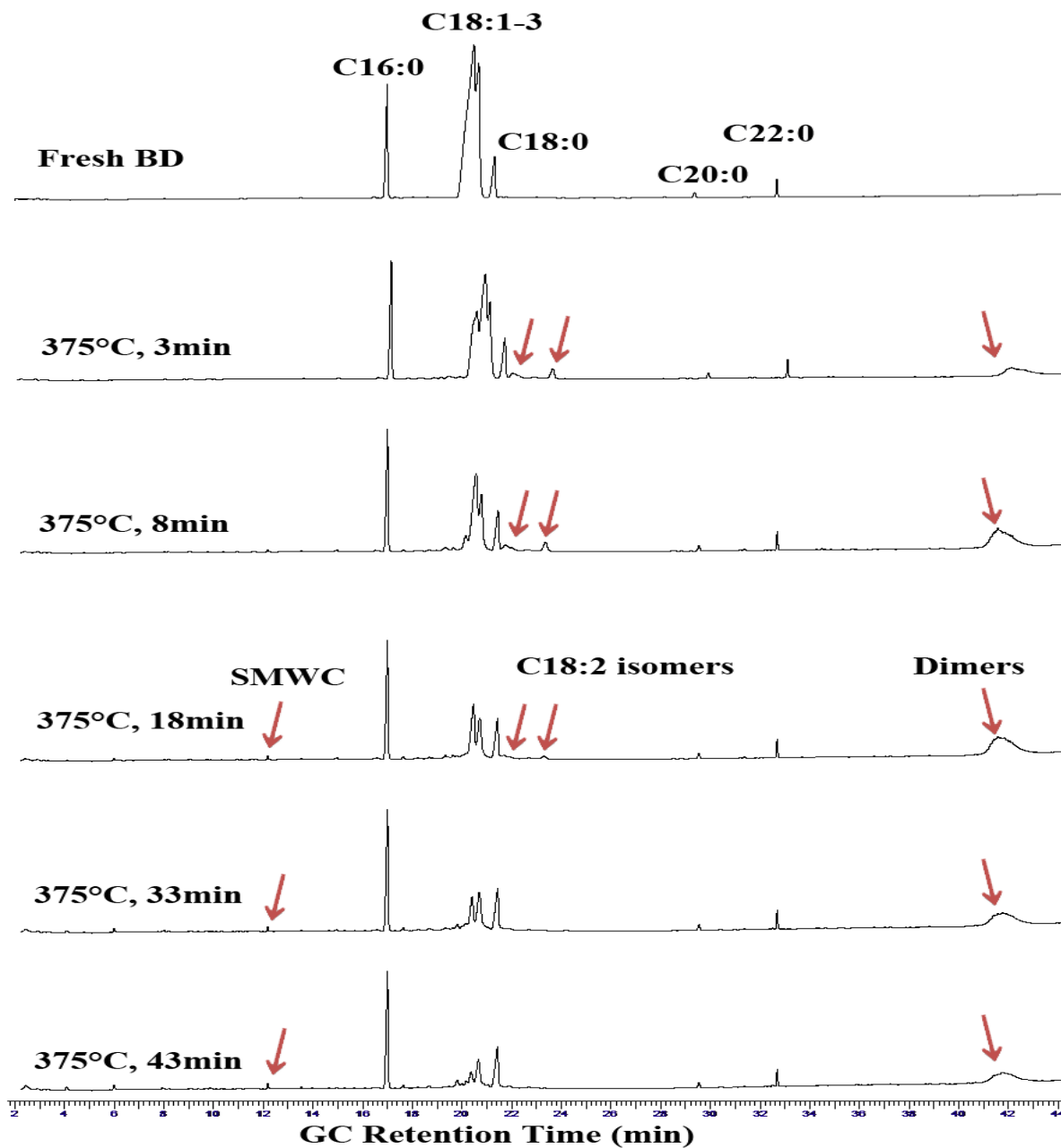


Fig. 16 GC/FID chromatograms of biodiesel fuel subjected to heat treatment at 375 °C. The red arrows indicate the formation of small molecular weight compounds, trans-type C18:2 isomers and dimers.

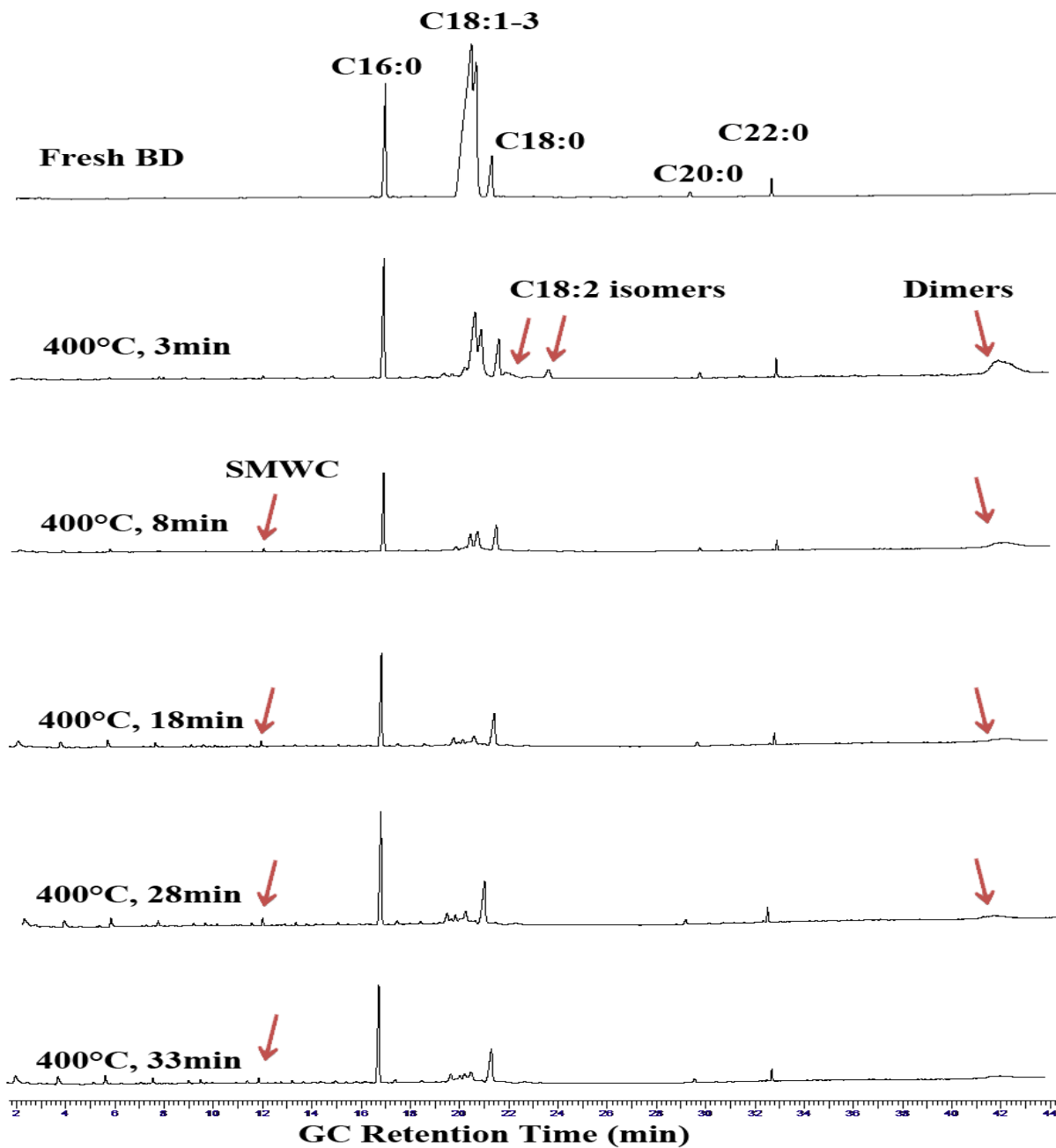


Fig. 17 GC/FID chromatograms of biodiesel fuel subjected to heat treatment at 400 °C, indicating the dynamic behavior of biodiesel decomposition and the formation of smaller molecular weight FAMES and hydrocarbons.

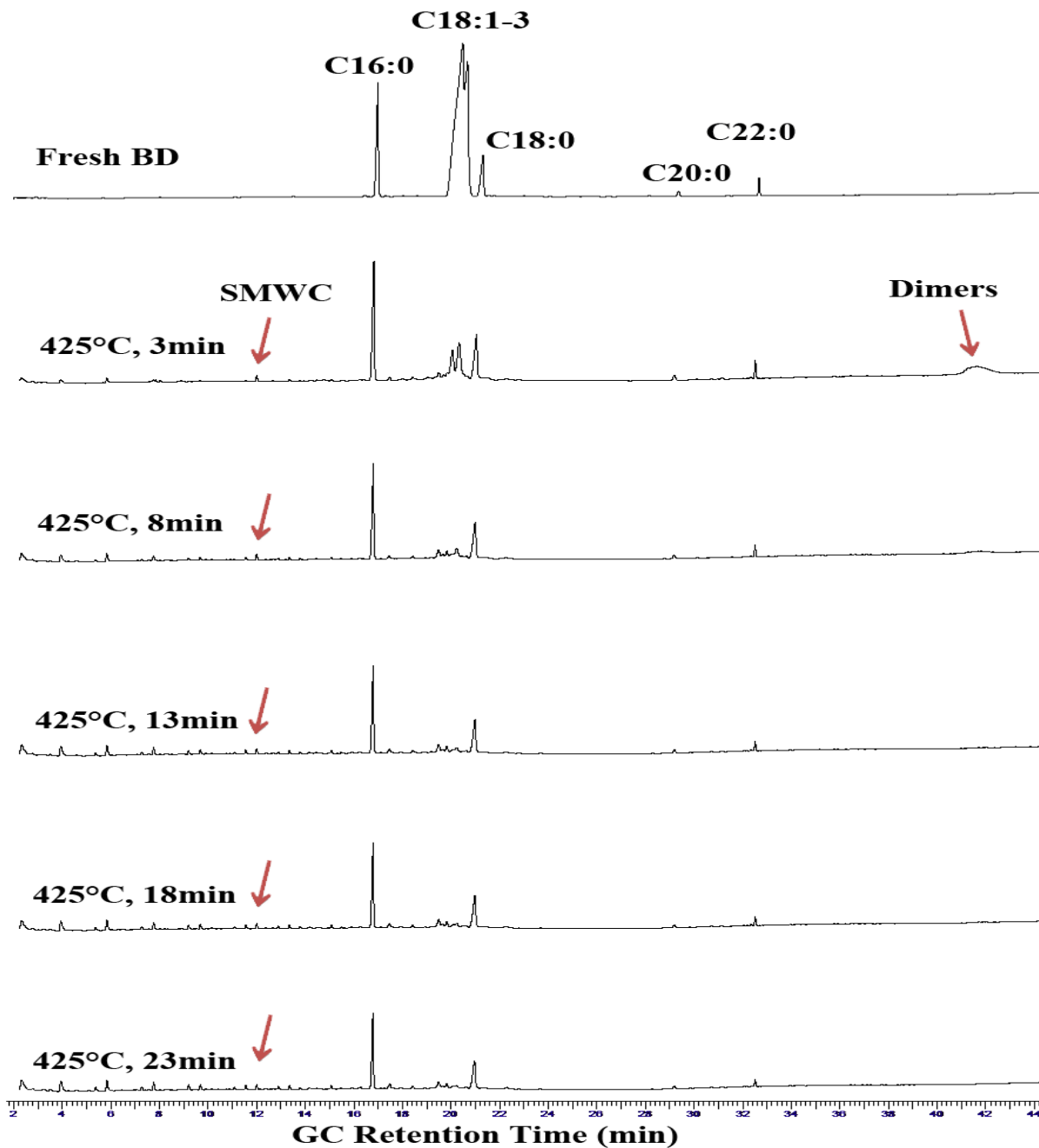


Fig. 18 GC/FID chromatograms of biodiesel fuel subjected to heat treatment at 425 °C, demonstrating the formation of significant amounts of smaller molecular weight FAMES and hydrocarbons owing to pyrolysis of FAMES.

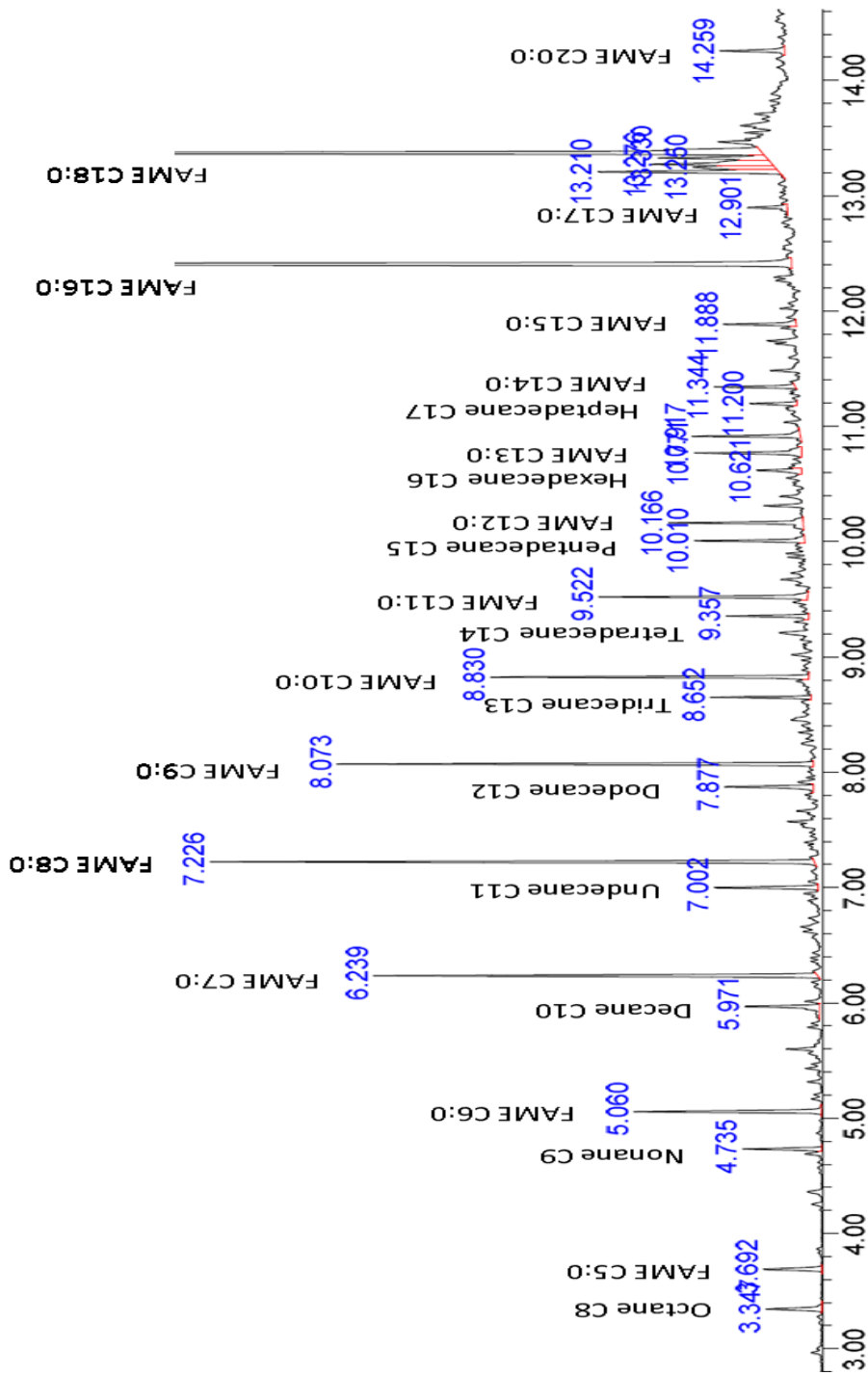


Fig. 19 GC/MS chromatogram of biodiesel fuel subjected to heat treatment at 425 °C for 23 min, demonstrating the distribution of decomposition productions. FAMEs C16:0, C18:0 and C20:0 are present in the fresh biodiesel.

help of GC-MS analysis, these emerging peaks were identified to be trans-type C18:2 isomers: either 9-cis, 11-trans C18:2 or 10-trans, 12-cis or both. They were formed via the cis-trans isomerization reaction, which meant that some portion of naturally existing cis-type C=C converted to trans-type C=C. Likewise, a previous publication declared that trans-isomerization of unsaturated FAMES happens as low as 270 °C (Imahara et al., 2008).

At 275 °C (**Fig. 11**) and 300 °C (**Fig. 12**), the aforementioned emerging isomerization peaks grew larger and larger as the residence time was increased. However, it was not the case at 325 °C (**Fig. 13**) and 350 °C (**Fig. 14**), at which temperature those two peaks kept enlarging initially as residence time increased up to 18 minutes and then maintained almost constant during the period from 18 minutes to 63 minutes. This phenomenon well demonstrates that the isomerization reactions reached equilibrium after certain amount of time and further suggests that the isomerization reactions are reversible.

Further, when the temperature increased to 360 °C (**Fig. 15**), 375 °C (**Fig. 16**), and 400 °C (**Fig. 17**), as the residence time increased, the two peaks areas reached maximum values first and then shrunk. In addition, higher thermal stressing temperature requires shorter residence time to reach the maximum areas. The reason for the peaks areas shrinking was that, although trans-isomers were stable than cis-isomers, they would also be consumed to form other compounds.

At 425 °C, no peaks of C18:2 isomers were observed in chromatograms. That the generated isomers were significantly decomposed to form small molecular weight would explain this case.

II. Polymerization reaction of FAMES

Accompanying with isomerization reactions, polymerization reactions took place.

Except for those two peaks, another peak with a bump shape first appeared at 300 °C for 63 minutes (**Fig. 12**). At 325 °C (**Fig. 13**), this peak became much more distinctive as time went on from 8 minutes to 63 minutes. Moreover, along with the stretching of this peak, the main original peaks of C18:1-3 contracted. Furthermore, the GC/FID retention time of this peak was almost twice as long as that of the C18:1-3 which implied that this compound had twice as much molecular weight as that of C18:1-3. Though identification of this compound was restricted to the analytical instrument used in this study, the compound was believed to be dimers due to the well-known Diels-Alder reaction of C18:1 and C 18:2 (Jain & Sharma, 2011; Nicolaou, Snyder, Montagnon, & Vassilikogiannakis, 2002), as mentioned in Eq. (1) in part “**2.5 Mechanism of thermal decomposition of biodiesel fuel**”. In this reaction, a conjugated diene group of one fatty acid chain formed from the isomerization reaction and a mono-olefin of another fatty acid chain generates a cyclohexene ring. The products are named dimers in which R₁, R₂, R₃ is and R₄ are functional groups.

At 350 °C and 360 °C (**Fig. 14** and **Fig. 15**), the polymerization composite peak continued to expand in the early stage and then remained nearly unchanged, this suggests that this Diels Alder reaction is also an equilibrium reaction.

At the temperature of 375 °C or higher, shown in **Fig. 16** to **Fig. 18**, the dimer peaks kept on enlarging firstly to a maximum value and shrinking afterward with the increasing of the residence time. Also, it required a shorter time for the peak to grow to the maximum value at higher temperature.

III. Pyrolysis reactions of FAMES

At sufficiently high temperatures, a series of pyrolysis (or thermal cracking) reactions were

observed. According to previous report, pyrolysis reactions were stated to start at around 370 °C and prominent pyrolysis proceeds at temperature above 400 °C (Luo et al., 2010). When thermal stressing temperature was raised to 350 °C for 33 minutes, a few small peaks appeared, one was indicated by the red arrow in **Fig. 14**. This phenomenon was relatively more evident at 375 °C (**Fig. 15**). According to their short retention time displayed in the GC/FID chromatograms, they were believed to be small molecular weight substances of these peaks. The reason for the occurrence of pyrolysis reactions was that FAMEs, dimers and polymers produced via the Diels-Alder reaction were very reactive at high temperatures, they ultimately formed lower molecular weight FAMEs, hydrocarbons and gas products.

In comparison to the small number of peaks showed at 350 °C and 375 °C, a large number of peaks emerged at 400 °C for 18 minutes, 425 °C for 8 minutes and above, even though there was a limited number of peaks at 400 °C for 8 minutes, 425 °C for 3 minutes and above. It was important to note that, the flood of peaks of GC retention time less than 16 minutes came with the fading of isomer and dimer peaks and the withdrawal of the C18:1-3 peaks. This trend showed a significance of decomposition of biodiesel fuel due to the pyrolysis reactions.

Fig. 19 is the GC-MS chromatogram of the biodiesel thermal stress at 425 °C for 23 minutes, revealing that the created pyrolysis products are mainly C5:0 to C18:0 FAMEs and C8 to C17 n-alkanes. This result is similar to the discoveries about formed small-molecular-weight products reported previously (Marulanda, Anitescu, & Tavlarides, 2010a; Seames et al., 2010; Shin et al., 2011).

Besides finding the diverse pathways of biodiesel decomposition, it can also be inferred from the chromatograms that unsaturated FAMEs were much more unstable than saturated

FAMES. The unsaturated C18:1-3, as the main components of BD-100 biodiesel, their peak height began to reduce gradually as the residence time increased once thermal treated at 300°C, which was shown in **Fig. 12**. This is consistent with the start-to-decompose temperature reported before (He et al., 2007; Imahara et al., 2008; Quesada-Medina & Olivares-Carrillo, 2011). The trend became more critical when temperature was further increased. When the temperature was elevated to 400 °C and the residence time was raised to 18 minutes or above, it was conspicuous that the C18:1-3 almost decomposed completely. The same situation happened at 425 °C for 8 minutes and above.

However, after a careful examination of the saturated FAMES peak areas, it was found that C16:0 only started decomposing at 375 °C and beyond, which is consistent with the conclusion proposed by Imahara et al. (Imahara et al., 2008) and results reported by Shin et al. (Shin et al., 2011). C20:0 and C22:0 were also observed to decompose at 375 °C and above in this research. It is a much higher decomposition temperature compared to that of C18:1-3. Not only is the decomposition temperature differential apparent, but also the extent of decomposition differs significantly under the same thermal stressing conditions between saturated and unsaturated FAMES. While the peaks of C18:1-3 nearly vanished, a small portion of the peak of saturated FAMES decomposed at 400 °C and beyond.

Relying on these, it should be emphasized that saturated FAMES have better thermal stability than unsaturated ones.

4.3.3 Effect of temperature on thermal stability of biodiesel

On the basis of the above discussion, results showed that temperature strongly affects the thermal stability of biodiesel.

This research demonstrated that biodiesel remained stable up to 275 °C despite the formation of new peaks. The main FAMES underwent a negligible change at this temperature and the trans-isomerization minimally occurred. This conclusion generally agrees with a former statement that all these FAMES were stable at 270 °C or below (Imahara et al., 2008).

Within the temperature range of 275 °C to 400 °C, the cis-trans isomerization reaction took place. In addition, the formed trans-type isomers were unstable at 360°C and higher. They would further decompose into small molecular weight products.

Another major reaction that occurred in biodiesel degradation was Diels-Alder reaction which took place at a temperature range of 300 °C to 425 °C, concurrently, the dimers decomposed at 375 °C and even higher temperatures.

It can also be concluded that biodiesel slightly decomposed at 300 °C which can be seen as the start-to-decompose temperature. Higher temperature leads to greater decomposition, especially for unsaturated FAMES of C18:1-3. Biodiesel is totally unstable at 400 °C and above.

Adequately high temperature also promotes the occurrence of pyrolysis reaction of biodiesel, not only FAMES, but also formed dimers and polymers. This study proved that pyrolysis started at 350 °C or above. When the temperature reaches 400 °C or above, a significant pyrolysis reaction will progress. Additionally, this research indicated that bad smell gas products were produced after exposure to 360 °C or above. It was unambiguous that biodiesel is much more reactive and has less thermal stability at higher temperature when keeping all other conditions the same.

All in all, temperature places an extraordinary important role in affecting thermal stability of biodiesel fuel.

4.3.4 Effect of thermal stressing time on thermal stability of biodiesel

Based on analyzing chromatograms **Fig. 10** to **Fig. 18**, it can be noted that thermal stressing time has a great influence on thermal stability of biodiesel as well. Longer residence time results in larger extent of thermal decomposition.

Isomerization reaction was observed from at 275 °C for 28 minutes or longer, which meant that shorter residence time at the same temperature can avoid this change. Likewise, Diels-Alder reaction happens at 300 °C for 63 minutes. The residence time control is also effective.

Pyrolysis reaction commences to take place at 350 °C. Whereas, significant pyrolysis occurs at 400 °C for 18 minutes or above and 425 °C for 8 minutes or above. In the meantime, formed dimers almost disappear at these points. In order to prevent large decomposition, the residence time should be shortened below 18 minutes at 400 °C or 8 minutes at 425 °C.

Another observation is that, gas products are generated at 360 °C for 33 minutes or above, at 375 °C for 8 minutes or above, and at 400 °C and 425 °C for all residence times in this thermal stressing study. Reducing the residence is one of the practical and effective measures for decreasing gas generation.

In sum, thermal stressing time on thermal stability of biodiesel is of great importance. Both thermal stressing time and temperature contribute to biodiesel fuel degradation. In fact, thermal stability of biodiesel is governed by a combination of factors, and temperature and residence time are powerful enough to cancel the influence of others.

4.4 Quantitative analysis of the extent of thermal decomposition of biodiesel

A quantitative analysis of the chromatograms for thermal stressed biodiesel samples was

carried out to study the extent of degradation.

To assess the thermal decomposition extent, fresh BD-100 biodiesel samples serve as the point of reference. Five samples of fresh biodiesel were run in GC-FID to minimize the optional errors. **Table 11** displays the peak areas of FAME compositions, which were manually integrated from the instrument. The average data were chosen as the indicator of fresh biodiesel for later calculations.

The subsequent **Table 12** presents concentrations of fresh biodiesel samples deduced from their peak areas by the means of calibration curve equations. The calibration curve described the relationship of two variables, the instrument response (peak area) for each standard and the concentration of each analyte. The average concentration were derived to represent that of fresh biodiesel and used for the later calculations.

Likewise, **Table A-5** in Appendix presents the peak areas of thermal stressed biodiesel samples and **Table A-6** shows the inferred concentrations. It should be pointed out that the concentrations of samples thermal stressed at 360 °C or below were corrected by a factor of $C_{16:0, \text{fresh}}/C_{16:0, \text{TS}}$, where C16:0 was used as a “native” internal standard. Whereas the concentrations of samples heated above 360 °C were directly calculated from the calibration curve equations without any further adjustment since C16:0 decomposed at these severe conditions.

Fig. 20 is the temporal profiles of the concentration of biodiesel at different thermal stressing temperatures. **Fig. 21** plots biodiesel decomposition percentage as a function of the thermal stressing time over a temperature range of 250 °C to 425 °C. It can be noticed that biodiesel decomposition increases with the increasing thermal stressing time. In addition, it is

Table 11 GC-FID data for fresh biodiesel

	Peak Area ($\times 10^6$)					Total
	C16:0	C18:1-3	C18:0	C20:0	C22:0	
Sample 1	1.599	11.867	0.891	0.053	0.141	14.551
Sample 2	1.510	11.201	0.786	0.075	0.145	13.717
Sample 3	1.732	12.784	0.904	0.087	0.167	15.674
Sample 4	1.565	11.620	0.819	0.079	0.153	14.236
Sample 5	1.610	11.774	0.834	0.073	0.149	14.440
Average	1.603	11.849	0.847	0.073	0.151	14.524
STDEV	0.082	0.581	0.050	0.013	0.010	0.718

Table 12 Concentrations of fresh biodiesel samples

	Concentration (ppm by volume) ^a					Total
	C16:0	C18:1-3	C18:0	C20:0	C22:0	
Sample 1	114.5	879.8	68.2	8.2	17.9	1088.6
Sample 2	108.6	832.2	61.1	9.7	18.2	1029.9
Sample 3	123.3	945.3	69.1	10.6	19.7	1167.9
Sample 4	112.3	862.2	63.3	10.0	18.8	1066.5
Sample 5	115.2	873.2	64.3	9.6	18.5	1080.8
Average	114.8	878.5	65.2	9.6	18.6	1086.8
STDEV	5.4	41.5	3.4	0.9	0.7	50.7

^a Calculated by the calibration curve equation $A_i = a_i C_i + b_i$ using parameters from **Table 11**.

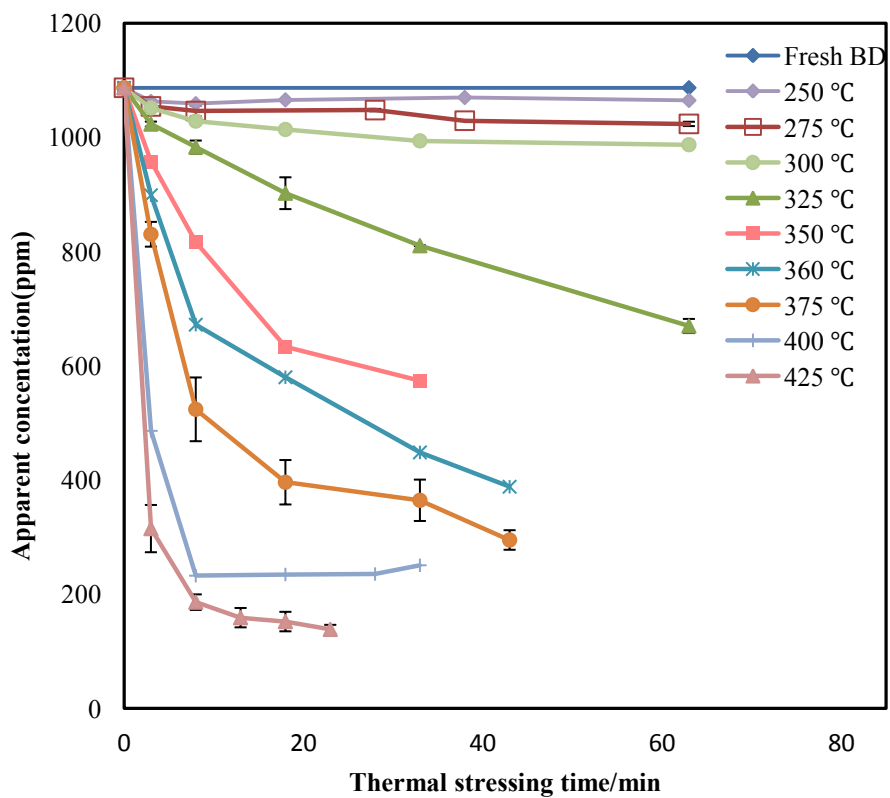


Fig. 20 Plot of concentration of biodiesel sample as a function of thermal stressing time at different temperatures.

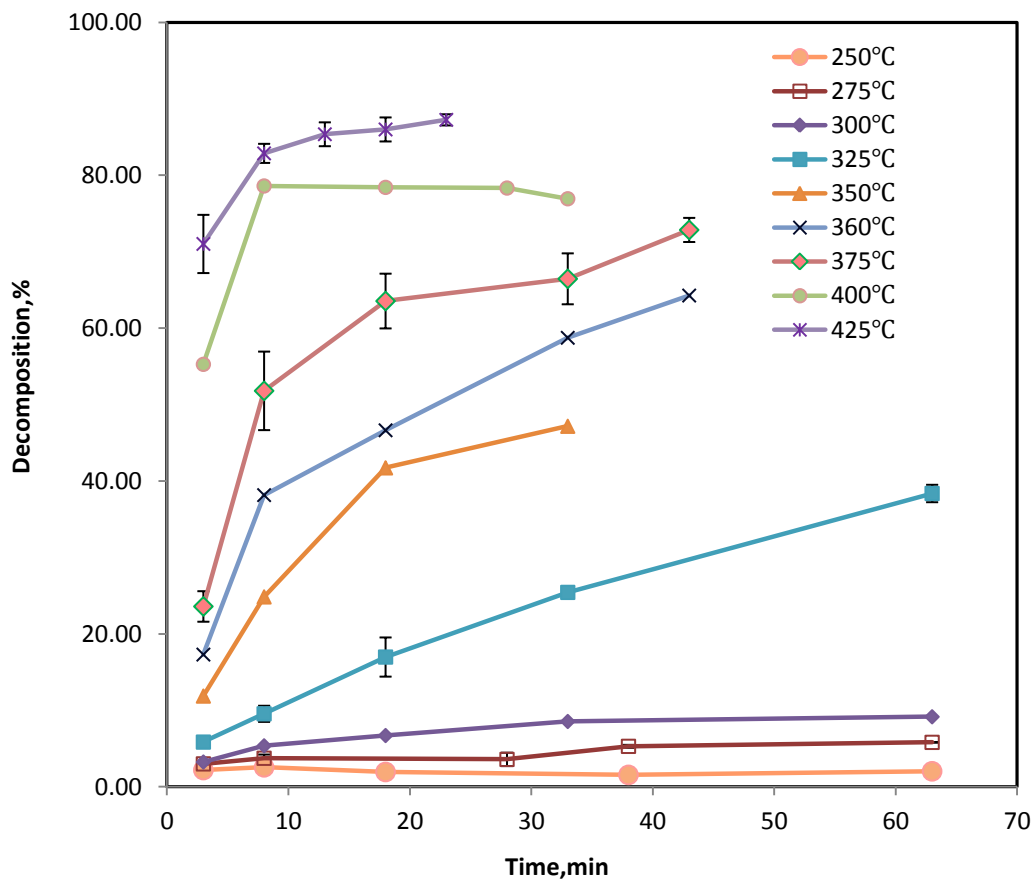


Fig. 21 Thermal decomposition percentage of biodiesel fuel variation as a function of time at different temperatures.

evident that the decomposition accelerates as the temperature rises.

Biodiesel remains relatively stable at 300 °C or below with less 10% decomposition, especially at 275 °C or below with only less than 6% decomposition. Cis-trans Isomerization reaction is responsible for the small-scale degradation.

At 325 °C, the decomposition increases gradually up to 40% after thermal stressed for 63 minutes, which mainly resulting from the increasing contribution of the polymerization reaction. As temperature rises from 350 °C to 425 °C, the pyrolysis reaction commences and speeds up the decomposition rapidly. The decomposition percent achieves about 80% within 10 minutes at 400 °C to 425 °C. After 23 minutes of heat treatment at 425 °C, it increases up to 87%. The decomposition percentage data is organized in **Table A- 6** in **Appendix A**.

4.5 Discussion on the impact of thermal decomposition on biodiesel fuel properties and synthesis

Thermal decomposition caused by excessive temperature may denature the fuel. Both large molecular weight compounds through Diels-Alder reaction and the decomposed products such as gases through pyrolysis reactions belong to denatured products of biodiesel (Marulanda, Anitescu, & Tavlarides, 2010a). The denaturalization of FAMES has a direct impact on fuel quality. The isomerization reaction also alters the characteristic of biodiesel to some extent. After all, the presence of these products inevitably brings about some changes of biodiesel fuel properties.

Studies so far have suggested that thermal decomposition influence the production and characteristics of biodiesel in primarily two aspects. Firstly, it is stated to cause the decrease of the biodiesel yield at high temperatures and long residence time. Therefore, the proposed optimal

temperature conditions for biodiesel synthesis through supercritical methanol/ethanol method is within 270 °C to 350 °C (He et al., 2007; Imahara et al., 2008; Kusdiana & Saka, 2001; Saka & Kusdiana, 2001; Shin et al., 2011). In spite of this, the Tavlarides group (Anitescu et al., 2008; Deshpande, Anitescu, Rice, & Tavlarides, 2010; Marulanda, Anitescu, & Tavlarides, 2010a; Marulanda, Anitescu, & Tavlarides, 2010b) have recently shown that a higher synthesis temperature (400 °C) would actually favour biodiesel production in fact since the formed decomposition products can serve as fuel components. Secondly, thermal decomposition is assumed to have a positive effect on fuel qualities such as viscosity, cold flow properties and cetane numbers (Imahara et al., 2008; Marulanda, Anitescu, & Tavlarides, 2010a; Marulanda, Anitescu, & Tavlarides, 2010b). This field is still less understood and will be addressed in future work.

4.6 Kinetic model for thermal decomposition of biodiesel

The dynamic thermal decomposition of biodiesel fuel at a temperature within the range of 250 °C to 425 °C was investigated. There has been no literature available on this aspect up to now, and the kinetics of thermal decomposition of biodiesel fuel is less understood. Therefore, this part of research is also aimed to shorten this gap.

4.6.1 Biodiesel decomposition mechanism

Based on previous studies (Seames et al., 2010; Shin et al., 2011), it is distinct that thermal decomposition of biodiesel fuel is an intricate process. A conventional pyrolysis study even demonstrated that biodiesel will undergo coking to produce coke products at extreme high temperatures around 500 °C (Mohan, Pittman, & Steele, 2006). However, in comparison, the thermal stressing temperatures included in the current research are relatively lower. Therefore,

coke products are not necessary to be considered here. Despite this, thermal decomposition of biodiesel via other pathways is still complex enough to pose great challenges for the kinetic study. Each pathway may yield multiple disproportional products instead of one. In order to better explore the kinetics of this part, it is better to simplify the mechanism for a general investigation.

From the observations of this research, cis-trans isomerization reaction, Diels-Alder reaction and pyrolysis reaction are predominantly involved in the thermal decomposition of biodiesel under the conditions studied.

As temperature rises, biodiesel will initially go through reversible isomerization and Diels-Alder reaction to form isomers and dimers, respectively. When the temperature is increased further, produced isomers, dimers and remaining FAMES will decompose to form lower molecular weight FAMES, hydrocarbons and gaseous products.

More specifically, isomerization occurs from 250 °C to 400 °C, converting natural cis-type unsaturated FAMES to trans-type FAMES; the Diels-Alder reaction occurs from 300 °C to 425 °C, creating dimers and possibly polymers; and pyrolysis of unsaturated FAMES, saturated FAMES, and formed dimers commences approximately at 350 °C, 375 °C and 375 °C, respectively. Without a shred of doubt, thermal stressing time is also crucial to determine the degree of biodiesel decomposition.

Taking into account the main reactions involved and the behaviors of biodiesel changes over time and temperature, a three-lump mechanism model of biodiesel thermal decomposition is proposed which is shown in **Fig. 22**. This kinetic mechanism consists of an initial reversible

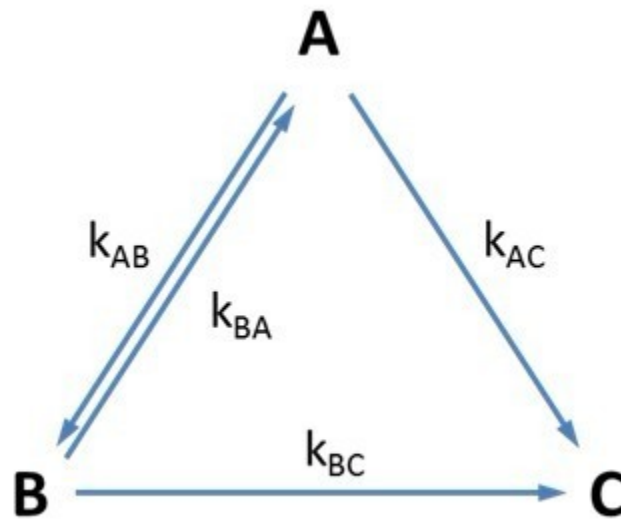


Fig. 22 A mechanism of biodiesel thermal decomposition. \Leftrightarrow reversible reaction; \rightarrow irreversible reaction; A: biodiesel; B: isomers, dimers, etc.; C: smaller FAMES, hydrocarbons, gases, etc.; k_{AB} , k_{BA} , k_{AC} and k_{BC} are reaction rate constants.

isomerization and Diels-Alder reactions followed by a pyrolysis reaction, where A represents biodiesel, B denotes the products of isomers, dimers, etc, and C stands for summation of smaller FAMEs, hydrocarbons, gases.

4.6.2 Proposed kinetic model

Although the three-lump mechanism provides a straightforward way for modeling thermal decomposition, it will also bring great challenges. The complexity of the biodiesel product mixture and the limitations of current analytical method are the major problems. Owing to these restrictions, it is demanding to differentiate and quantify products B and C since they spread out in terms of a fairly large number of small overlapped low concentrated peaks, rather than a few detached large ones in the chromatograms.

Consequently, this model calls for additional adjustment. Widegren and Bruno (Widegren & Bruno, 2008) suggested to use the first order kinetic model to describe the thermal decomposition of aviation turbine fuel Jet A. Inspired by this case, the current model is further simplified to a reversible first order reaction model similarly (Eq. (6)). Reversible first-order reaction is also a simplest type to describe thermal decomposition in which a reactant (A) thermally converts to a product (P). All kinds of products generated are bracketed together. This assumption provides a practical base for a quantitatively kinetic study of the overall thermal stability of biodiesel.



Here, P is all reaction products which take into account both B and C, and k_1 and k_2 are the rate constants for the forward and the reverse reactions.

The rate of reaction (6) is given by

$$-\frac{dC_A}{dt} = k_1 C_A - k_2 C_P \quad (7)$$

By assuming $C_P = C_{A0} - C_A$, Eq. (7) can be rewritten in the following form

$$-\frac{dC_A}{dt} = (k_1 + k_2) \left[C_A - \frac{k_2}{k_1 + k_2} C_{A0} \right] \quad (8)$$

Integrating Eq. (8) gives

$$C_A = \frac{k_1}{k_1 + k_2} C_{A0} \exp[-(k_1 + k_2)t] + \frac{k_2}{k_1 + k_2} C_{A0} \quad (9)$$

Then let $C_A = \sum C_{i,TS}$ and $C_{A0} = \sum C_{i,fresh}$ and the reaction rate constants k_1, k_2 for each reaction temperature can be obtained by fitting the experimental data.

4.6.3 Simulation results

As stated previously, the kinetic analysis was conducted through the proposed model. The forward and reverse rate constants, at each temperature were determined in association with the assembled data at differed reaction time. After k_1, k_2 are achieved, the equilibrium constant $K = k_1 / k_2$ is calculated. All of the results are presented in **Table 13**. After close scrutiny of the derived rate constants in **Table 13**, it is found that the rate constant for the forward reaction (k_1) is faster than that for the reverse reaction (k_2) at $T \geq 350$ °C, which is another indication for the occurrence of pyrolysis reactions.

In this current kinetic modeling, the experimental data shows a good fit into the simulation curves, as displayed in **Fig. 23** and **Fig. 24**.

Table 13 Rate constants and equilibration constant for biodiesel thermal decomposition reactions

T, °C	k_1 (min ⁻¹)	k_2 (min ⁻¹)	K
250	0.0005	0.0068	0.0728
275	0.0016	0.0109	0.1424
300	0.0032	0.0170	0.1901
325	0.0133	0.0202	0.6585
350	0.0397	0.0348	1.1389
360	0.0658	0.0418	1.5737
375	0.1067	0.0469	2.2737
400	0.3220	0.0891	3.6144
425	0.5079	0.0840	6.0464

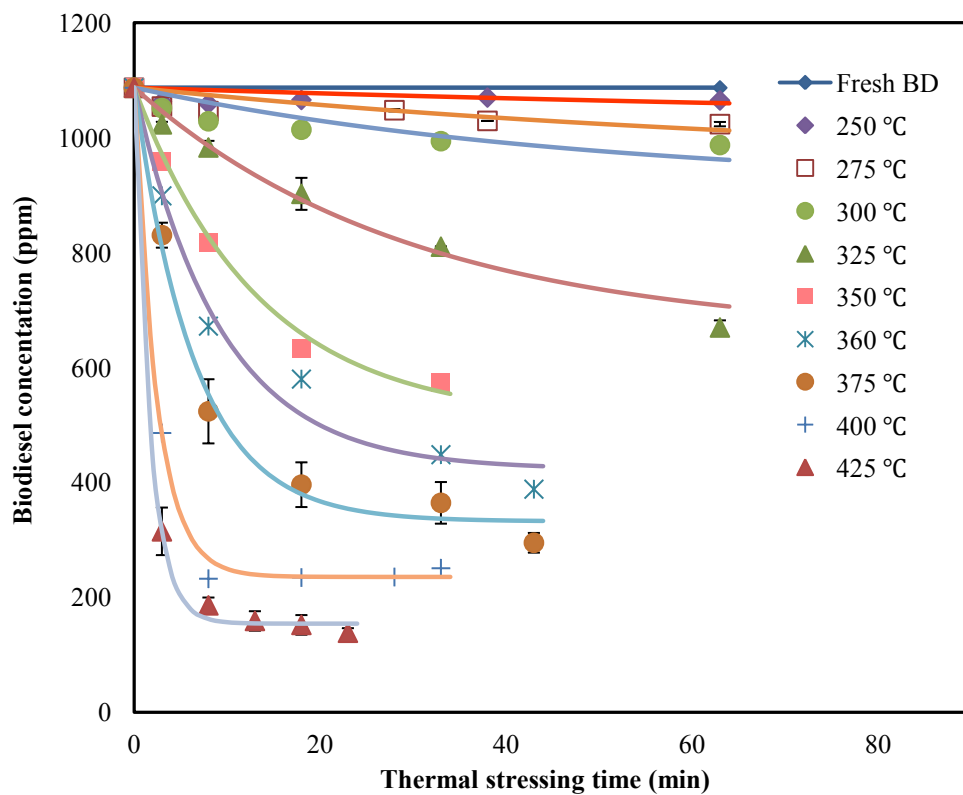


Fig. 23 Modeling of biodiesel concentration as a function of time for various stressing temperatures using the reversible first-order kinetics fitted with experimental data.

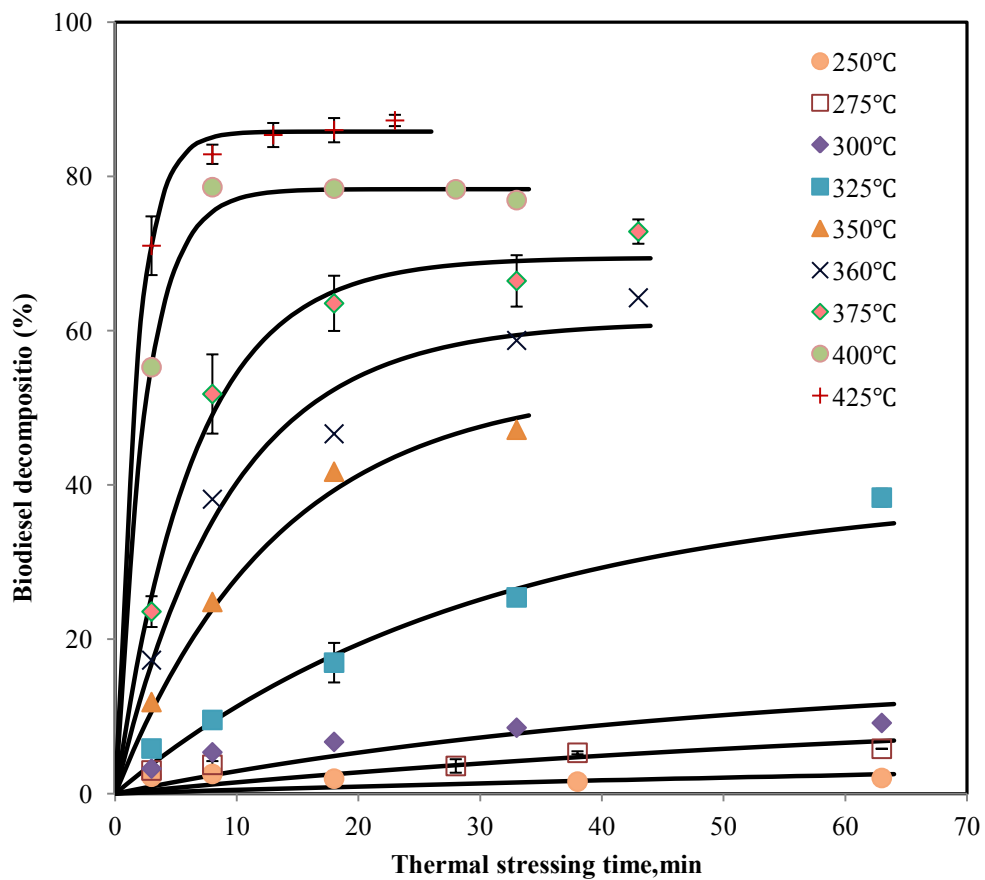


Fig. 24 Plot of predictions of biodiesel thermal decomposition as a function of time under different stressing conditions using the reversible first-order kinetic model fitted with experimental data.

Again, as mentioned above, this kinetic model pays attention to the overall reaction which ignores the detailed intermediate reactions. The well fitted result ascertains that the reversible first-order reaction model is properly determined. It well represents the mechanism and kinetics of thermal decomposition of biodiesel fuel. This result also supports the argument that both isomerization and polymerization via the Diels-Alder reaction play a significant role in biodiesel decomposition in the temperature range studied.

4.6.4 Determination of Arrhenius parameters

Referring to the well-known Arrhenius equation, reaction rate constants are expressed as a function of temperature, as shown below:

$$k = A \exp(-E_a / RT) \quad (10)$$

where A is the pre-exponential factor, E_a is the activation energy, and R is the universal gas constant. The value of R is $8.314 \text{ J}/(\text{mol}\cdot\text{k})$. Here, for the reversible first-order reaction kinetics, the units of the reaction rate constant k and pre-exponential A are min^{-1} identically.

About the equilibrium constant, it can be expressed as a function of temperature as well by the van't Hoff equation, as shown below:

$$\frac{d \ln K}{d(1/T)} = -\frac{\Delta H^\circ}{R} \quad (11)$$

where ΔH° is the standard reaction enthalpy. The values for $\ln k_1$ and $\ln k_2$ were calculated from **Table 13** and listed in **Table A- 5** in **Appendix A**. By plotting $\ln k_1$, $\ln k_2$ and $\ln K$ versus $1/T$ (**Fig. 25**, **Fig. 26** and **Fig. 27**), values of A , E_a and ΔH° can be determined. A for k_1 and k_2 are

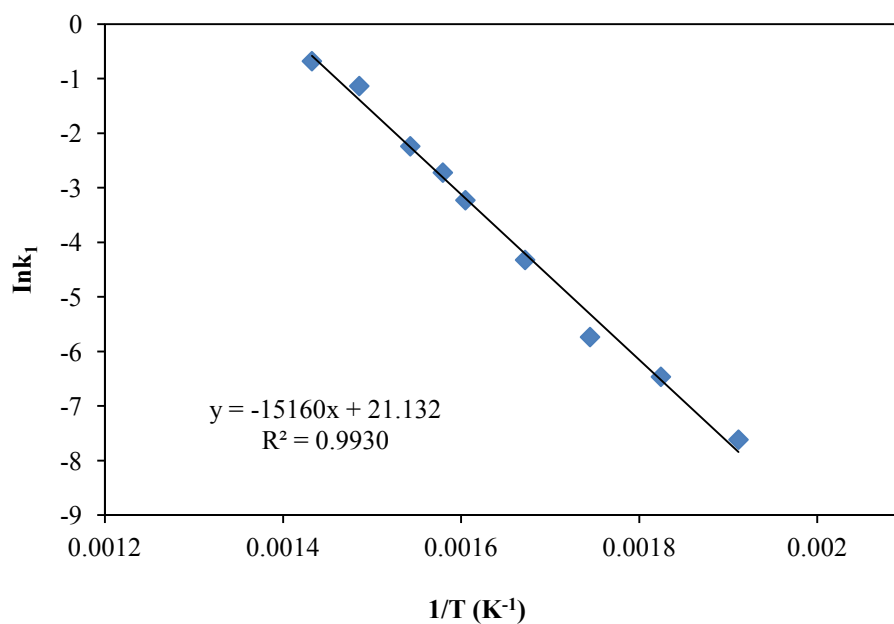


Fig. 25 Arrhenius plot for the first-order forward decomposition of biodiesel. The Arrhenius parameters determined from the fit to the data are $A = 1.50 \times 10^9 \text{ min}^{-1}$ and $E_a = 126.0 \text{ KJ/mol}$.

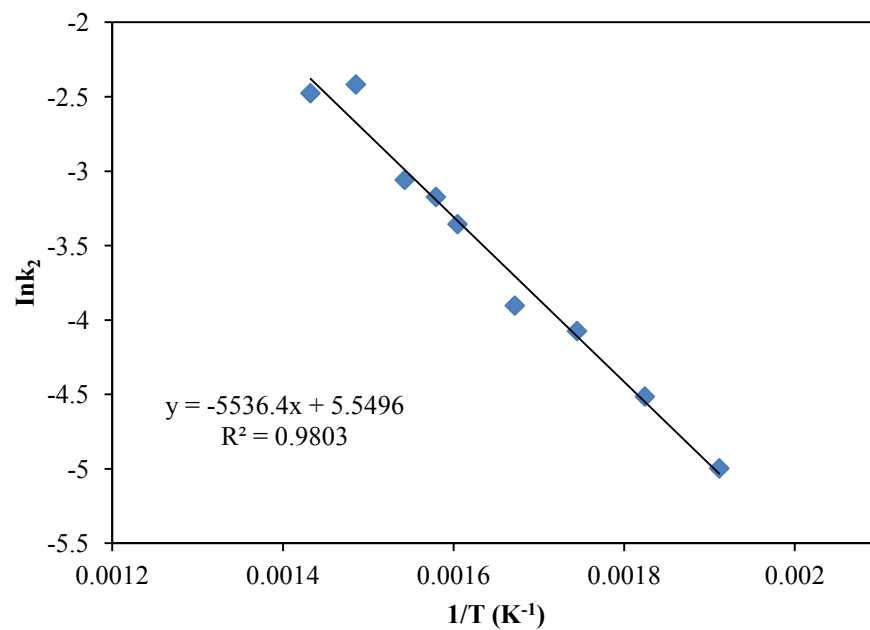


Fig. 26 Arrhenius plot for the first-order reverse decomposition of biodiesel. The Arrhenius parameters determined from the fit to the data are $A = 257 \text{ min}^{-1}$ and $E_a = 46.0 \text{ KJ/mol}$.

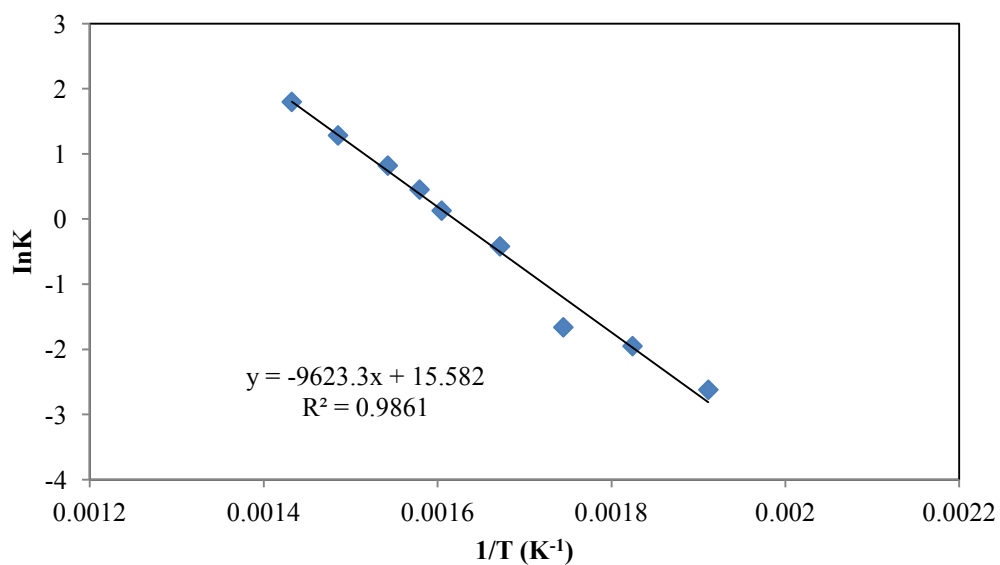


Fig. 27 Van't Hoff plot for the reversible first order decomposition of biodiesel. The determination of the reaction enthalpy ΔH° for biodiesel thermal decomposition is 80.0 KJ/mol, indicating an overall endothermic reaction.

1.50×10^9 and 257 min^{-1} , respectively, and Ea for the forward and reverse reactions are 126.0 and 46.0 KJ/mol, respectively. The reaction enthalpy ΔH° for biodiesel thermal decomposition is 80.0 KJ/mol, indicating an overall endothermic reaction. In turn, the high linearity of the Arrhenius plots ($R^2 > 98\%$) powerfully validates the rationality of the hypothesis of reversible first-order kinetics.

Chapter V

Conclusions

In this study, thermal stressing of biodiesel in batch reactors was carried out at reaction temperatures ranging from 250 °C to 425 °C for 3 to 63 minutes. Degree to which thermal decomposition occurred was analyzed qualitatively and quantitatively. A reversible first-order reaction model was proposed thereafter to describe the kinetics of biodiesel thermal decomposition processes. The following text summarizes the main conclusions we draw from this study:

1. Appropriate calibration curves of the constituents of biodiesel were constructed by utilizing two analytical standards GLC-10 FAME mix and GLC-100 FAME mix. Since the R-squared (R^2) is a good criterion to measure the calibration curve quality, the values in these created calibration curves close to 1 strongly demonstrated that the perfect fit of the linear regression lines to the data. The calibration curves serve as a good index and guideline of converting the manual integrated peaks areas of FAMES to their concentrations.
2. With the help of GC-FID and GC-MS as analytical tools, this study gained insight into the decomposition pathways and advanced some new finds. It can be concluded that decomposition of FAMES takes place at 275 °C or above and largely depends on the thermal stressing temperature and time of stress; and the decomposition involves cis-trans isomerization (275-400 °C), polymerization (Diels-Alder reaction) (300-425 °C) and pyrolysis (≥ 350 °C) reactions. Specially, isomerization converts unsaturated FAMES from naturally occurring cis to trans carbon double bonds; polymerization forms the dimers and/or polymers via the well known Diels-Alder reaction; and pyrolysis (also known as thermal

cracking or thermal decomposition) develops the lower molecular weight FAMES hydrocarbons and gas products. What deserves special mention is that the formed isomers and dimers are not stable at high temperature; they will decompose to smaller molecular weight products under severe conditions.

3. A three-lump model is proposed to describe the decomposition mechanism. For convenience and feasibility, the kinetic model based on this proposed mechanism is simplified to a reversible general first order reaction model. Owing to the good fitted data, the concentrations and thermal decomposition percentage of biodiesel can be well predicted by this kinetic model. That is, the decomposition kinetic can be well modeled by this simplified reaction.
4. During the fitting process, the forward and reverse reaction rate constants were derived in for each temperature. The Arrhenius plots were drawn afterwards with these kinetic data, the Arrhenius parameters pre-exponential factor A and activation energy E_a for thermal decomposition of biodiesel are determined. A for k_1 and k_2 are 1.50×10^9 and 257 min^{-1} , respectively, and E_a for the forward and reverse reactions are 126.0 and 46.0 KJ/mol, respectively. The validity of these kinetics is further validated by the high linearity of the Arrhenius plots.
5. The proposed kinetic model not only plays as an important role in describing and predicting the global behavior of biodiesel when exposed to high temperatures, but also offers some valuable information. From the established Van't Hoff plot, the reaction enthalpy ΔH° for biodiesel thermal decomposition is 80.0 KJ/mol, indicating an overall endothermic reaction.

Chapter VI

Future work

As mentioned above in **section 4.5**, this research has not explored the effects of thermal decomposition on fuel qualities such as viscosity, cold flow properties, and cetane number. Now some researchers recommended that supercritical transesterification should be performed below the start-to-decompose temperature which is 300 °C (Imahara et al., 2008), while others claim that a certain extent of decomposition is beneficial to the promotion of the fuel qualities (Marulanda, Anitescu, & Tavlarides, 2010a). Without strong support, it is hasty to draw a conclusion.

For better understanding and effort to discover more information concerning biodiesel fuel, future work is recommended. The challenges present in the future work offer chances for developments and breakthroughs that will advance the biodiesel fuel science and technology. These efforts are meaningful since it will allow biodiesel to be produced and consumed in a more efficient and environmentally friendly way.

Appendix A Supplementary information

Additional information is provided in this section to enrich the subject studied in more detail. First, **Fig.A- 1** shows more calibration curves for the analytes except for these present in the fresh biodiesel constructed. Although there was no C19:0, C21:0 contained in the BD-100 biodiesel samples, they were included in the analytical standards GLC-10 and GLC-100 FAME mix. Therefore, the calibration curves for C19:0, C21:0 and analytical standards GLC-10 and GLC-100 FAME mix were created.

Fig.A- 2 is the chromatograms for the fresh biodiesel, analytical standard GLC-10 FAME mix and the mix of fresh biodiesel and GLC-100 FAME mix. By comparing these chromatograms, the constituents existing in the fresh biodiesel can be identified without the help of GC-MS.

Fig.A- 3 to **Fig.A- 28** show the original chromatograms for the thermal stressed samples at different temperatures and residence time.

Table A- 1 and **Table A- 2** record the GC-FID data for analytical standard GLC-10 FAME mix and GLC-100 mix separately. The calibration curves for the analytes were established based on these data.

Table A- 3 is the GC-FID data for thermal stressed biodiesel samples, and **Table A- 4** is the corresponding concentrations. It should be pointed out that the concentrations for the samples stressed at 360 °C or below were corrected by a factor of $C_{16:0, \text{fresh}}/C_{16:0, \text{TS}}$, where C16:0 was used as a “native” internal standard. Since methyl palmitate decomposed at 375 °C or above, it could not serve as an internal standard at these conditions.

Table A- 5 and the following table are designate for the kinetic study. **Table A- 5** assembles the data of $\ln k_1$, $\ln k_2$ and $\ln K$ for each temperature. These data are used for the Arrhenius plots and Van't Hoff plot where the Arrhenius parameters A , activation energy and the overall reaction enthalpy were solved.

Table A- 6 displayed the modeling data and the experimental data of biodiesel concentration and decomposition percentage at different temperature and residence time. This table vividly demonstrated the good fitness of the proposed kinetic model and the data, which also validated that the thermal decomposition can be well modeled by this reversible first-order reaction kinetics.

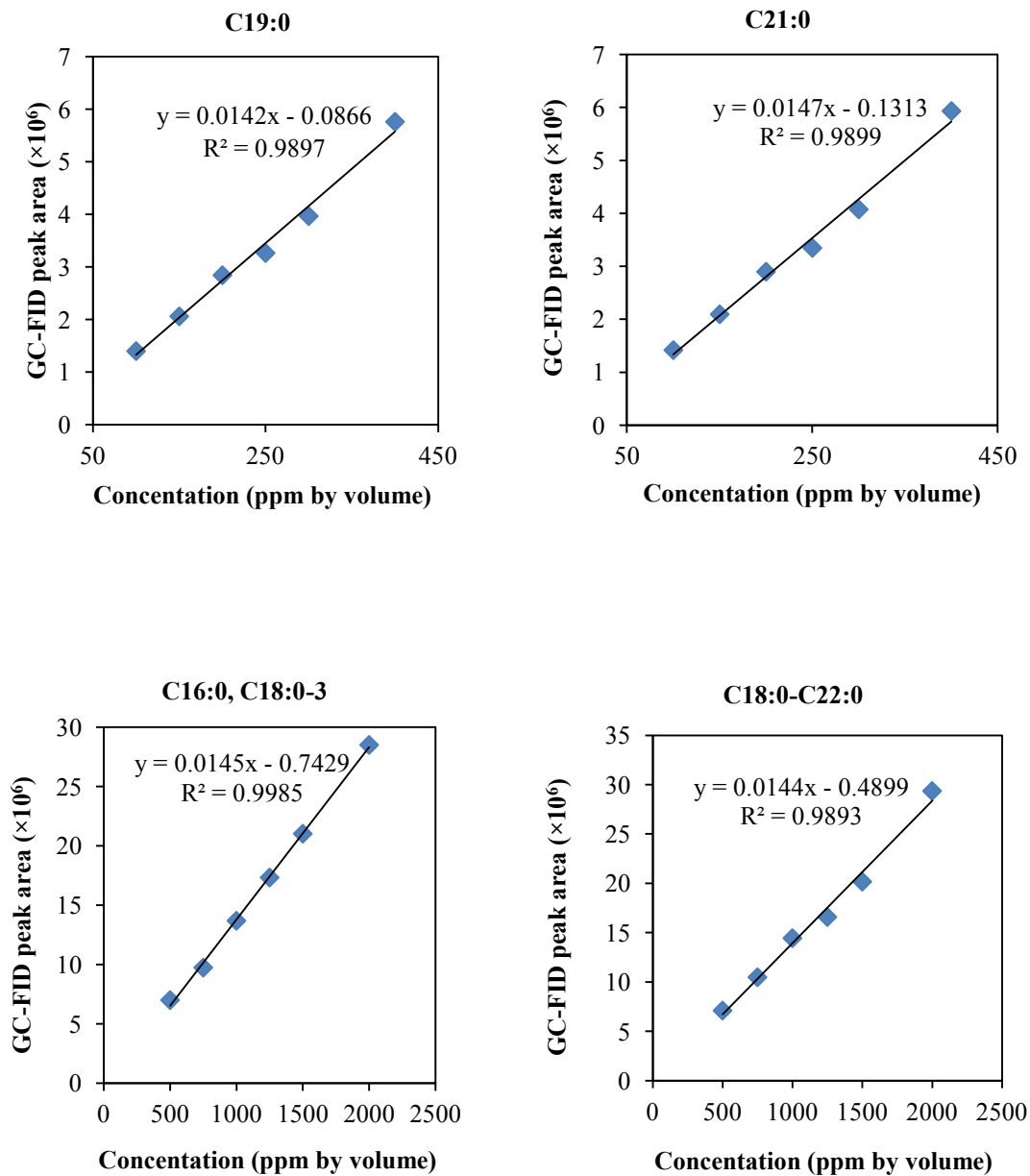


Fig.A- 1 GC-FID calibration curves for supplementary FAME analytes and mixtures (C19:0, C21:0 and analytical standard mixtures)

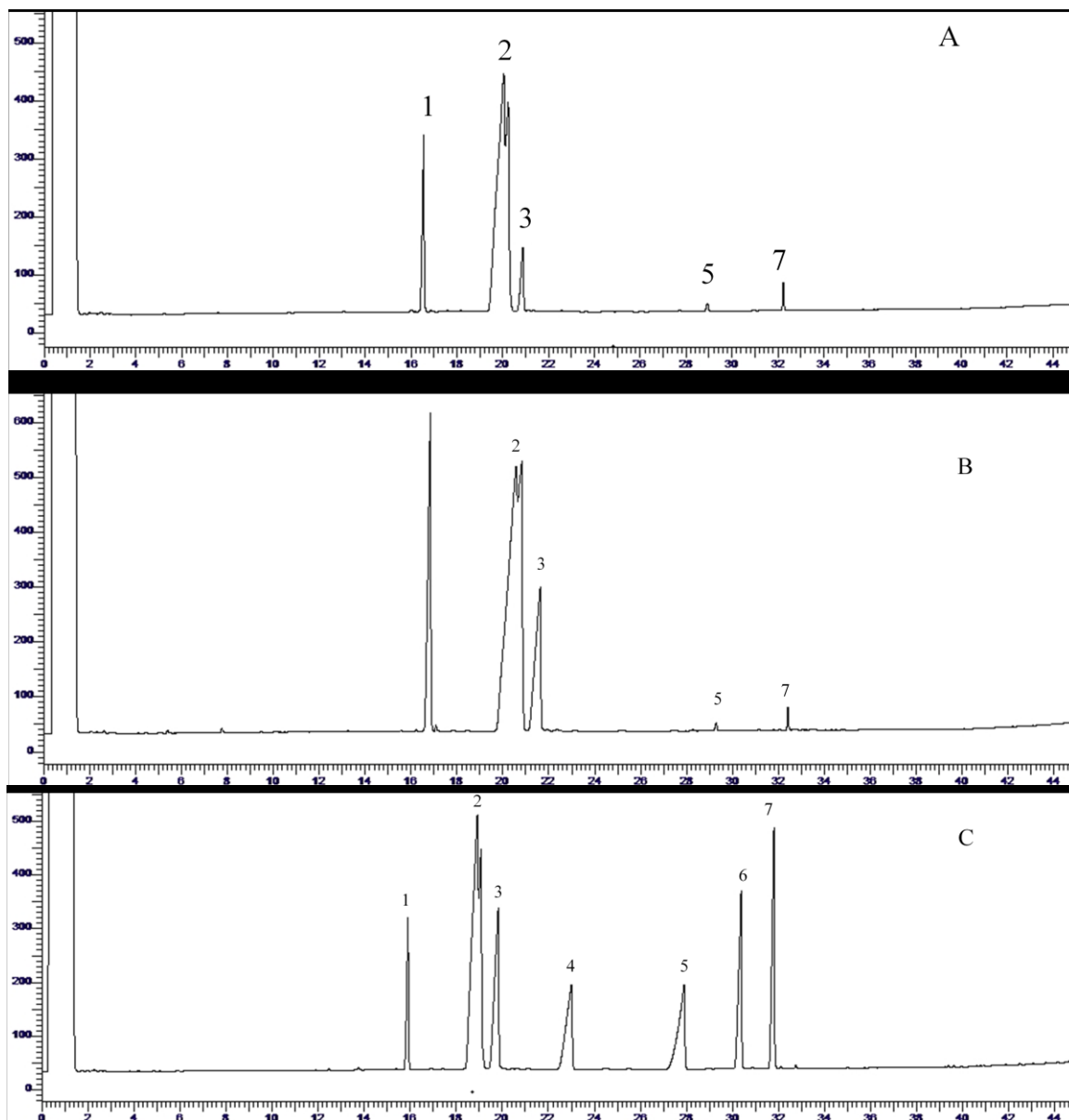


Fig.A- 2 Chromatograms of fresh biodiesel (A), fresh biodiesel and GLC-10 FAME mix (B), fresh biodiesel and GLC-100 FAME mix (C). Peaks shown in the chromatograms are C 16:0 (1), C 18:1-3 (2), C 18:0 (3), C 19:4 (4), C20:0 (5), C 21:0 (6), C 22:0 (7).

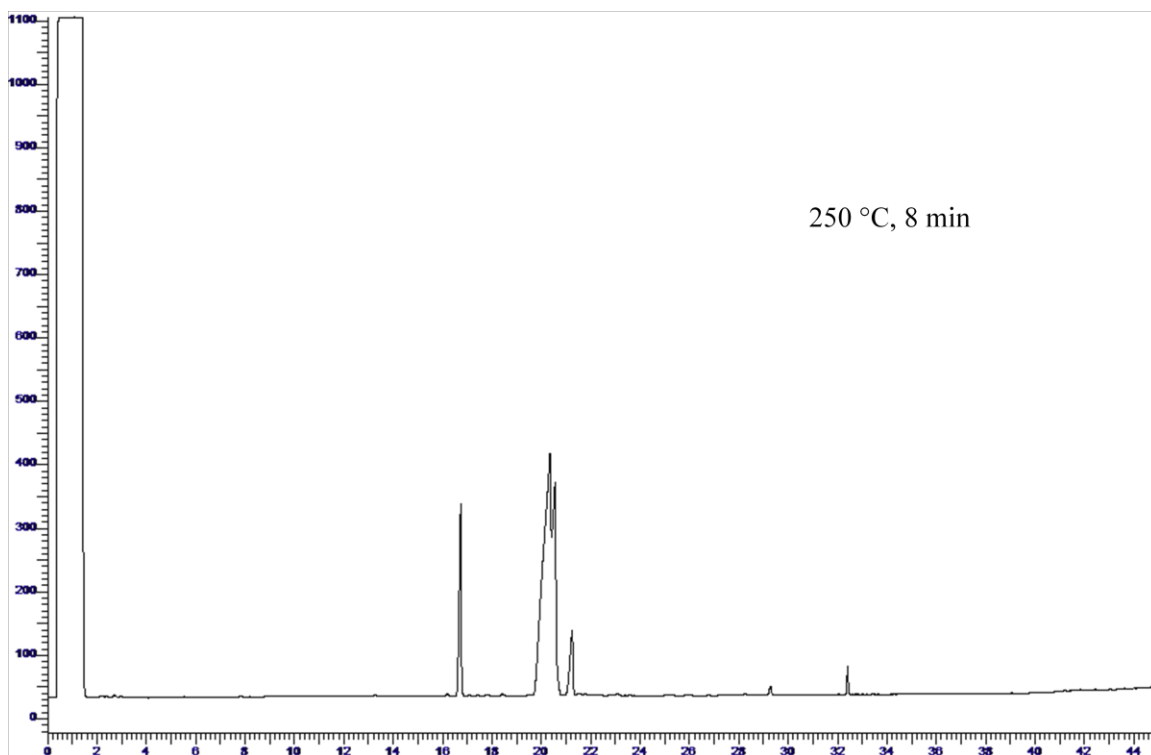
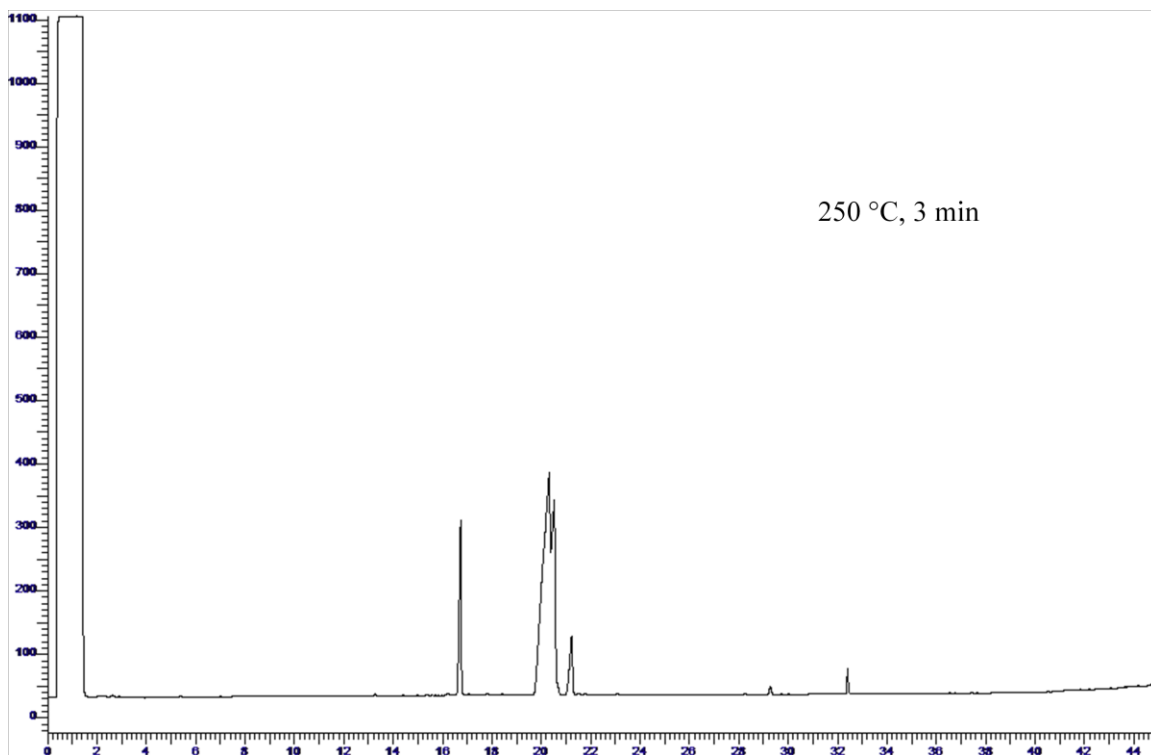


Fig.A- 3 Chromatograms of biodiesel samples thermal stressed at 250 °C for 3 and 8 minutes.

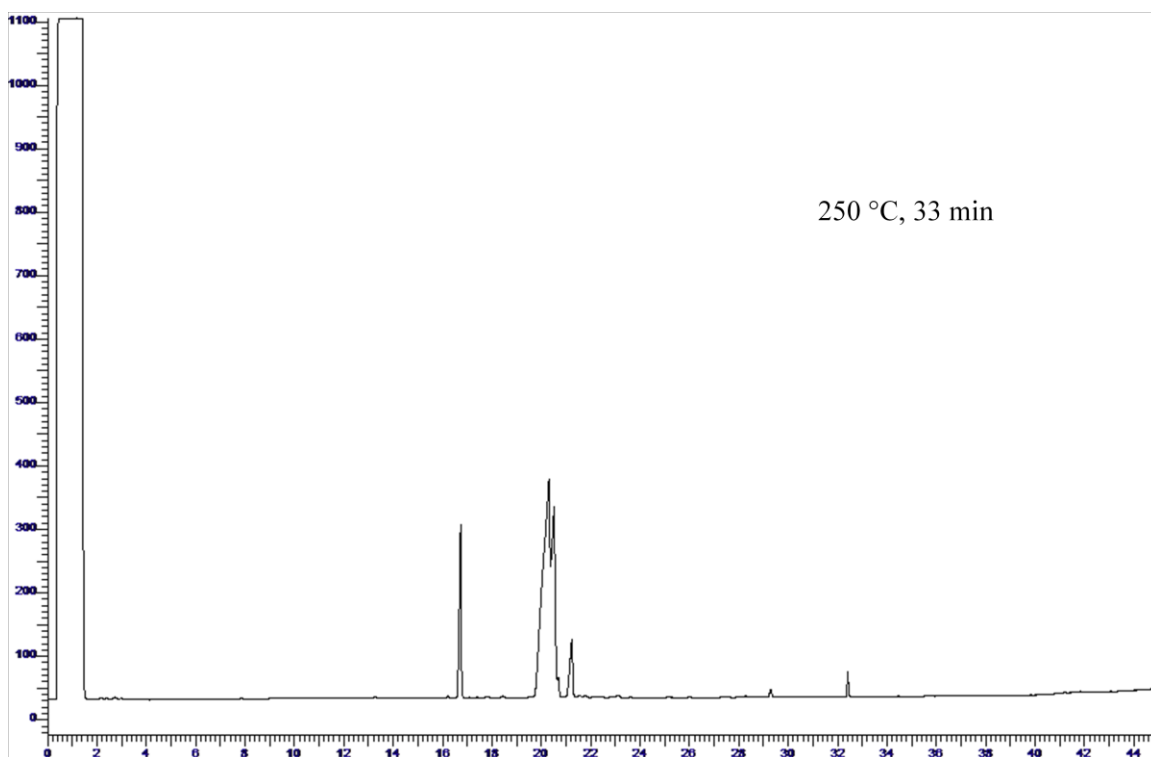
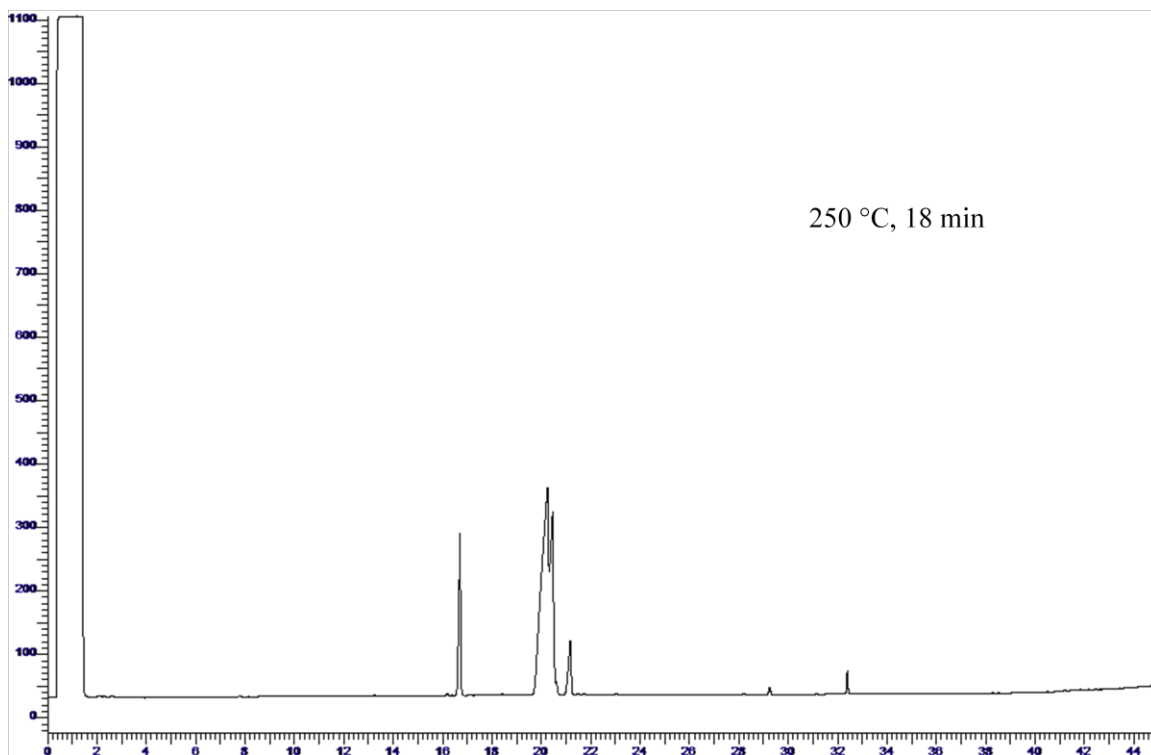


Fig.A- 4 Chromatograms of biodiesel samples thermal stressed at 250 °C for 18 and 33 minutes.

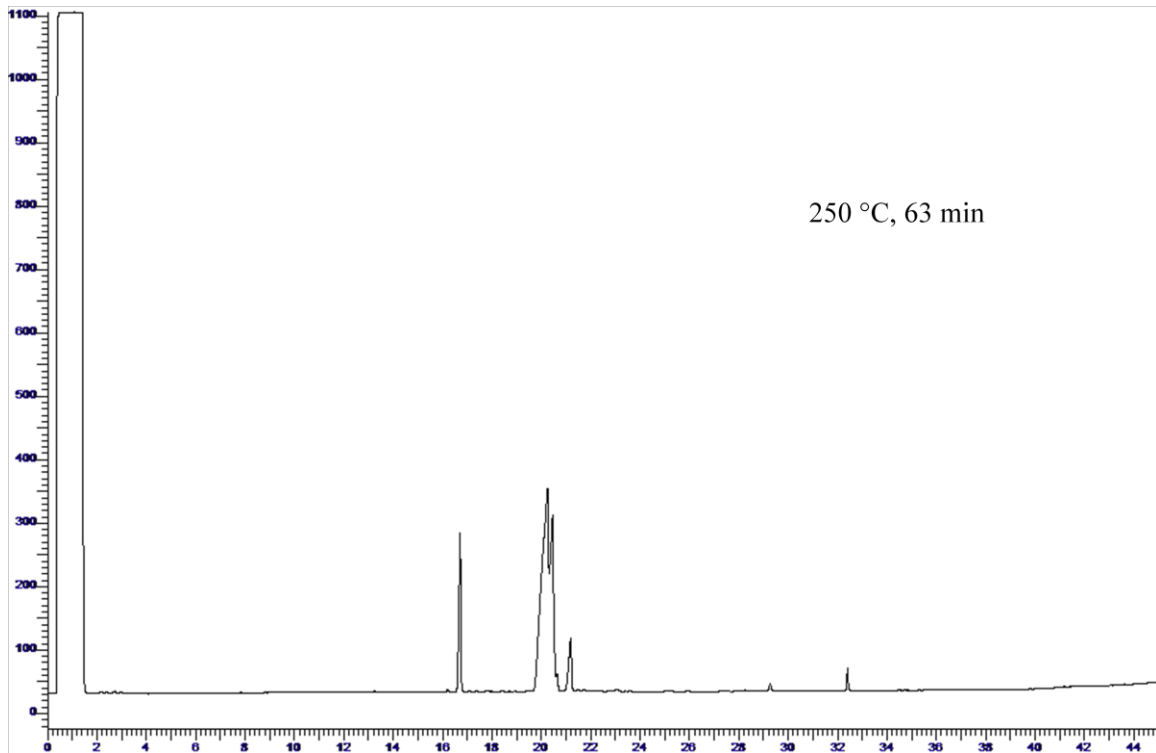


Fig.A- 5 Chromatogram of biodiesel sample thermal stressed at 250 °C for 63 minutes.

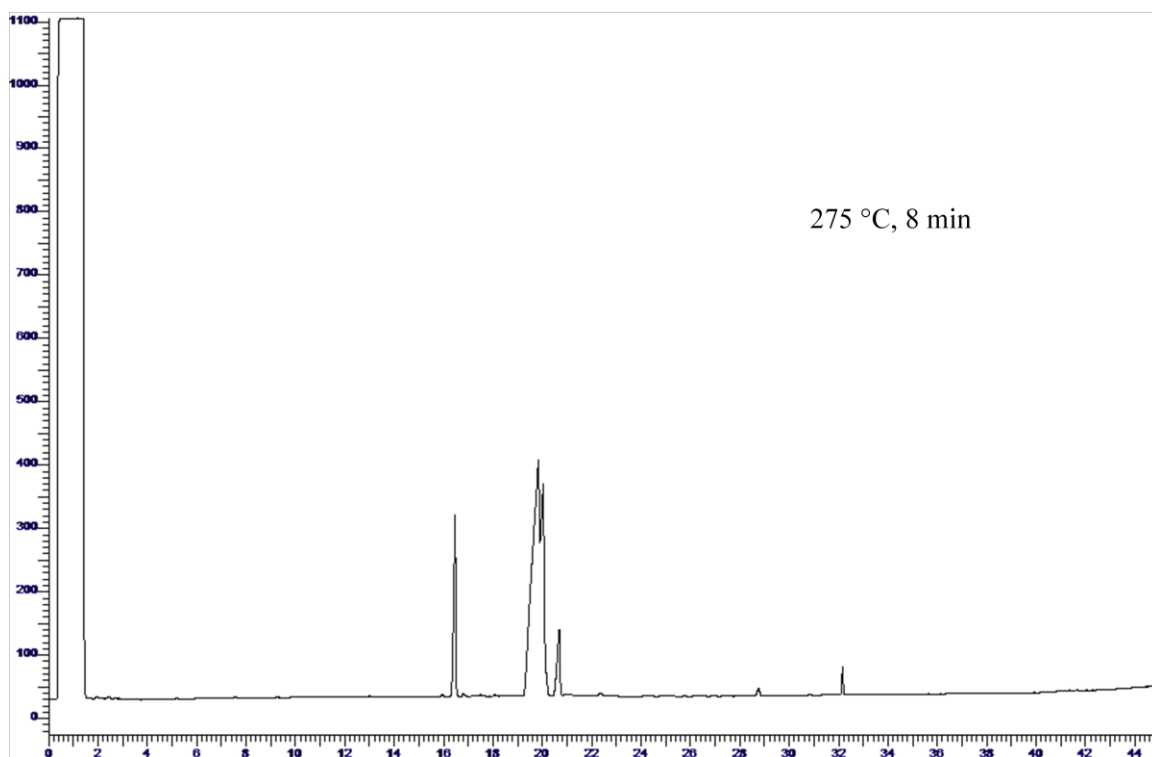
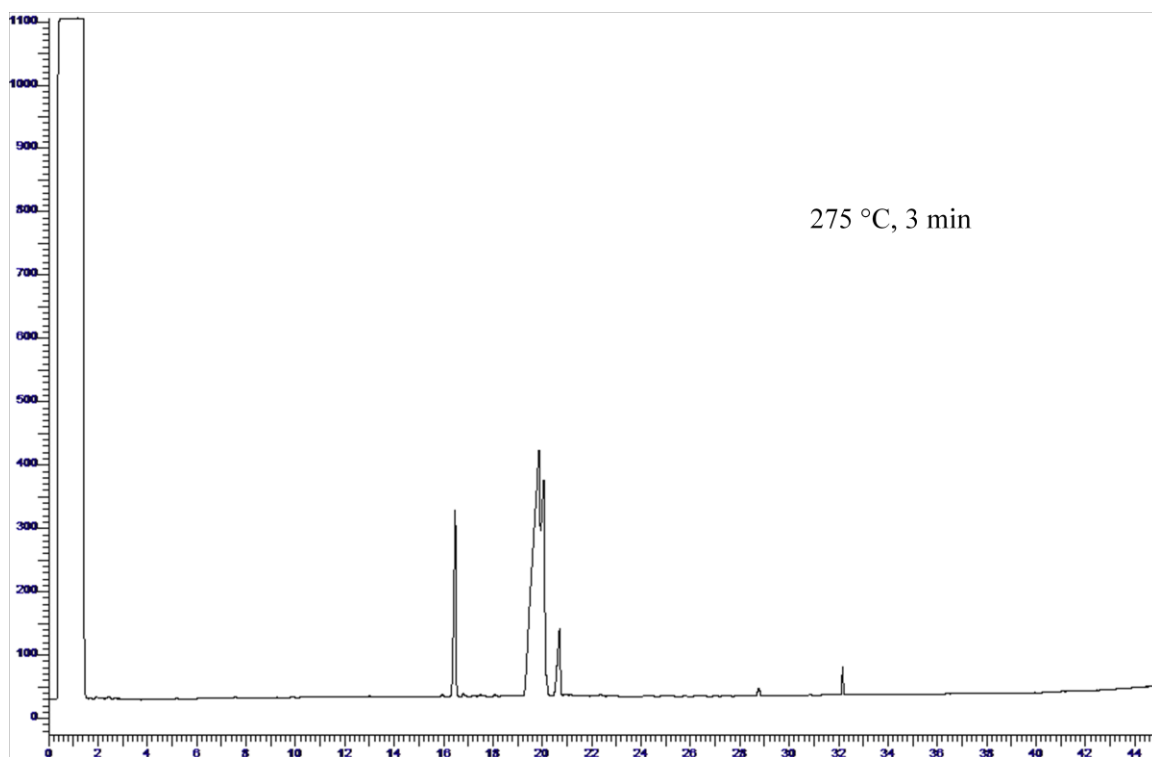


Fig.A- 6 Chromatograms of biodiesel samples thermal stressed at 275 °C for 3 and 8 minutes.

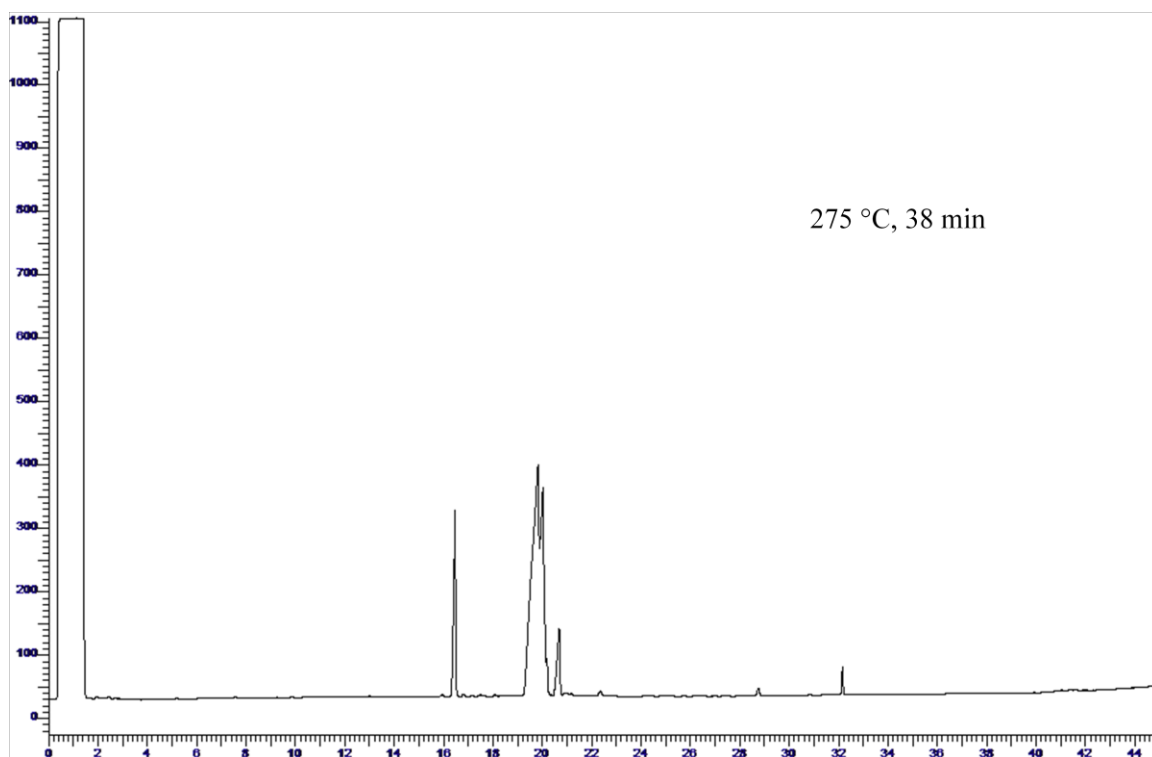
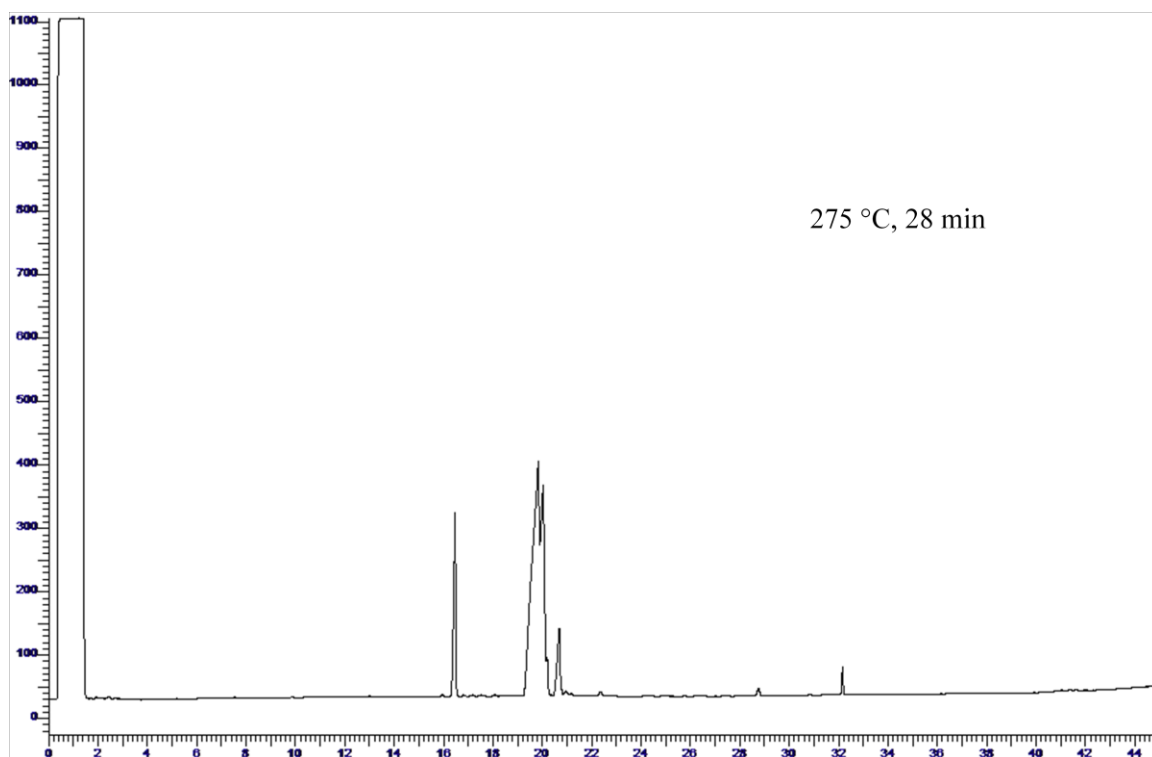


Fig.A- 7 Chromatograms of biodiesel samples thermal stressed at 275 °C for 28 and 38 minutes.

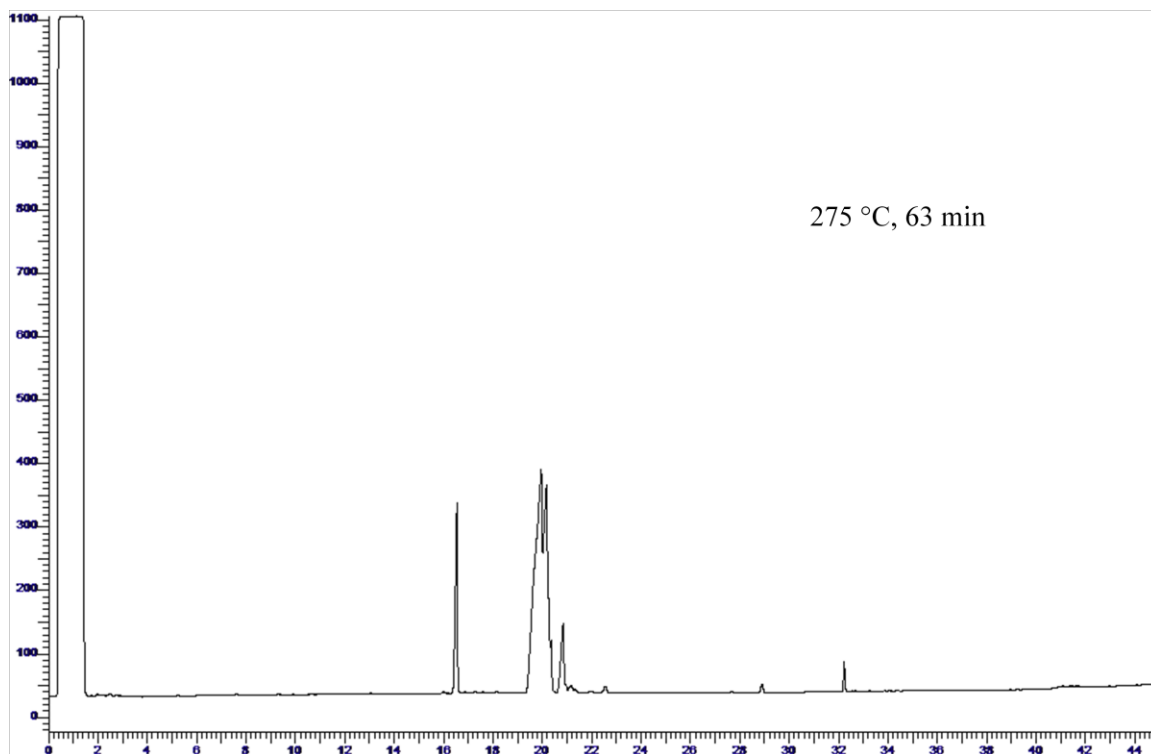


Fig.A- 8 Chromatogram of biodiesel samples thermal stressed at 275 °C for 63 minutes.

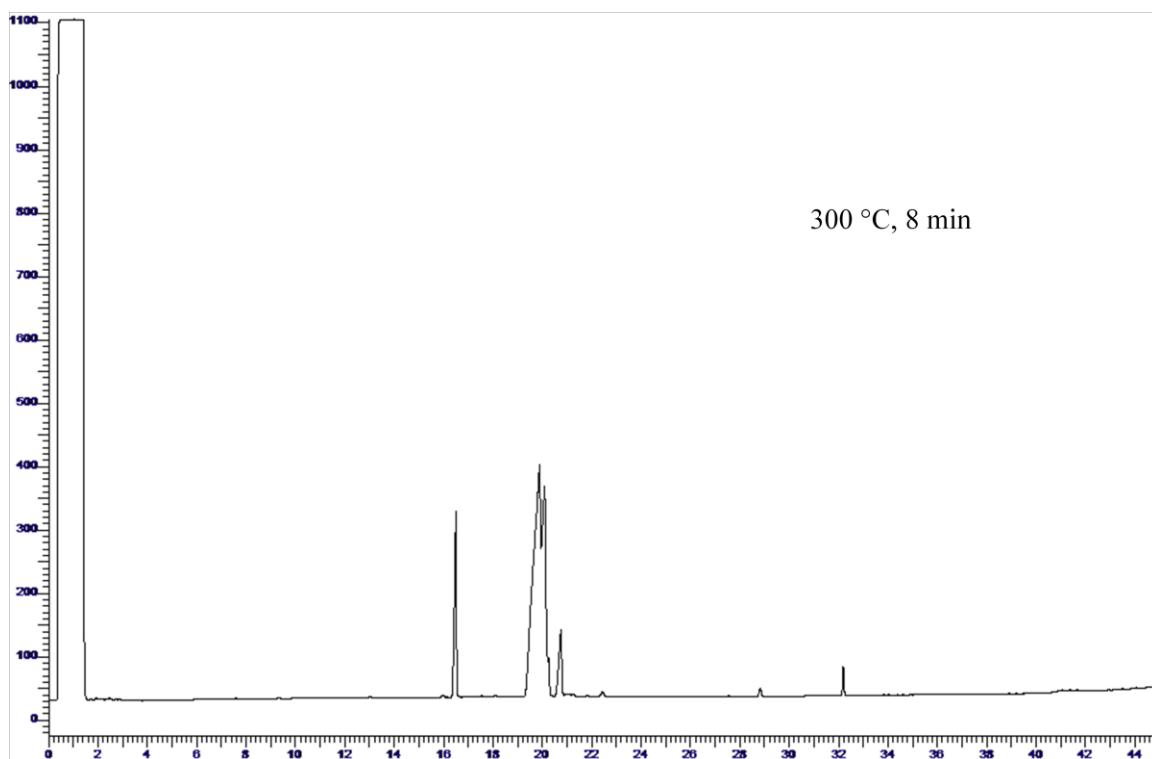
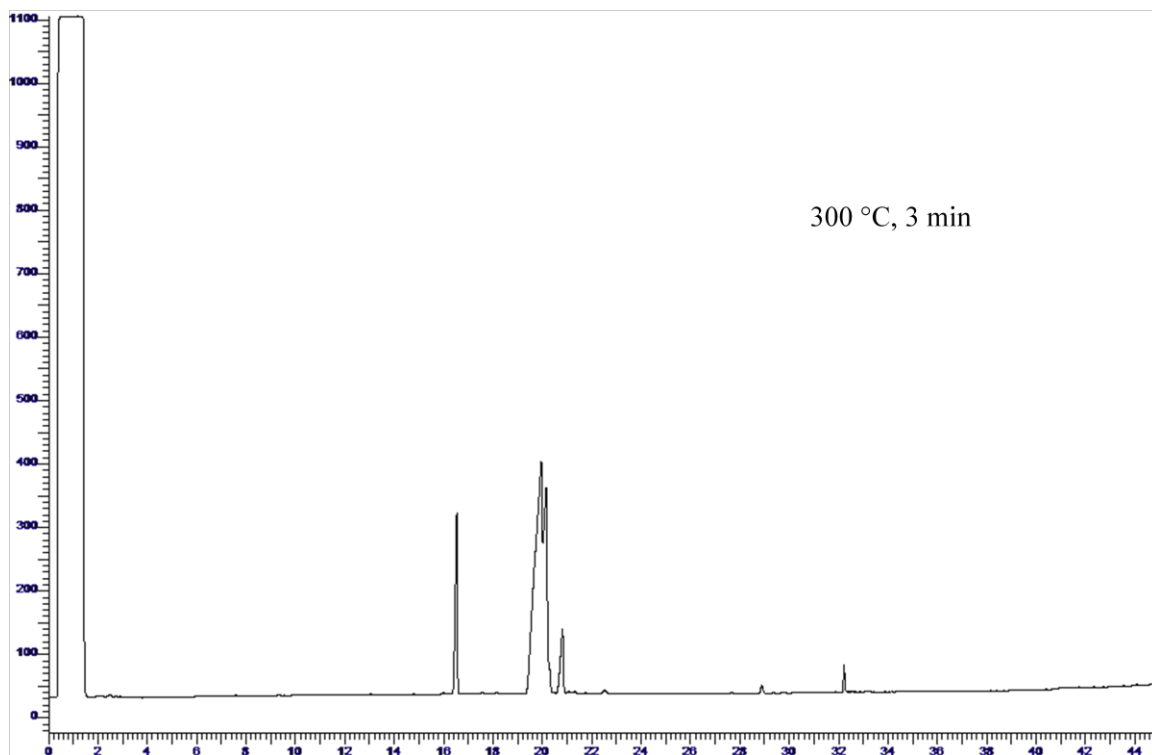


Fig.A- 9 Chromatograms of biodiesel samples thermal stressed at 300 °C for 3 and 8 minutes.

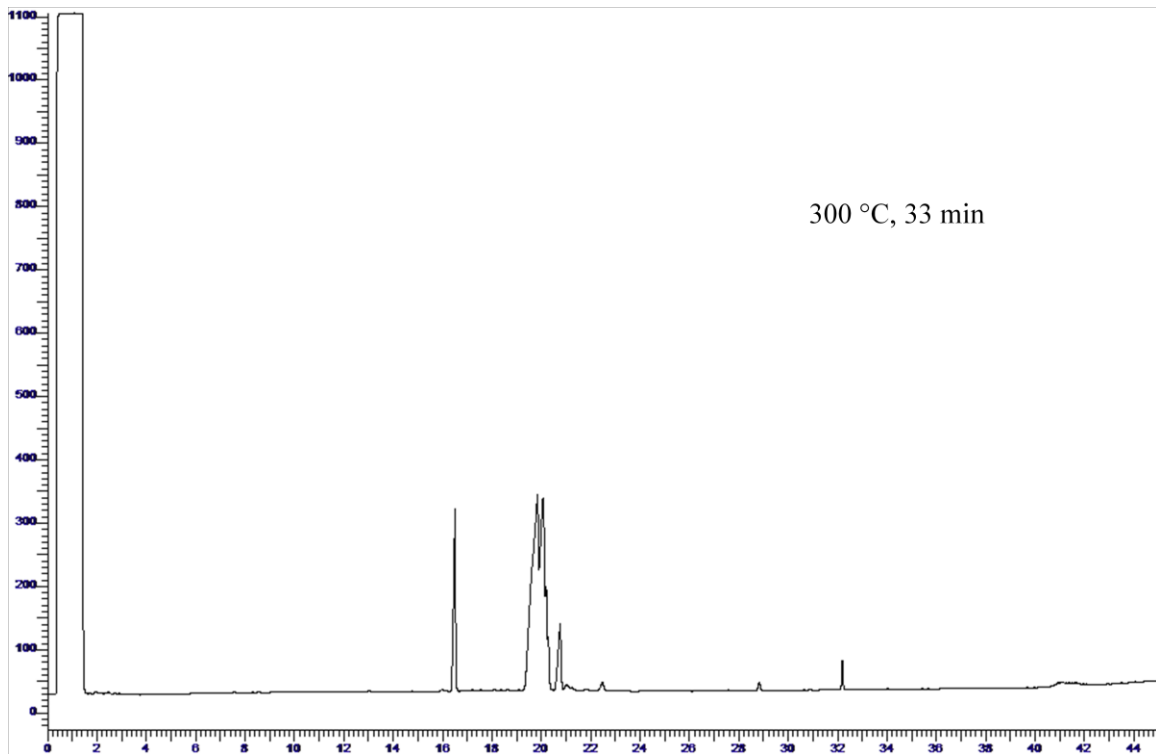
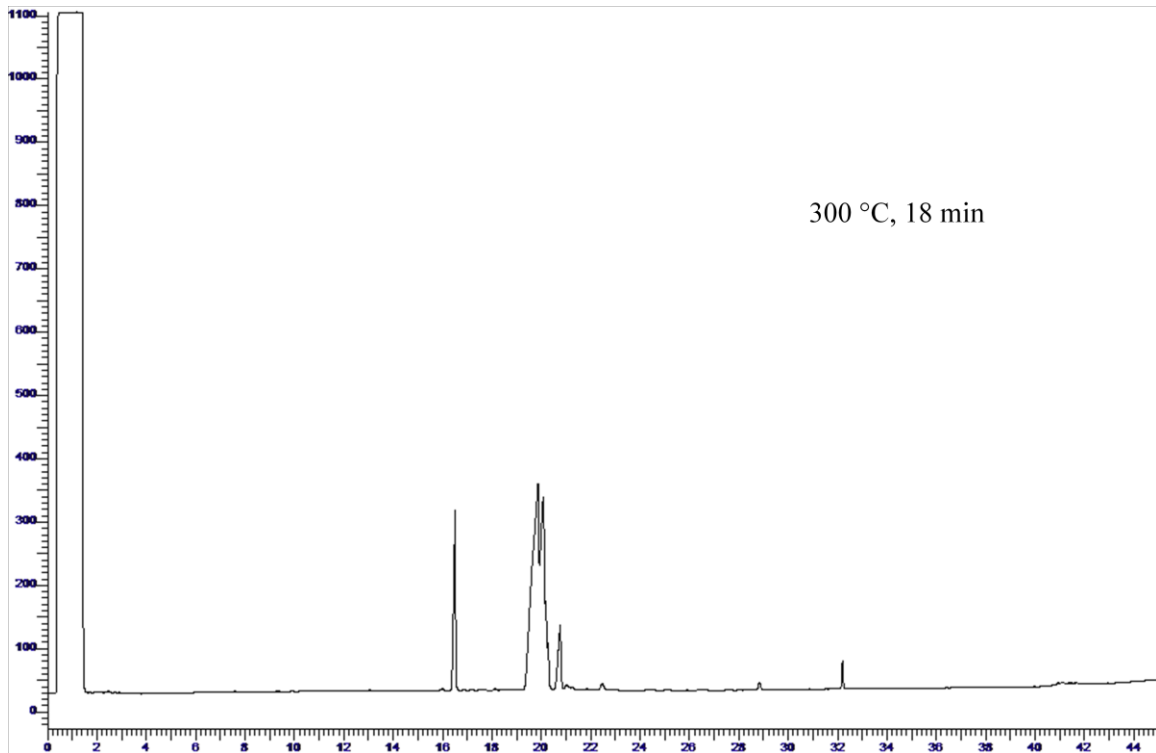


Fig.A- 10 Chromatograms of biodiesel samples thermal stressed at 300 °C for 18 and 33 minutes.

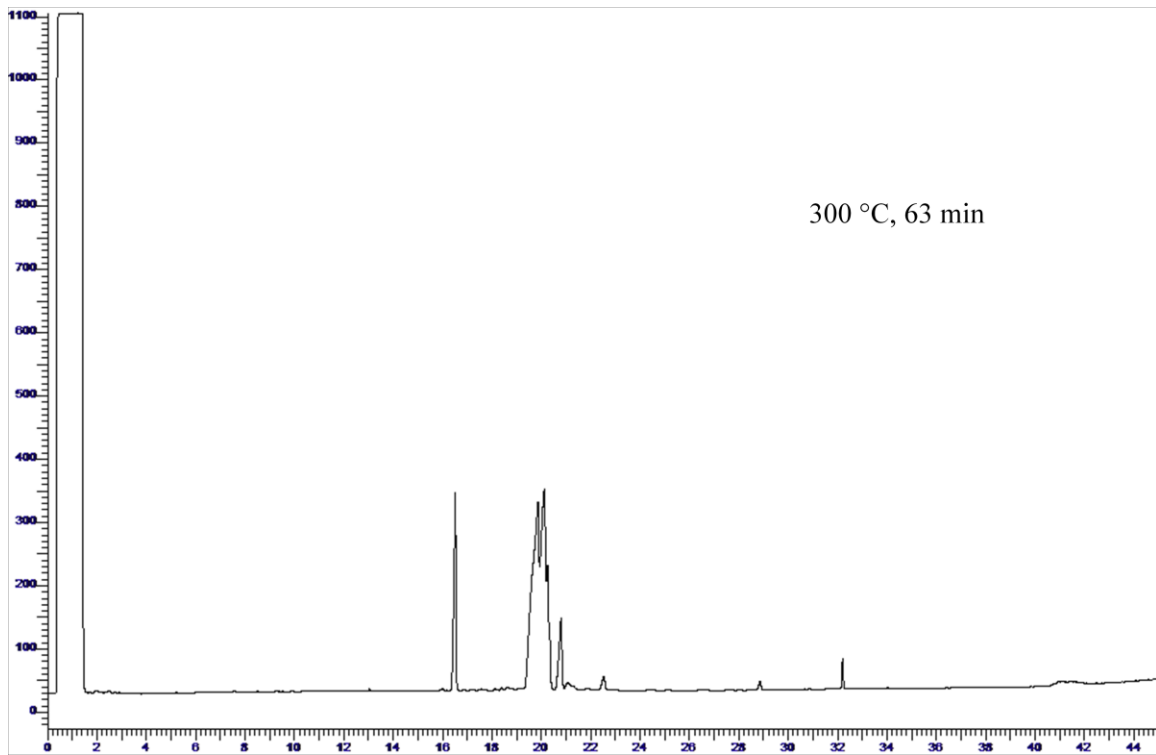


Fig.A- 11 Chromatogram of biodiesel sample thermal stressed at 300 °C for 63 minutes.

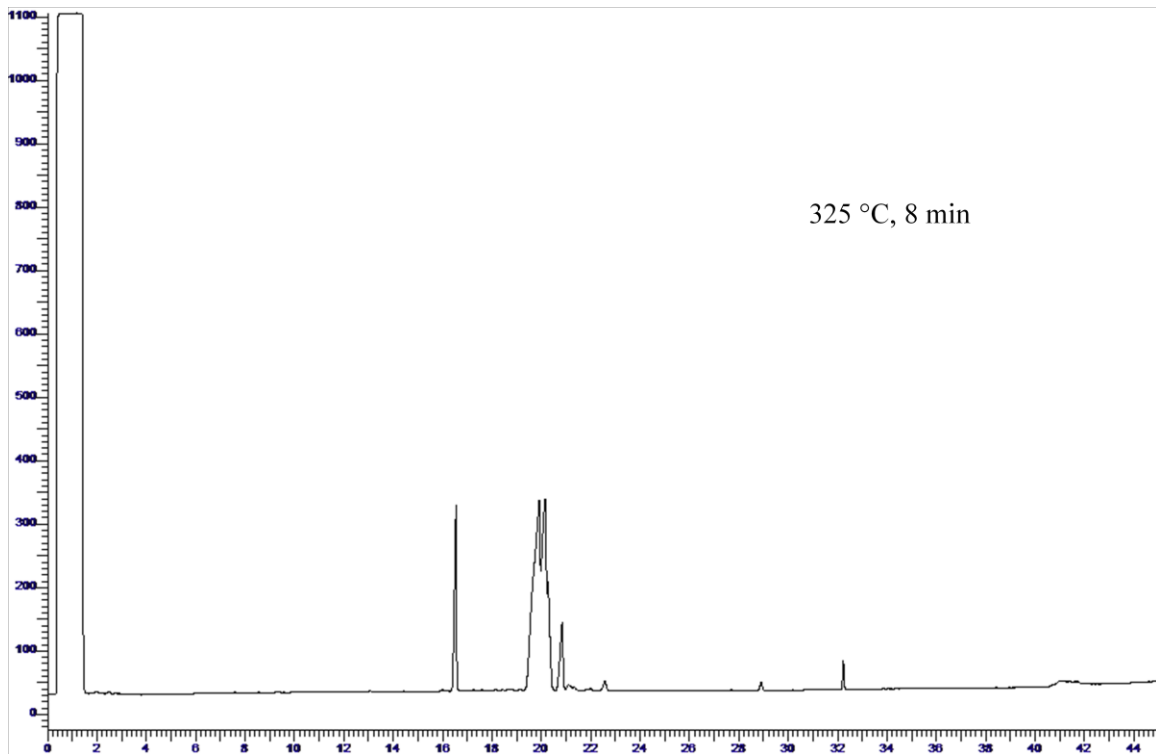
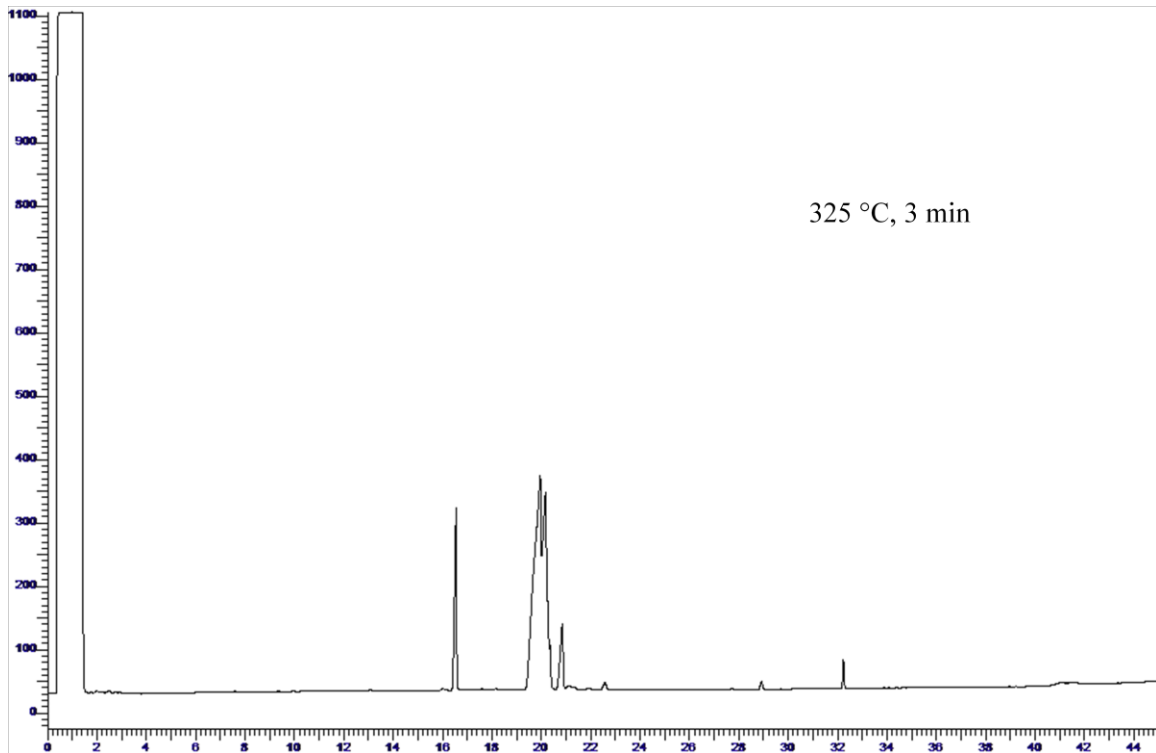


Fig.A- 12 Chromatograms of biodiesel samples thermal stressed at 325 °C for 3 and 8 minutes.

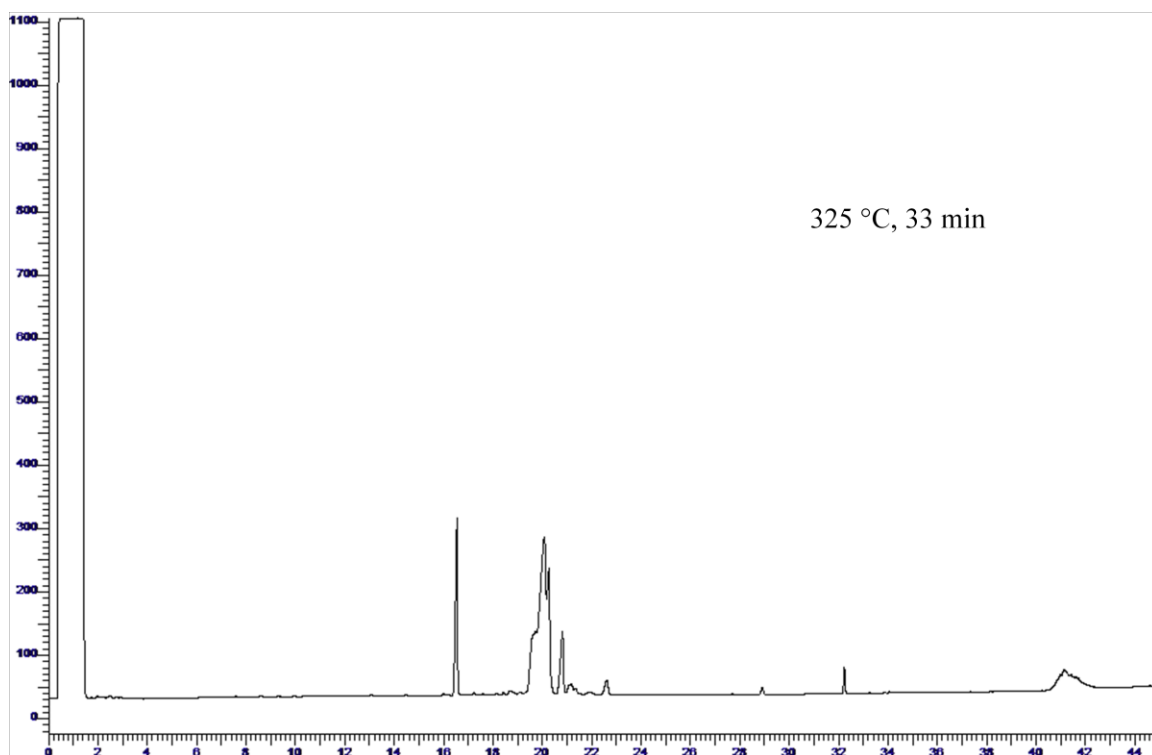
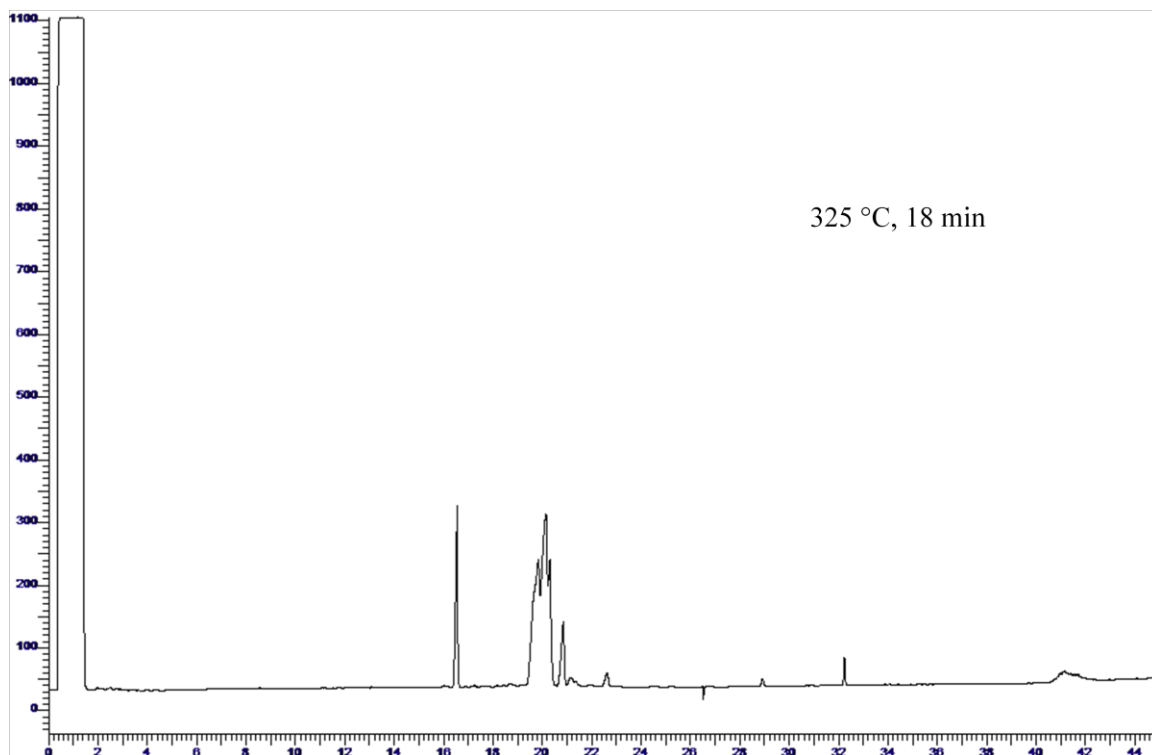


Fig.A- 13 Chromatograms of biodiesel samples thermal stressed at 325 °C for 18 and 33 minutes.

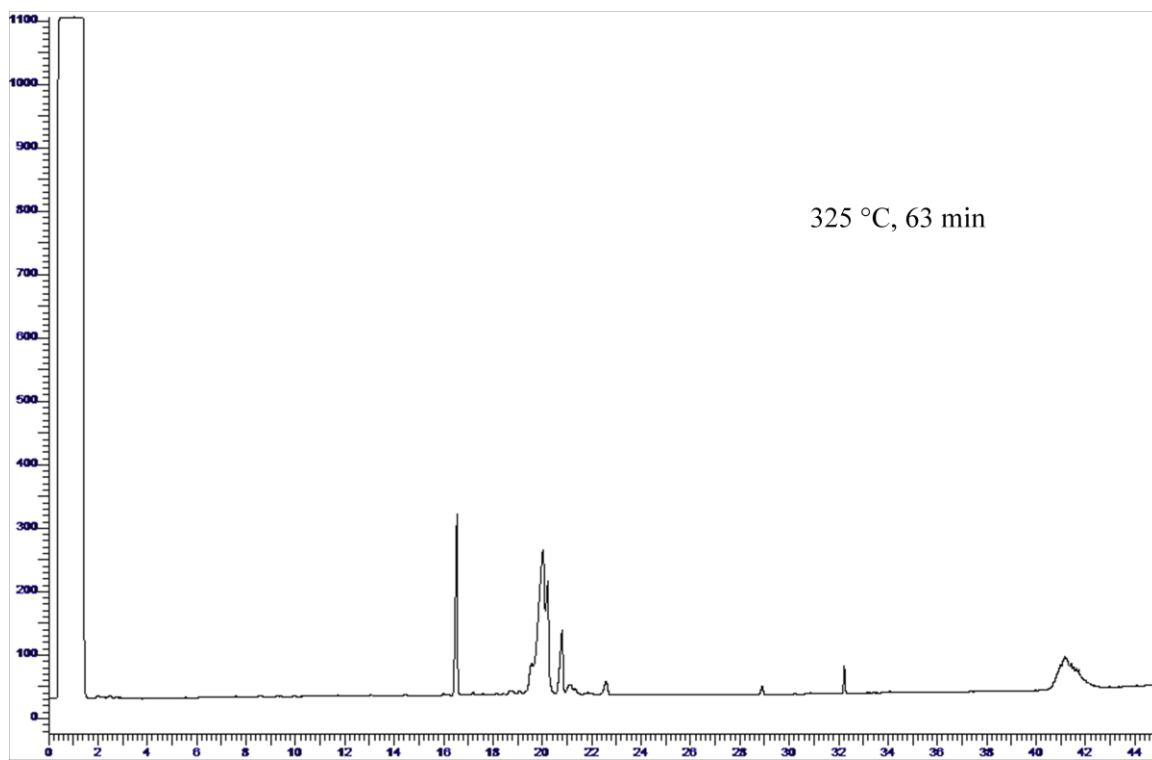


Fig.A- 14 Chromatogram of biodiesel sample thermal stressed at 325 °C for 63 minutes.

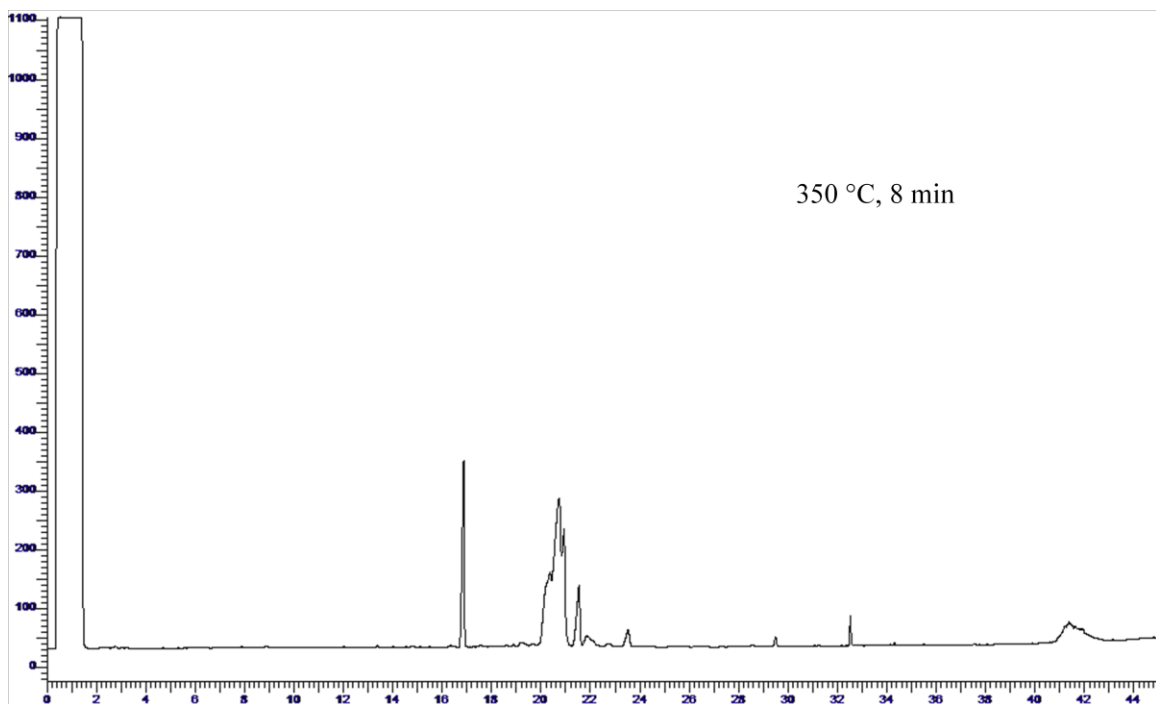
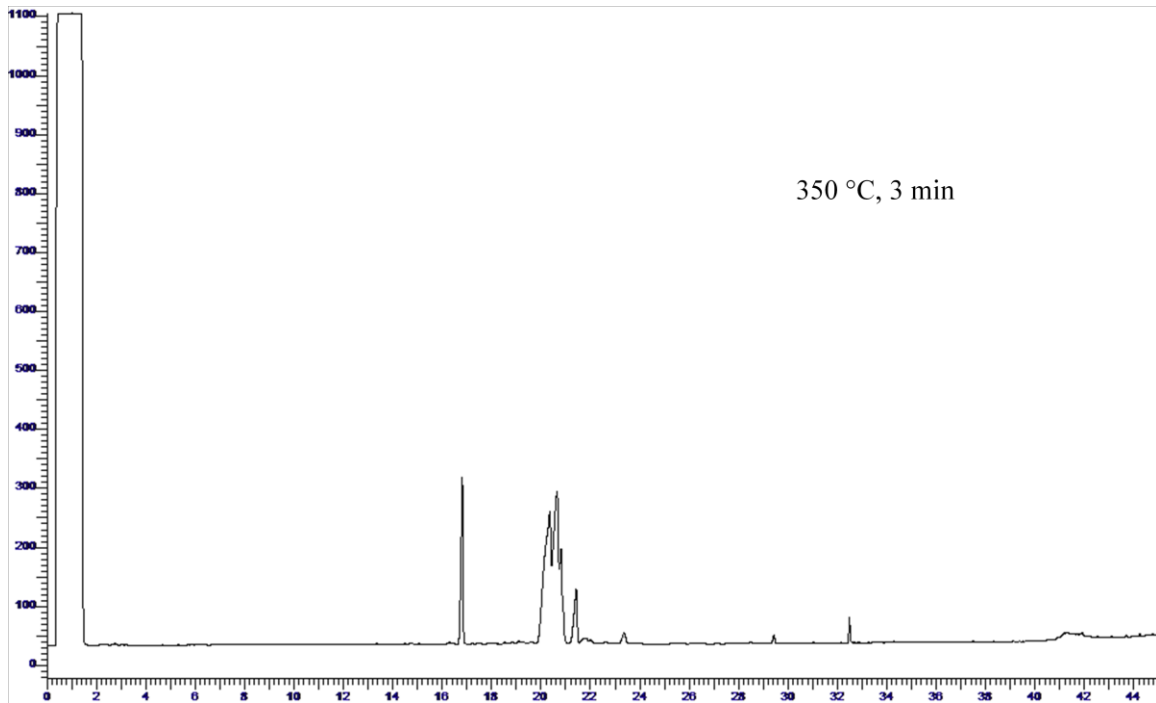


Fig.A- 15 Chromatograms of biodiesel samples thermal stressed at 350 °C for 3 and 8 minutes.

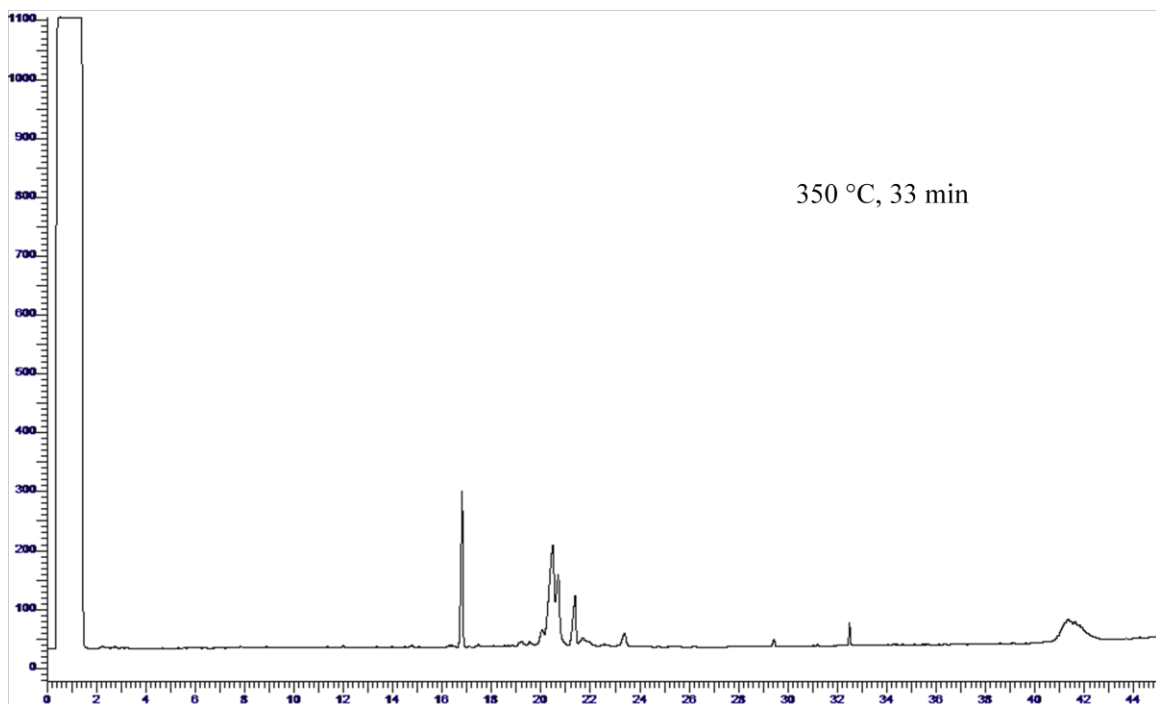
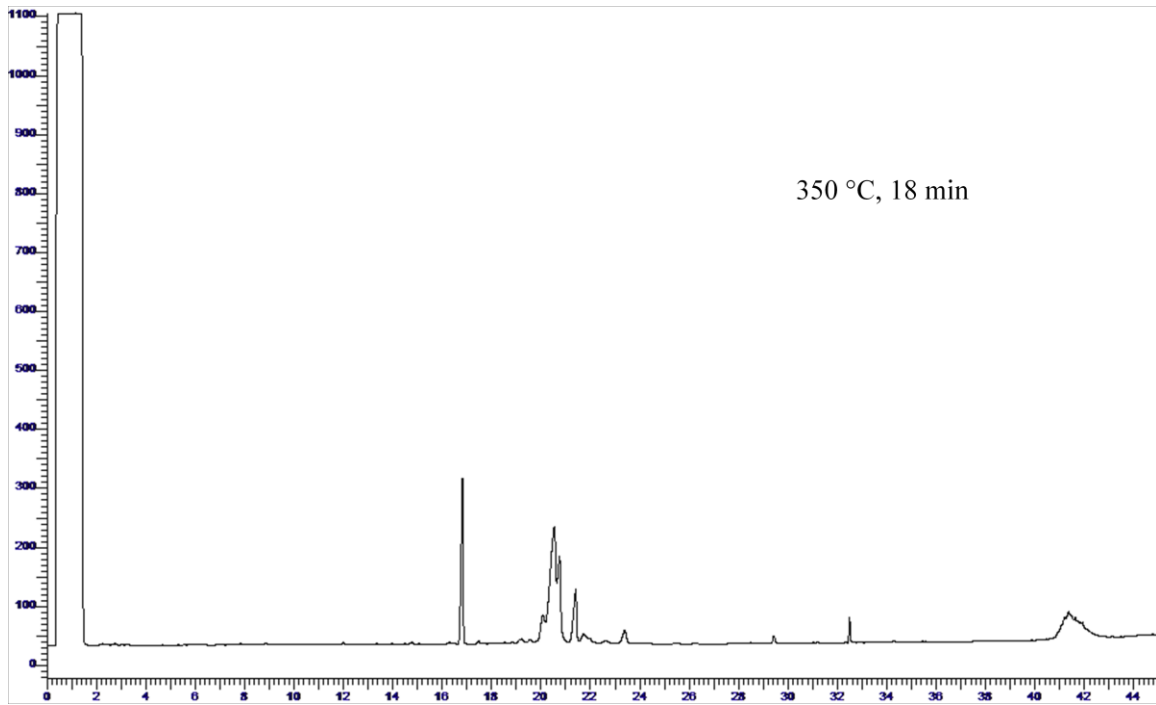


Fig.A- 16 Chromatograms of biodiesel samples thermal stressed at 350 °C for 18 and 33 minutes.

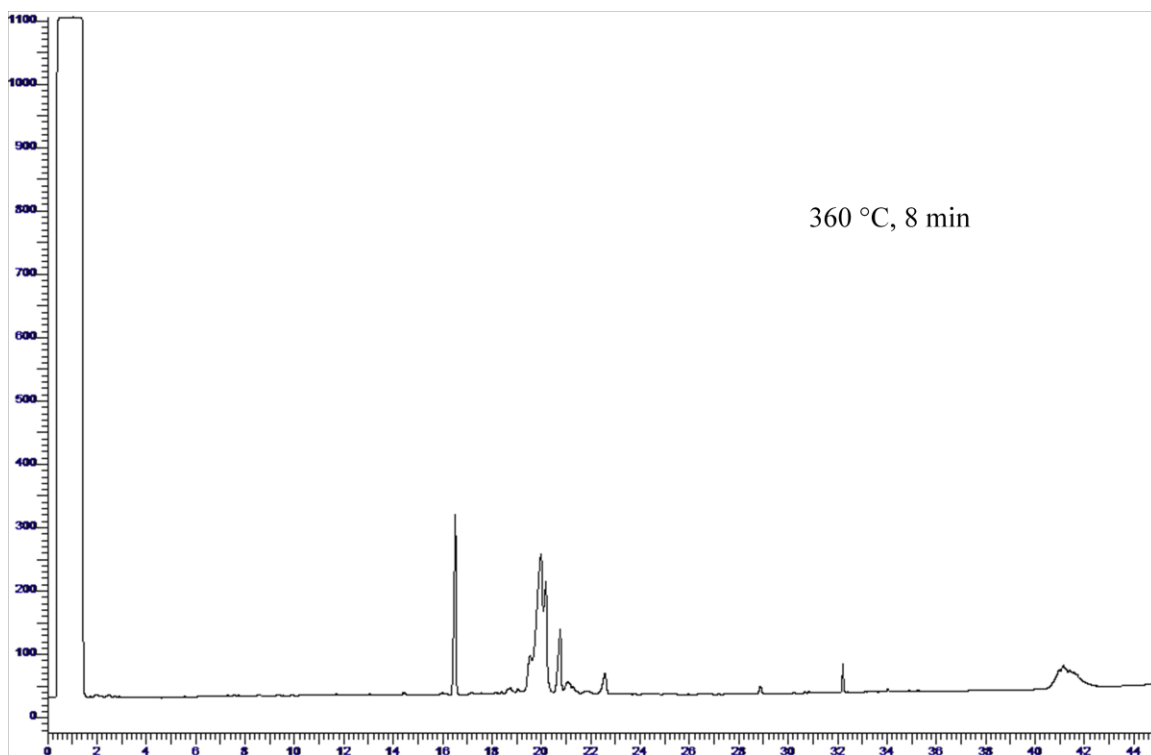
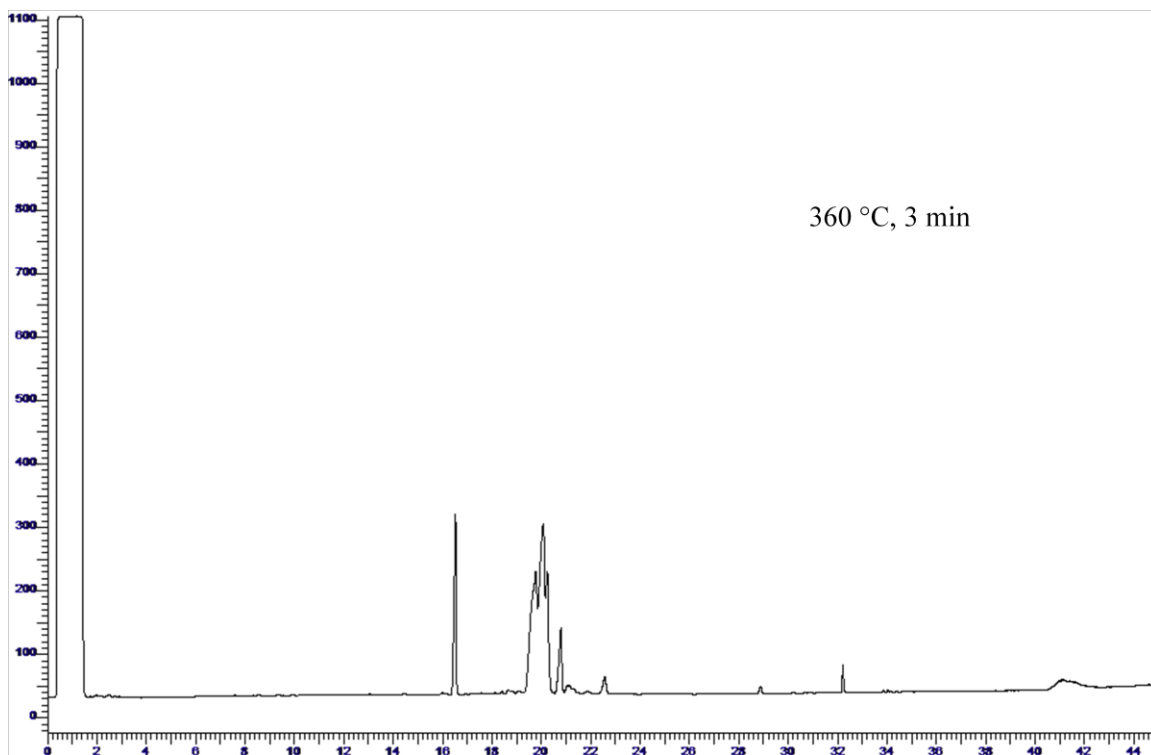


Fig.A- 17 Chromatograms of biodiesel samples thermal stressed at 360 °C for 3 and 8 minutes.

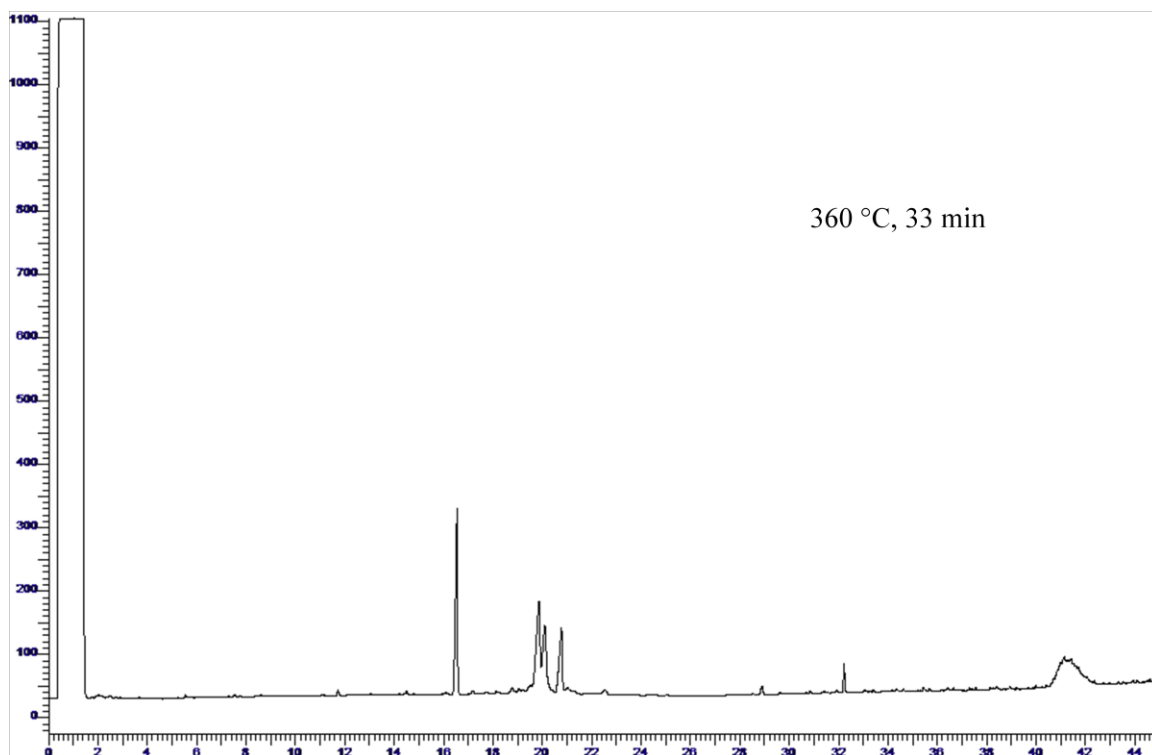
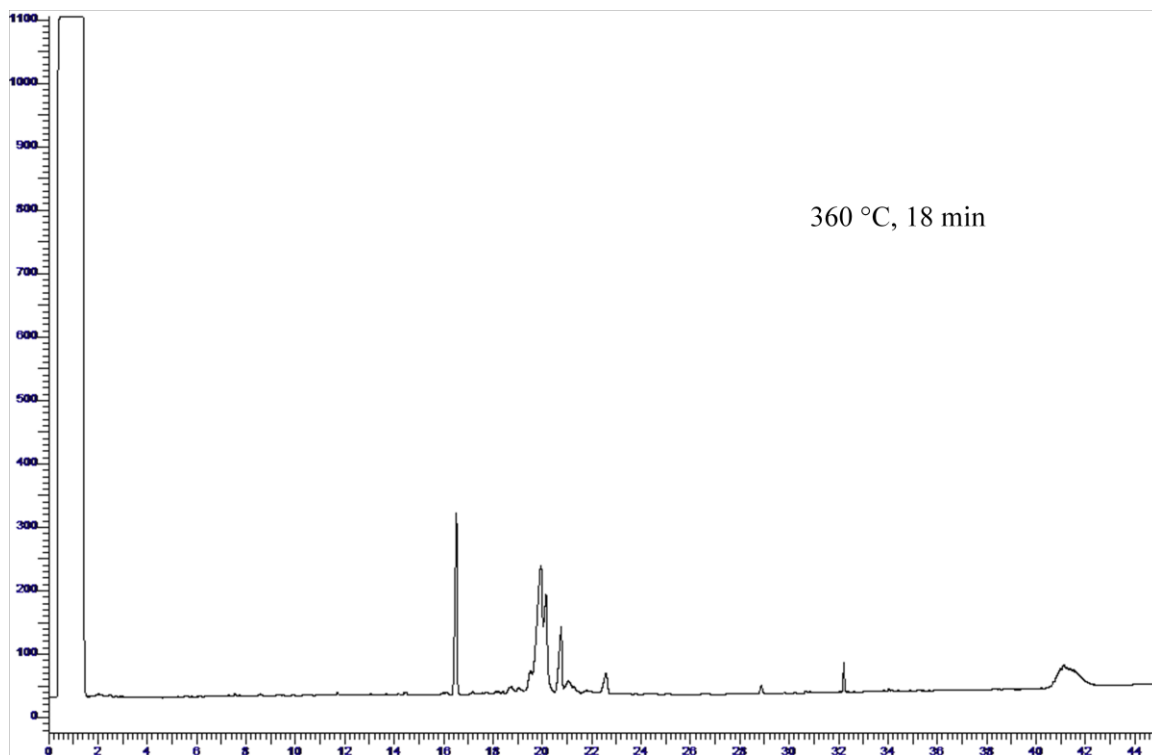


Fig.A- 18 Chromatograms of biodiesel samples thermal stressed at 360 °C for 18 and 33 minutes.

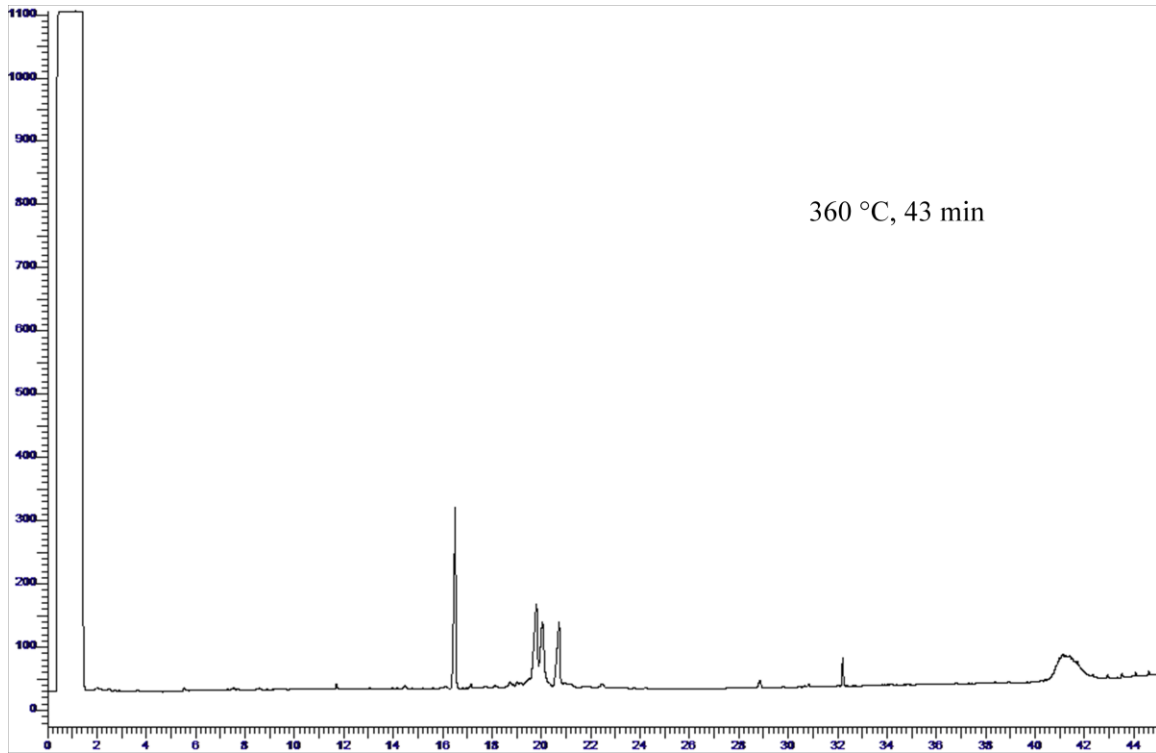


Fig.A- 19 Chromatogram of biodiesel sample thermal stressed at 360 °C for 43 minutes.

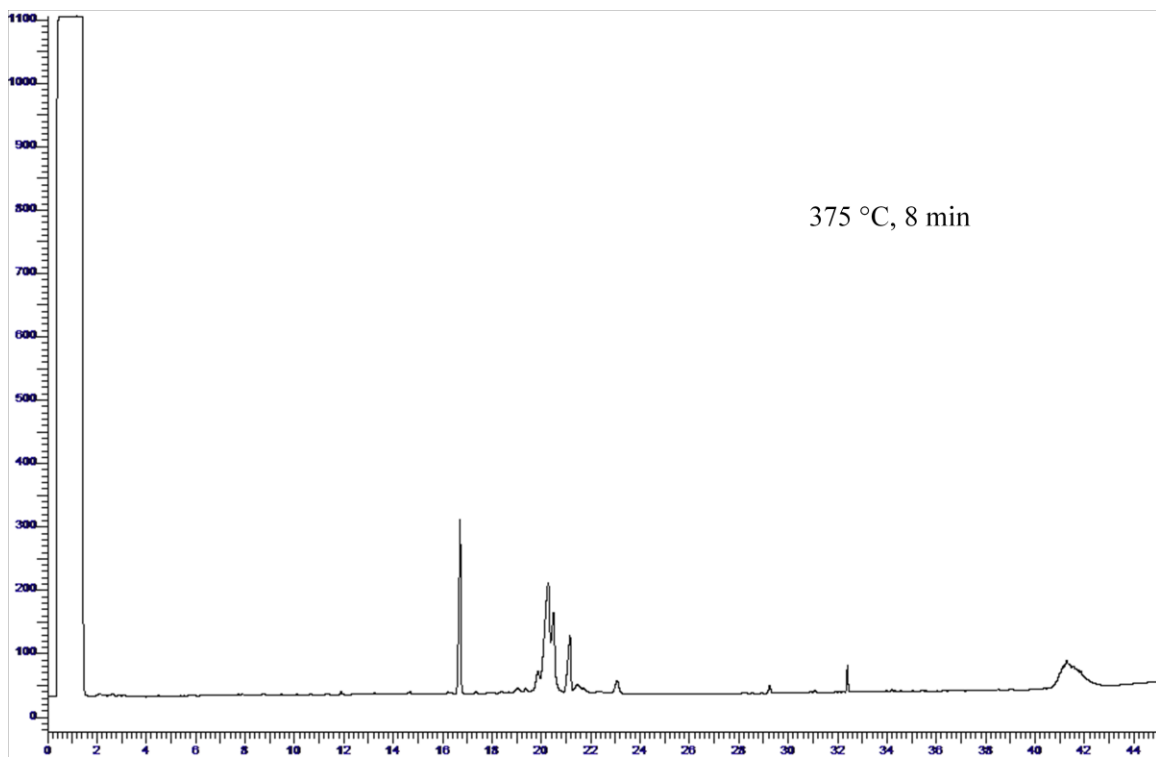
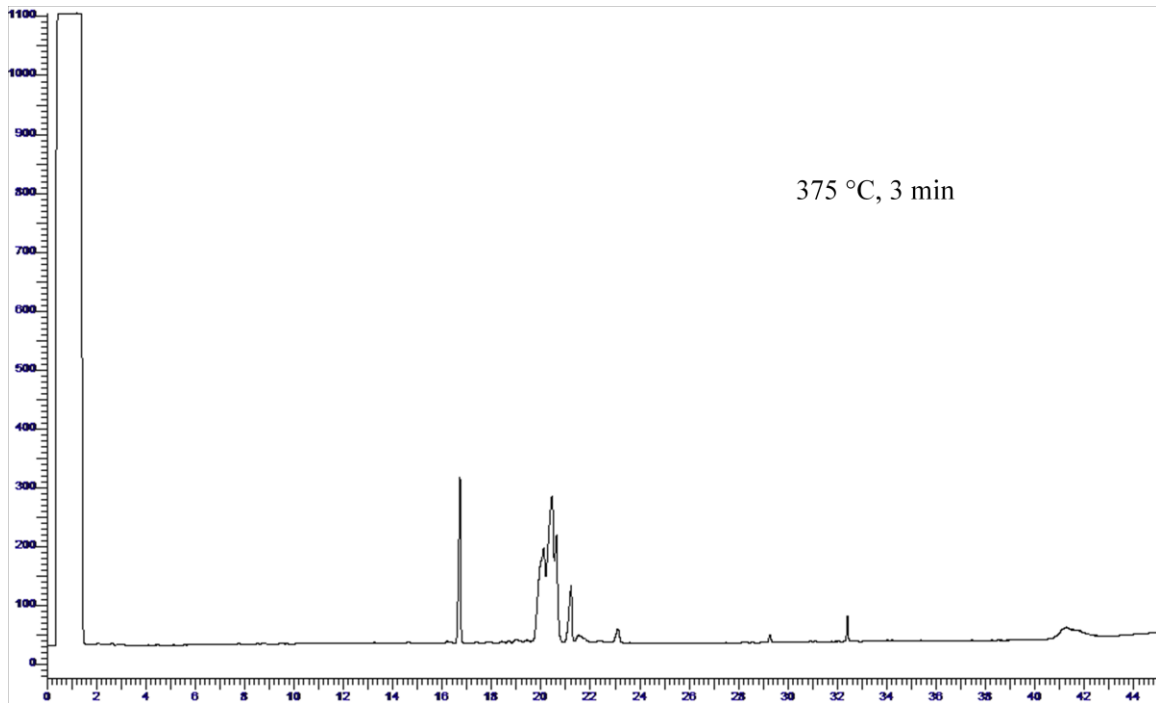


Fig.A- 20 Chromatograms of biodiesel samples thermal stressed at 375 °C for 3 and 8 minutes.

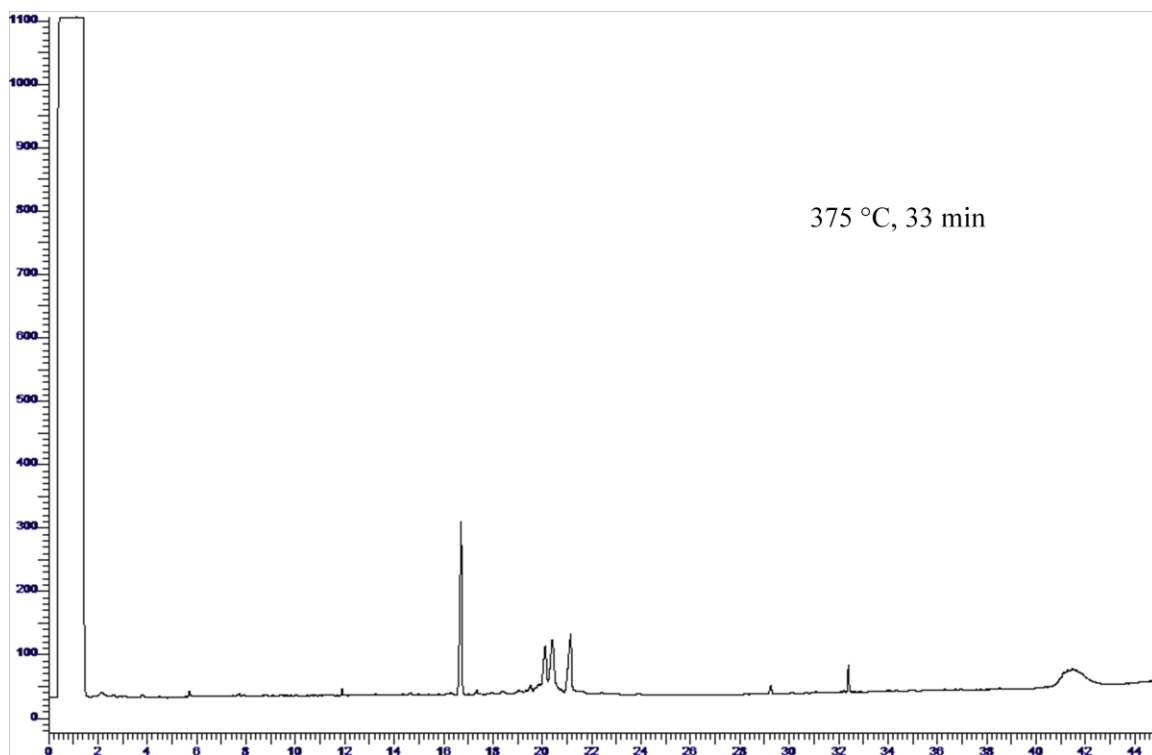
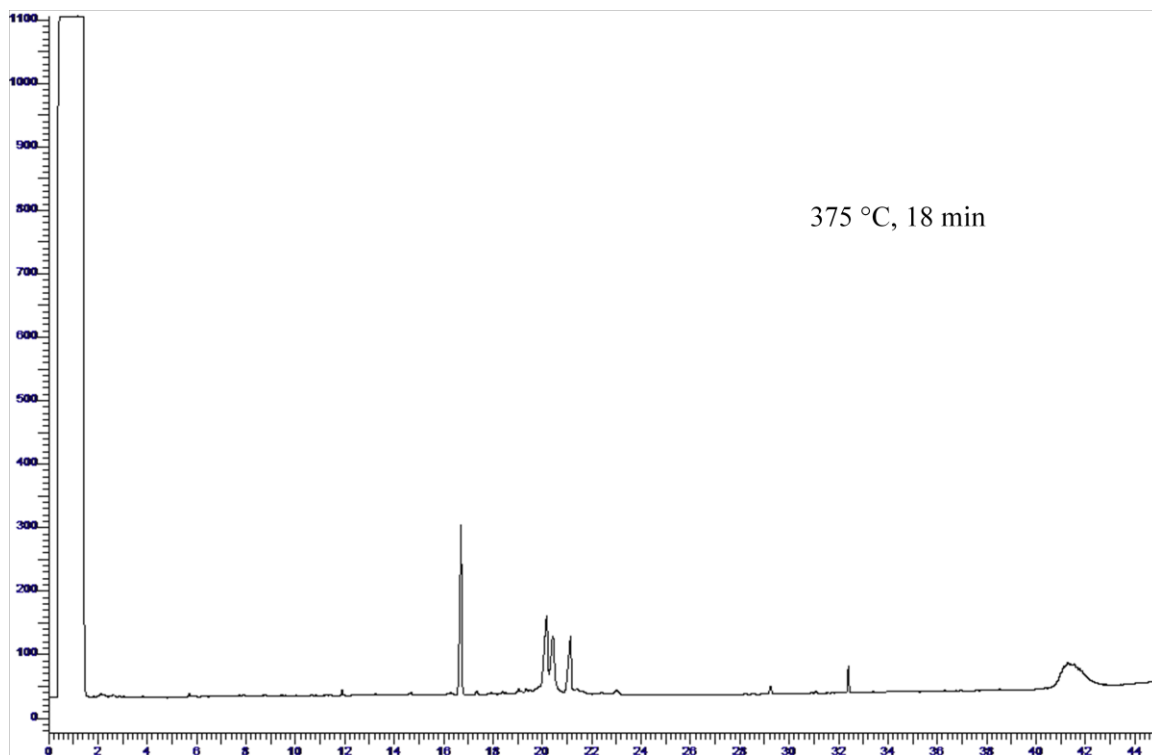


Fig-A- 21 Chromatograms of biodiesel samples thermal stressed at 375 °C for 18 and 33 minutes.

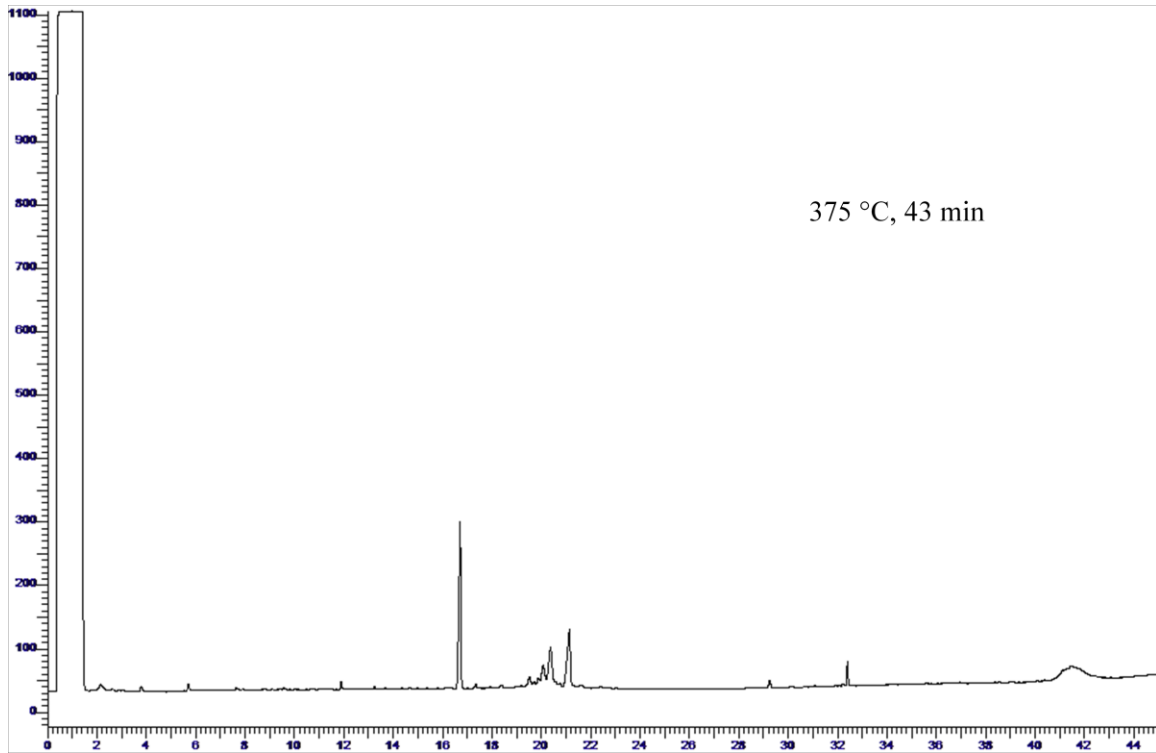


Fig.A- 22 Chromatogram of biodiesel sample thermal stressed at 375 °C for 43 minutes.

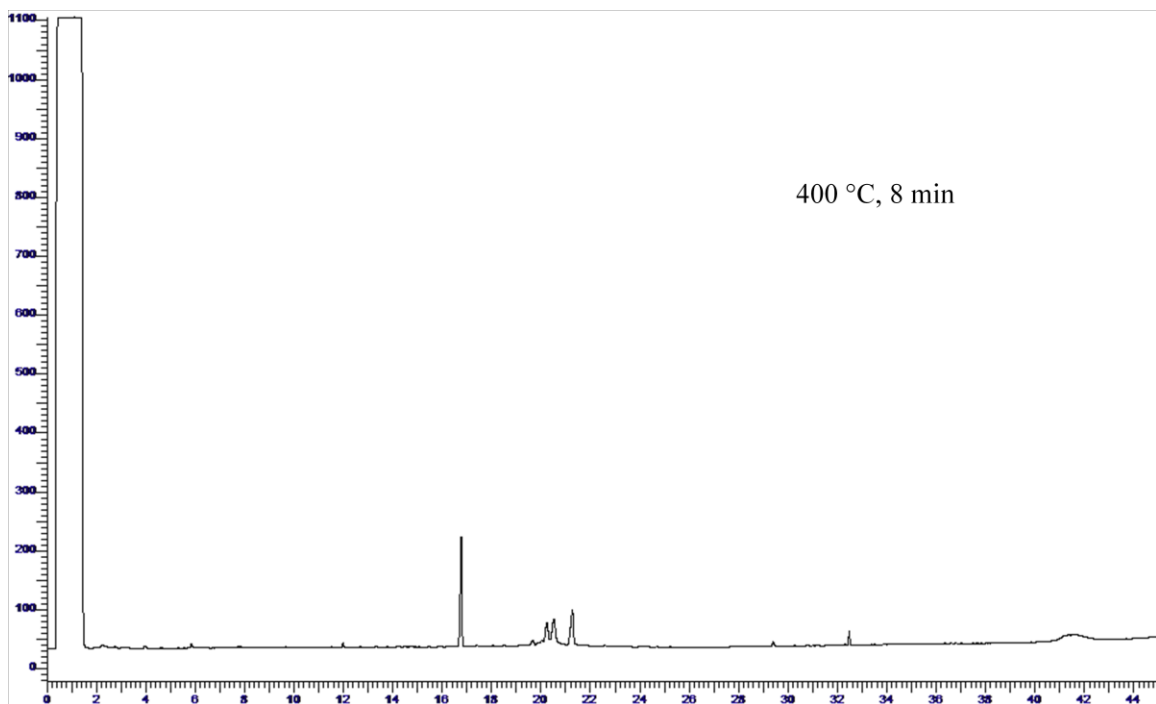
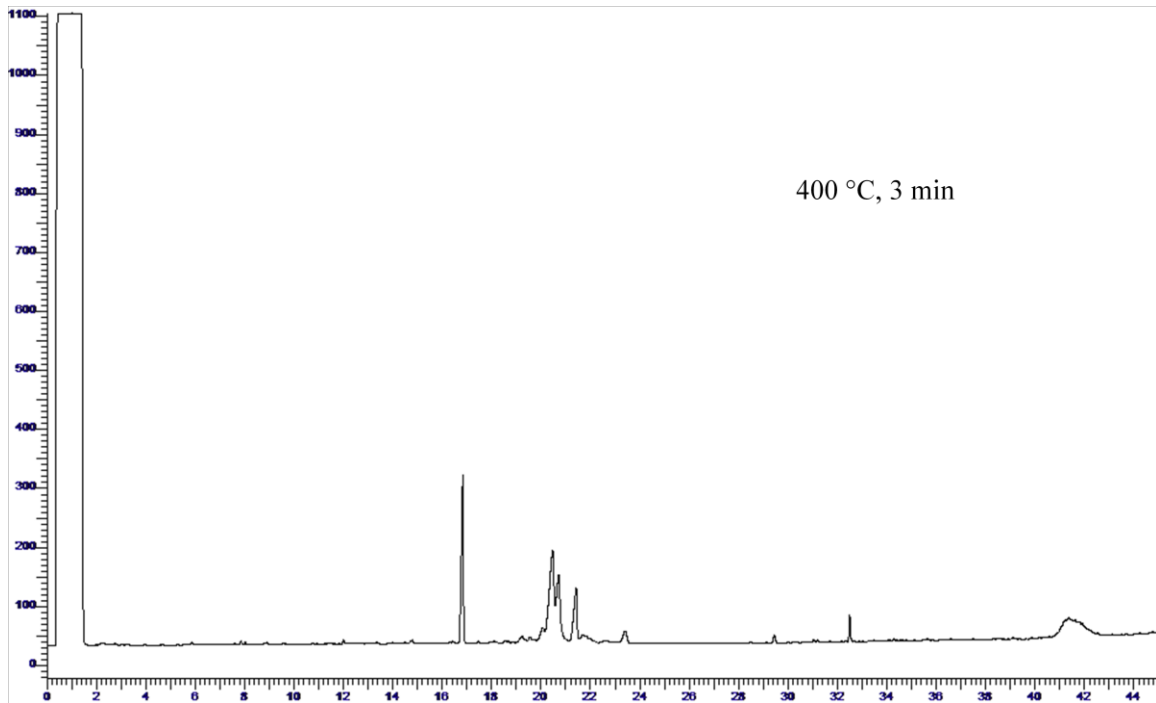


Fig.A- 23 Chromatograms of biodiesel samples thermal stressed at 400 °C for 3 and 8 minutes.

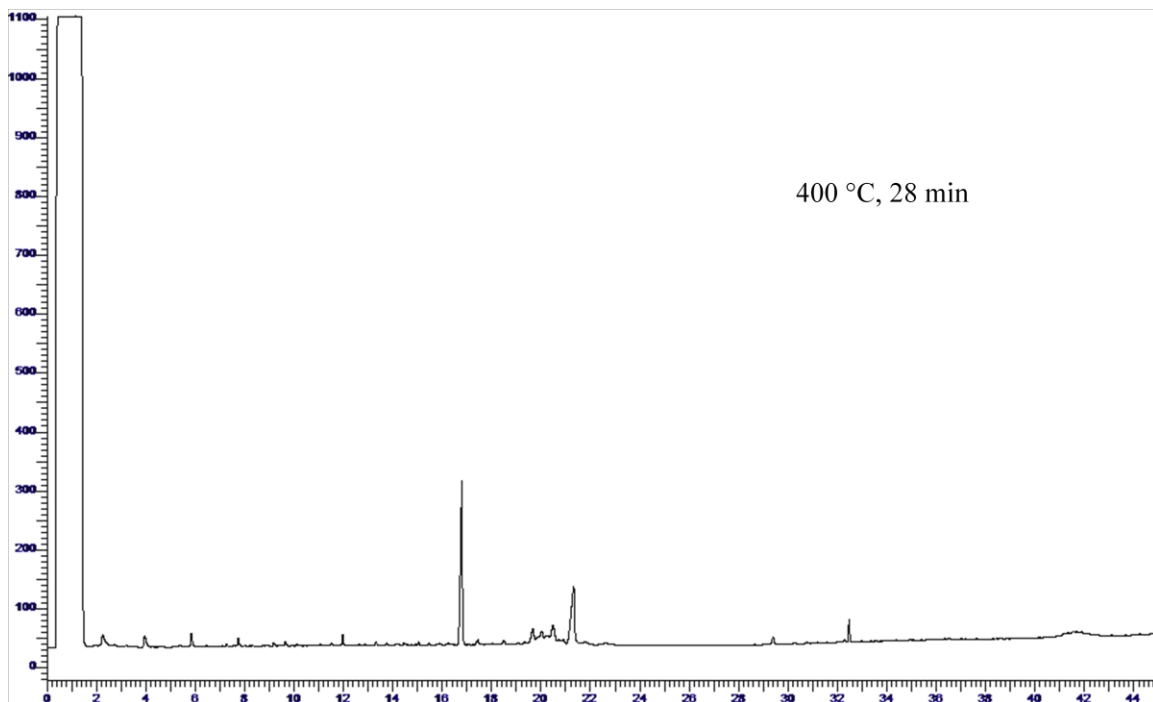
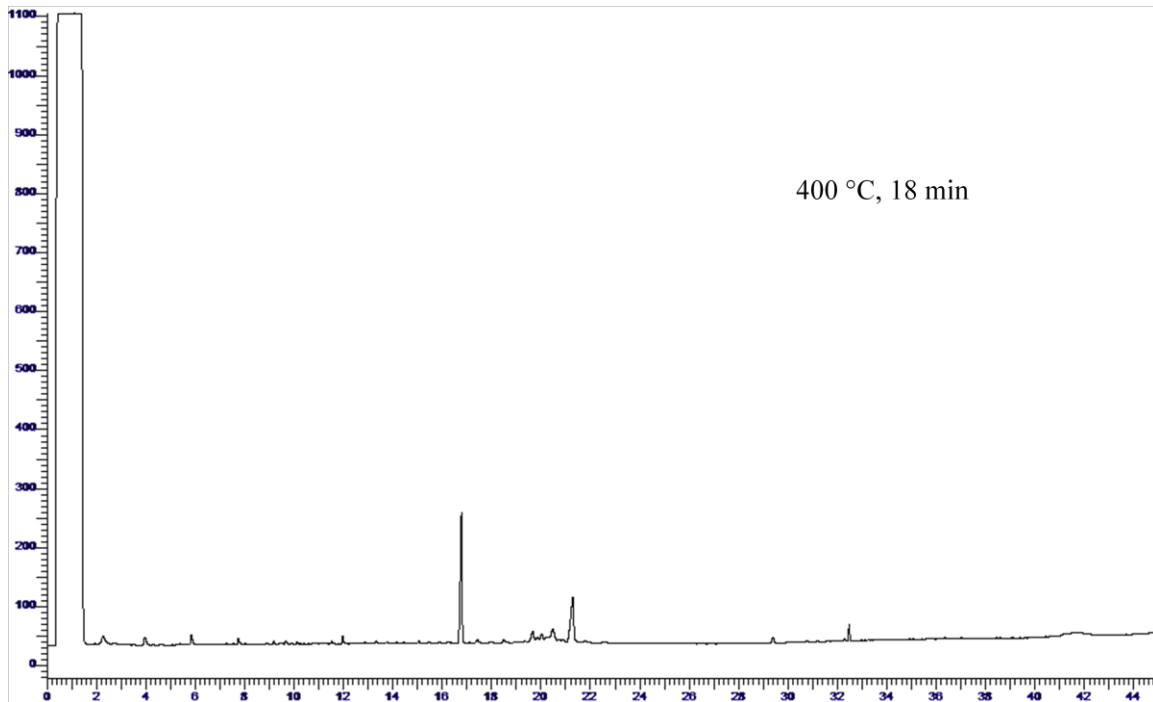


Fig.A- 24 Chromatograms of biodiesel samples thermal stressed at 400 °C for 18 and 28 minutes.

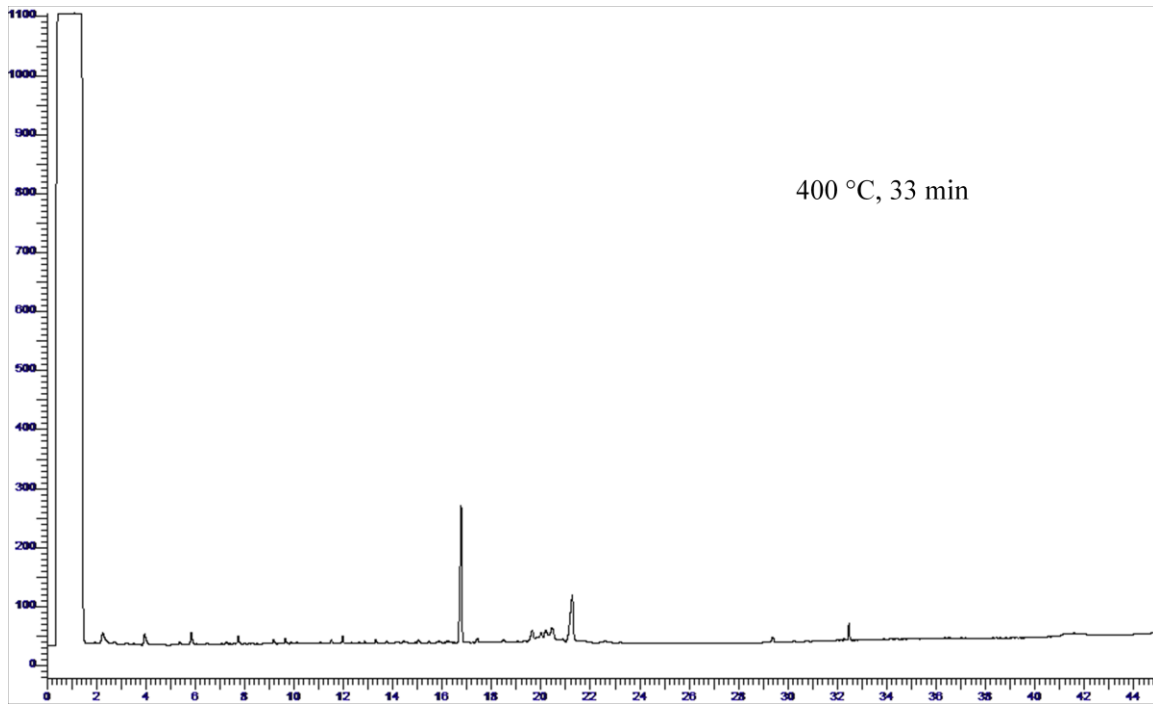


Fig.A- 25 Chromatogram of biodiesel sample thermal stressed at 400 °C for 33 minutes.

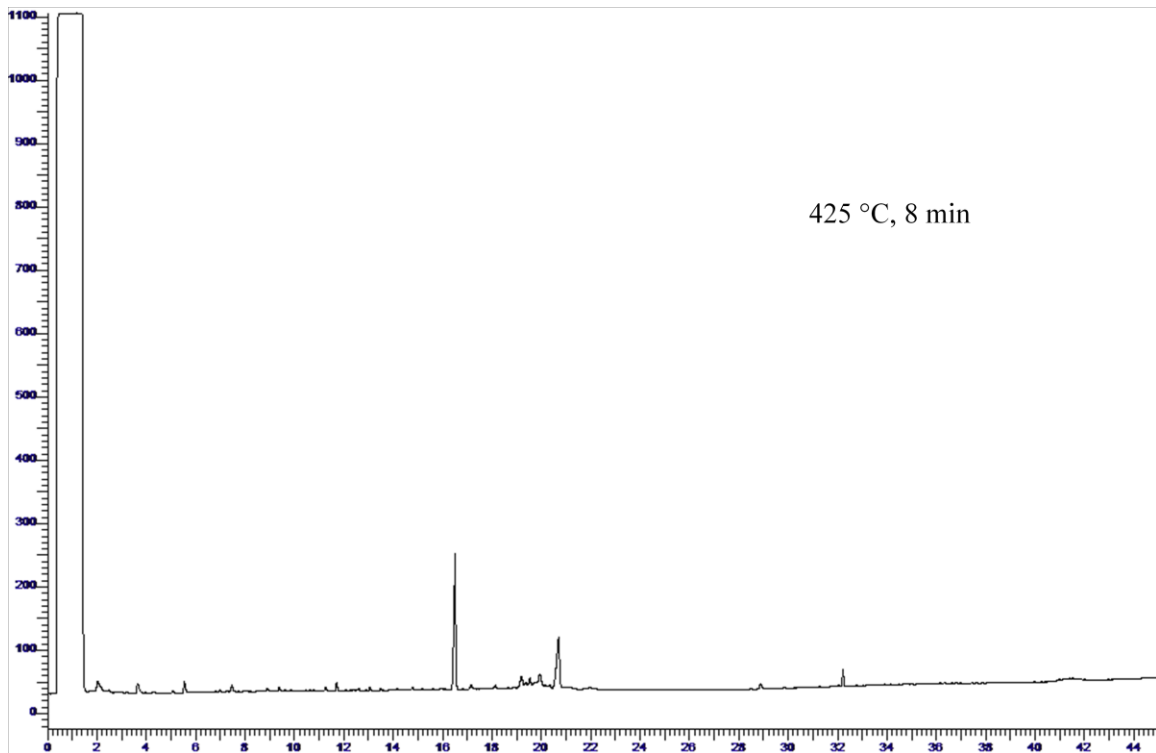
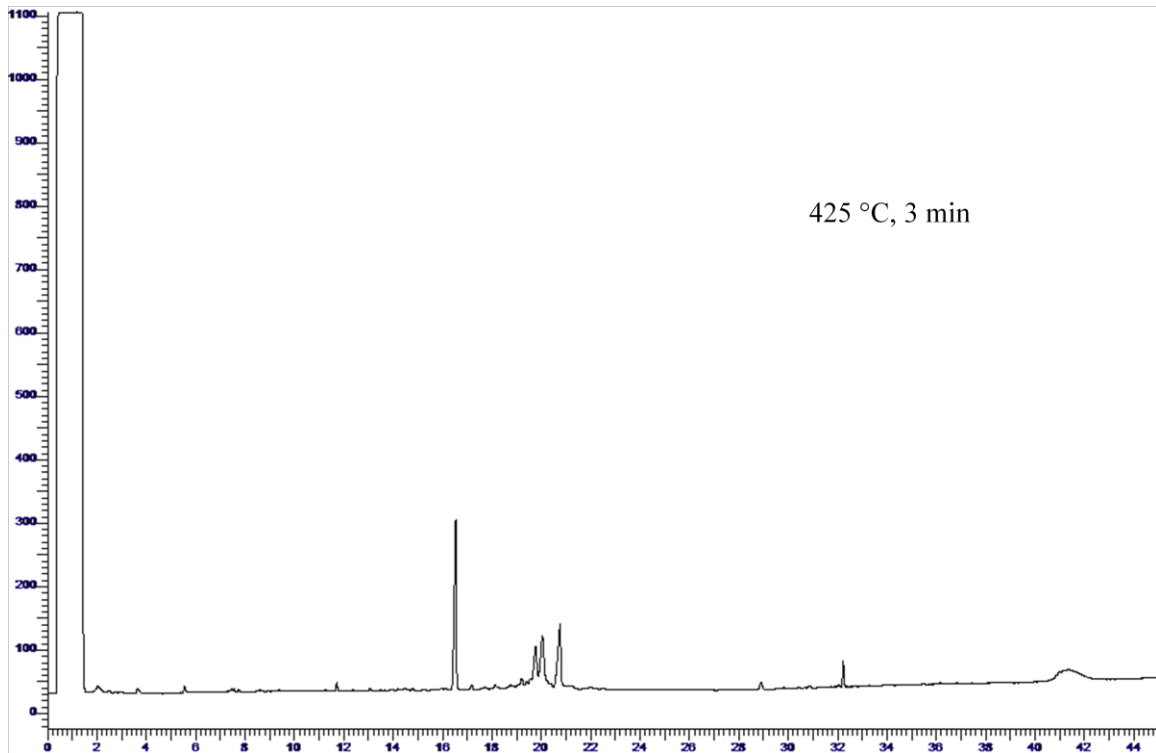


Fig-A- 26 Chromatograms of biodiesel samples thermal stressed at 425 °C for 3 and 8 minutes.

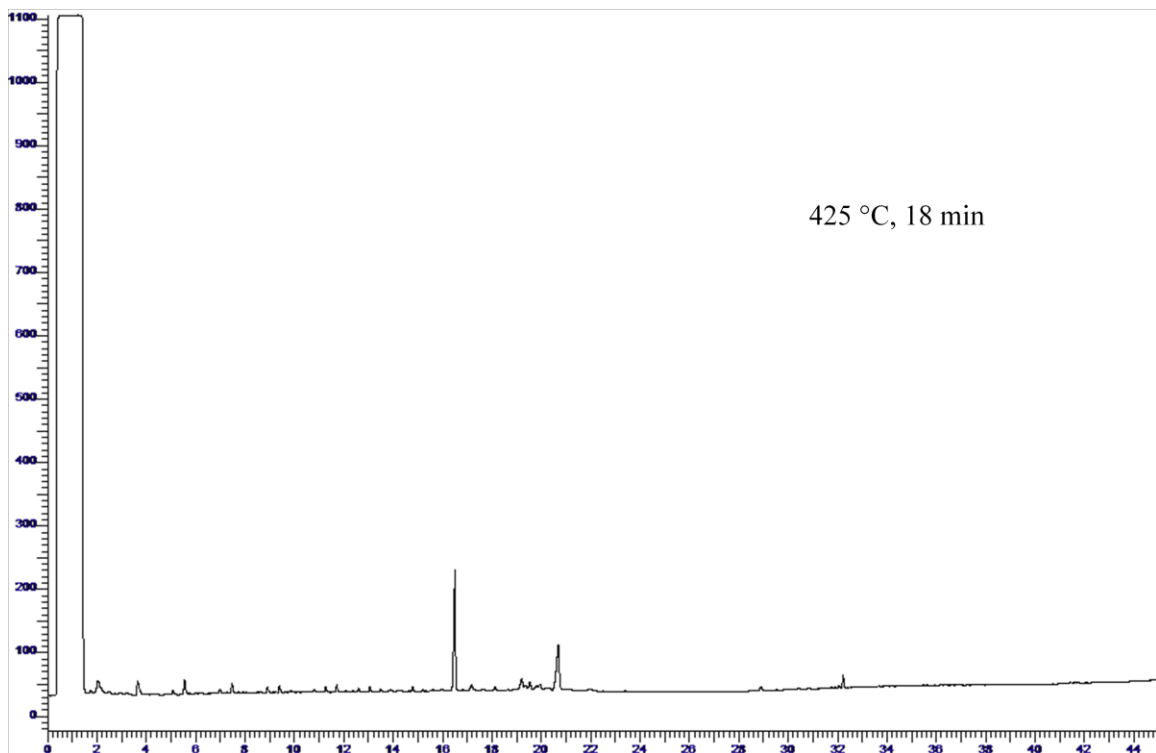
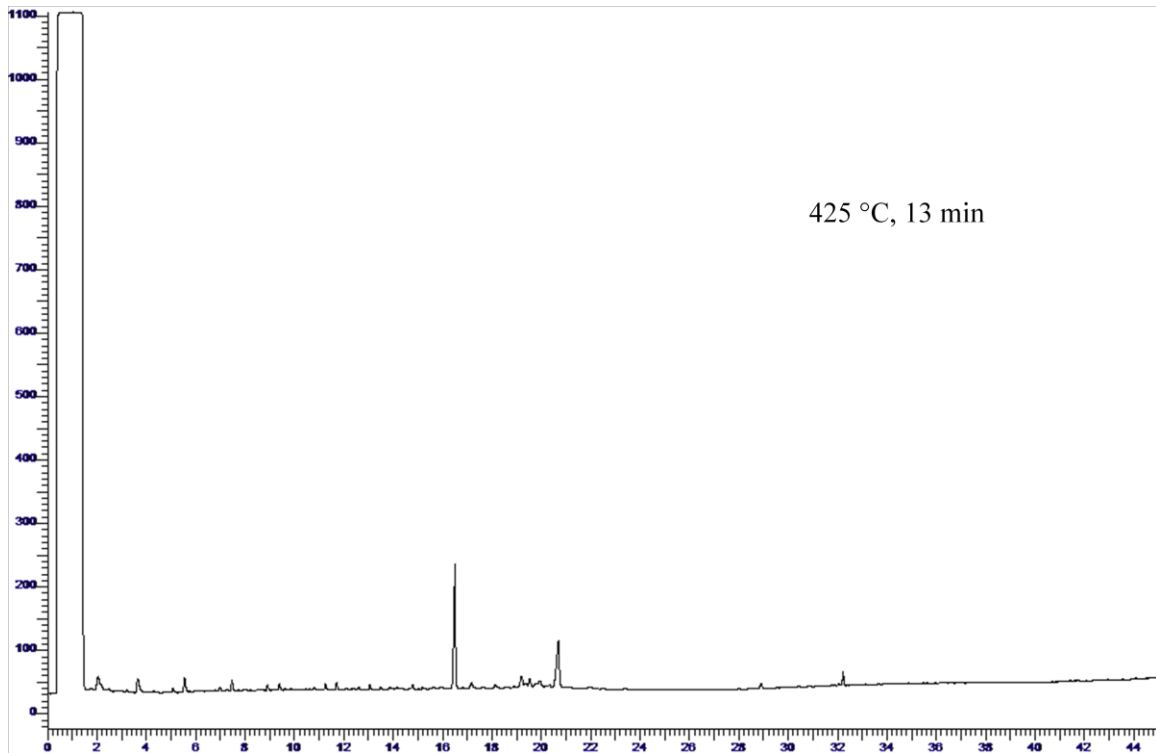


Fig-A- 27 Chromatograms of biodiesel samples thermal stressed at 425 °C for 13 and 18 minutes.

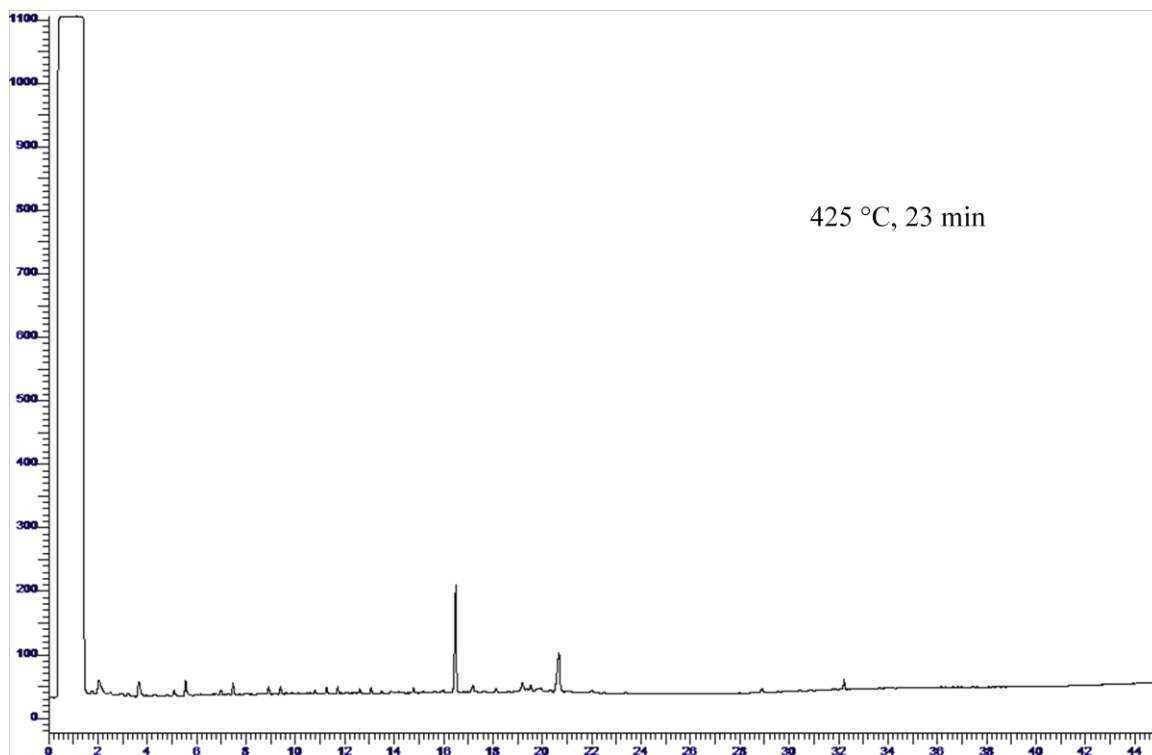


Fig.A- 28 Chromatogram of biodiesel samples thermal stressed at 425 °C for 23 minutes.

Table A- 1 GC-FID data for analytical standard GLC-10 FAME mix

FAME Con. (ppm by vol.)			GC Peak Area ($\times 10^6$)		
Total	Individual	Combined	GLC-10 FAME Mix (wt. %)		
			(20%)	(20%)	(60%)
	C16:0, C18:0	C18:1-3	C16:0	C18:0	C18:1-3
500	100	300	1.477	1.476	4.044
750	150	450	2.049	2.045	5.638
1000	200	600	2.877	2.898	7.903
1250	250	750	3.644	3.658	10.018
1500	300	900	4.413	4.440	12.154
2000	400	1200	5.972	5.996	16.515

Table A- 2 GC-FID data for analytical standard GLC-100 FAME mix

FAME Con.		GC Peak Area ($\times 10^6$)				
(ppm by vol.)		GLC-100 FAME Mix (wt. %)				
Total	Individual	(20%)	(20%)	(20%)	(20%)	(20%)
		C18:0	C19:0	C20:0	C21:0	C22:0
500	100	1.428	1.401	1.434	1.416	1.425
750	150	2.096	2.061	2.116	2.093	2.117
1000	200	2.878	2.843	2.926	2.896	2.898
1250	250	3.313	3.265	3.310	3.345	3.354
1500	300	4.022	3.967	4.019	4.073	4.086
2000	400	5.850	5.761	5.866	5.930	5.950

Table A- 3 GC-FID data for thermally-stressed biodiesel samples

Temperature (°C)	Residence Time(min)	GC Peak Area ($\times 10^6$)					Total
		C16:0	C18:1-3	C18:0	C20:0	C22:0	
250	3	1.471	10.575	0.785	0.071	0.145	13.047
	8	1.656	11.836	0.852	0.077	0.167	14.588
	18	1.305	9.451	0.699	0.065	0.124	11.644
	38	1.411	10.232	0.763	0.072	0.137	12.615
	63	1.263	9.140	0.678	0.065	0.124	11.270
275	3	1.632	11.510	0.857	0.095	0.167	14.261
	8	1.588	11.059	0.830	0.094	0.161	13.732
	28	1.621	11.360	0.871	0.092	0.165	14.109
	38	1.623	11.159	0.842	0.093	0.165	13.882
	63	1.703	11.700	0.841	0.091	0.171	14.506
275R ^a	3	1.382	9.893	0.735	0.072	0.134	12.216
	8	1.472	10.443	0.792	0.076	0.143	12.926
	28	1.488	10.382	0.930	0.078	0.145	13.023
	38	1.499	10.288	0.837	0.076	0.148	12.848
	63	1.500	10.240	0.775	0.078	0.150	12.743
300	3	1.568	11.086	0.830	0.087	0.158	13.729
	8	1.627	11.306	0.720	0.094	0.152	13.899
	18	1.545	10.505	0.731	0.084	0.153	13.018
	33	1.617	10.714	0.752	0.090	0.156	13.329
	63	1.760	11.448	0.906	0.097	0.177	14.388
325	3	1.601	10.957	0.858	0.084	0.159	13.659
	8	1.659	10.824	0.897	0.089	0.166	13.635
	18	1.590	9.426	0.859	0.082	0.161	12.118
	33	1.506	7.466	0.803	0.081	0.155	10.011
	63	1.570	6.003	0.803	0.082	0.164	8.622

Table A- 3 (continued) GC-FID data for thermally-stressed biodiesel samples

Temperature (°C)	Residence Time(min)	GC Peak Area ($\times 10^6$)					Total
		C16:0	C18:1-3	C18:0	C20:0	C22:0	
325R	3	1.461	9.952	0.776	0.076	0.145	12.410
	8	1.525	9.740	0.849	0.078	0.146	12.338
	18	1.499	8.393	0.793	0.080	0.150	10.915
	63	1.465	5.364	0.750	0.075	0.159	7.813
350	3	1.484	9.253	0.835	0.075	0.143	11.790
	8	1.765	8.805	1.011	0.088	0.156	11.825
	18	1.486	5.084	0.770	0.075	0.150	7.565
	33	1.361	3.949	0.691	0.061	0.140	6.202
360	3	1.538	8.842	0.790	0.082	0.161	11.413
	8	1.546	5.893	0.703	0.086	0.169	8.397
	18	1.606	4.869	0.694	0.089	0.175	7.433
	33	1.592	2.945	0.750	0.087	0.166	5.540
	43	1.551	2.231	0.530	0.085	0.164	4.561
375	3	1.507	8.171	0.804	0.074	0.152	10.708
	8	1.437	3.758	0.657	0.072	0.141	6.065
	18	1.406	2.246	0.583	0.069	0.134	4.438
	33	1.454	1.730	0.639	0.073	0.133	4.029
	43	1.374	1.067	0.606	0.069	0.12	3.236
375R	3	1.457	8.714	0.737	0.075	0.147	11.130
	8	1.423	4.803	0.722	0.074	0.151	7.173
	18	1.334	2.949	0.710	0.071	0.146	5.210
	33	1.450	2.318	0.766	0.077	0.142	4.753
	43	1.275	1.386	0.702	0.067	0.144	3.574

Table A- 3 (continued) GC-FID data for thermally-stressed biodiesel samples

Temperature (°C)	Residence Time(min)	GC Peak Area ($\times 10^6$)					Total
		C16:0	C18:1-3	C18:0	C20:0	C22:0	
400	3	1.543	3.480	0.850	0.076	0.160	6.109
	8	0.837	1.001	0.517	0.043	0.083	2.481
	18	1.059	0.642	0.682	0.054	0.100	2.537
	28	1.311	0.533	0.542	0.065	0.112	2.563
	33	1.119	0.780	0.713	0.058	0.100	2.770
425	3	1.490	1.712	0.687	0.078	0.142	4.109
	8	1.060	0.389	0.385	0.053	0.091	1.978
	13	0.938	0.239	0.325	0.044	0.071	1.617
	18	0.895	0.203	0.313	0.041	0.066	1.518
	23	0.767	0.134	0.231	0.035	0.054	1.221
425R	3	1.224	1.095	0.755	0.064	0.134	3.272
	8	0.927	0.098	0.549	0.054	0.079	1.707
	13	0.733	0.026	0.408	0.044	0.058	1.269
	18	0.680	0.013	0.381	0.039	0.053	1.166
	23	0.618	0.011	0.346	0.035	0.048	1.058

^a R-replicates.

Table A- 4 Concentrations of thermal stressed biodiesel samples

Temperature (°C)	Residence Time(min)	Concentration (ppm by volume)*					Total
		C16:0	C18:1-3	C18:0	C20:0	C22:0	
250	3	114.8	852.1	66.0	10.2	19.7	1062.8
	8	114.8	851.8	63.6	9.6	19.1	1058.9
	18	114.8	853.1	66.6	10.9	20.3	1065.6
	38	114.8	857.5	66.9	10.7	19.9	1069.7
	63	114.8	851.0	66.8	11.2	20.9	1064.6
275	3	114.8	840.4	64.8	11.0	19.4	1050.4
	8	114.8	829.3	64.6	11.2	19.5	1039.4
	28	114.8	835.1	66.1	10.8	19.4	1046.2
	38	114.8	819.9	64.1	10.9	19.4	1029.1
	63	114.8	820.9	61.3	10.3	18.9	1026.2
275R ^a	3	114.8	846.1	66.0	10.9	20.0	1057.8
	8	114.8	841.4	66.5	10.6	19.6	1052.8
	28	114.8	828.4	75.8	10.7	19.5	1049.2
	38	114.8	815.8	68.6	10.4	19.6	1029.2
	63	114.8	811.6	64.1	10.6	19.7	1020.8
300	3	114.8	841.0	65.4	10.8	19.5	1051.4
	8	114.8	828.4	55.9	10.9	18.4	1028.4
	18	114.8	809.5	59.3	10.7	19.4	1013.8
	33	114.8	791.2	58.3	10.7	18.8	993.8
	63	114.8	779.8	63.5	10.3	18.7	987.1
325	3	114.8	815.8	66.0	10.4	19.2	1026.2
	8	114.8	780.4	66.5	10.4	19.0	991.0
	18	114.8	710.8	66.5	10.3	19.5	921.9
	33	114.8	598.8	65.9	10.8	20.0	810.3
	63	114.8	469.9	63.4	10.4	19.9	678.4

Table A- 4 (continued) Concentrations of thermal stressed biodiesel samples

Temperature (°C)	Residence Time(min)	Concentration (ppm by volume)*					Total
		C16:0	C18:1-3	C18:0	C20:0	C22:0	
325R	3	114.8	809.0	65.8	10.7	19.8	1020.0
	8	114.8	762.0	68.4	10.4	19.1	974.8
	18	114.8	671.8	65.5	10.7	19.7	882.5
	63	114.8	451.0	63.7	10.6	20.8	660.9
350	3	114.8	743.9	69.1	10.5	19.4	957.7
	8	114.8	605.0	69.8	9.7	17.4	816.7
	18	114.8	423.8	64.3	10.4	19.9	633.2
	33	114.8	364.9	63.5	10.2	20.8	574.1
360	3	114.8	689.5	63.7	10.6	20.1	898.7
	8	114.8	468.5	57.4	10.9	20.5	672.0
	18	114.8	379.3	54.8	10.7	20.2	579.8
	33	114.8	244.1	59.0	10.6	19.8	448.3
	43	114.8	197.4	45.1	10.8	20.1	388.2
375	3	108.4	615.8	62.3	9.7	18.7	814.9
	8	103.8	300.6	52.4	9.5	17.9	484.3
	18	101.8	192.6	47.4	9.3	17.5	368.6
	33	105.0	155.7	51.1	9.6	17.4	338.9
	43	99.7	108.4	48.9	9.3	16.5	282.8
375R	3	105.2	654.6	57.8	9.7	18.4	845.6
	8	102.9	375.2	56.8	9.7	18.6	563.2
	18	97.1	242.8	55.9	9.5	18.3	423.6
	33	104.7	197.7	59.7	9.9	18.0	390.1
	43	93.2	131.2	55.4	9.2	18.1	307.1

Table A- 4 (continued) Concentrations of thermal stressed biodiesel samples

Temperature (°C)	Residence Time(min)	Concentration (ppm by volume)*					
		C16:0	C18:1-3	C18:0	C20:0	C22:0	Total
400	3	110.8	280.7	65.4	9.8	19.2	486.0
	8	64.4	103.7	42.9	7.5	14.0	232.4
	18	79.0	78.0	54.1	8.3	15.1	234.5
	28	95.6	70.2	44.6	9.0	16.0	235.4
	33	82.9	87.9	56.1	8.6	15.1	250.7
425	3	107.3	154.5	54.4	10.0	18.0	344.1
	8	79.0	60.0	34.0	8.2	14.5	195.7
	13	71.0	49.2	29.9	7.6	13.2	170.9
	18	68.2	46.7	29.1	7.4	12.8	164.2
	23	59.8	41.7	23.6	6.9	12.0	144.1
425R	3	89.8	110.4	59.0	9.0	17.5	285.6
	8	70.3	39.2	45.1	8.3	13.7	176.5
	13	57.5	34.0	35.5	7.6	12.3	147.0
	18	54.0	33.1	33.7	7.2	12.0	140.0
	23	50	33.0	31.4	6.9	11.6	132.8

* Calculated by the calibration curve equation $A_i = a_i C_i + b_i$ using parameters from **Table 12**.

Concentrations of biodiesel samples thermal stressed at 360 °C or below were corrected by a factor of $C_{16:0, fresh} / C_{16:0, TS}$, where C16:0 was used as a “native” internal standard.

^a R-replicate

Table A- 5 Data of Ink1, Ink2, and InK for each temperature

T, °C	Ink₁	Ink₂	InK
250	-7.6170	-4.9975	-2.6196
275	-6.4644	-4.5152	-1.9491
300	-5.7353	-4.0751	-1.6602
325	-4.3218	-3.9040	-0.4178
350	-3.2268	-3.3568	0.1301
360	-2.7205	-3.1739	0.4534
375	-2.2381	-3.0595	0.8214
400	-1.1333	-2.4182	1.2849
425	-0.6774	-2.4770	1.7996

Table A- 6 Comparison of modeling data and experimental data of biodiesel concentration and thermal decomposition percentage

Temperature (°C)	Residence Time(min)	Concentration (ppm)			Decomposition percentage (%)		
		Exp.	Molding	STDEV	Exp.	Modeling	STDEV
250	3	1062.8	1085.2	15.8	2.20	0.15	1.45
	8	1058.9	1082.6	16.8	2.56	0.38	1.54
	18	1065.6	1077.8	8.6	1.95	0.83	0.79
	38	1069.7	1069.0	0.5	1.57	1.63	0.04
	63	1064.6	1059.8	3.4	2.04	2.49	0.32
275	3	1054.1	1081.8	19.6	3.01	0.46	1.80
	8	1046.1	1073.9	19.7	3.74	1.19	1.80
	28	1047.7	1046.8	0.6	3.59	3.68	0.06
	38	1029.1	1035.6	4.6	5.30	4.71	0.42
	63	1023.5	1013.0	7.4	5.82	6.79	0.69
300	3	1051.4	1076.6	17.8	3.25	0.94	1.63
	8	1028.4	1060.9	23.0	5.37	2.39	2.11
	18	1013.8	1033.8	14.1	6.71	4.87	1.30
	33	993.8	1002.3	6.0	8.55	7.78	0.54
	63	987.1	961.8	17.9	9.17	11.51	1.65
325	3	1023.1	1045.6	15.9	5.86	3.79	1.46
	8	982.9	985.5	1.8	9.56	9.32	0.17
	18	902.2	891.7	7.4	16.98	17.95	0.69
	33	810.3	798.4	8.4	25.44	26.53	0.77
	63	669.7	707.8	26.9	38.38	34.87	2.48
350	3	957.7	970.9	9.3	11.88	10.67	0.86
	8	816.7	826.9	7.2	24.85	23.91	0.66
	18	633.2	659.4	18.5	41.73	39.33	1.70
	33	574.1	557.6	11.7	47.17	48.70	1.08

Table A- 6 (continued) Comparison of modeling data and experimental data of biodiesel concentration and thermal decomposition percentage

Temperature (°C)	Residence Time(min)	Concentration (ppm)			Decomposition percentage (%)		
		Exp.	Molding	STDEV	Exp.	Modeling	STDEV
360	3	898.7	903.4	3.3	17.30	16.88	0.30
	8	672.0	703.1	22.0	38.17	35.31	2.02
	18	579.8	517.9	43.8	46.65	52.34	4.02
	33	448.3	441.3	4.9	58.75	59.39	0.45
	43	388.2	428.8	28.7	64.28	60.55	2.64
375	3	830.3	808.1	15.7	23.60	25.64	1.44
	8	523.8	552.9	20.6	51.81	49.12	1.90
	18	396.1	379.5	11.7	63.56	65.08	1.07
	33	364.5	336.7	19.7	66.46	69.02	1.81
	43	295.0	333.0	26.9	72.86	69.36	2.47
400	3	486.0	483.6	1.7	55.28	55.50	0.16
	8	232.4	267.3	24.7	78.61	75.41	2.26
	18	234.5	236.0	1.1	78.42	78.28	0.10
	28	235.4	235.5	0.1	78.34	78.33	0.01
	33	250.7	235.5	10.7	76.94	78.33	0.98
425	3	314.9	312.1	2.0	71.02	71.28	0.18
	8	186.1	162.4	16.8	82.87	85.06	1.55
	13	159.0	154.6	3.1	85.37	85.77	0.28
	18	152.1	154.2	1.5	86.00	85.81	0.13
	23	138.4	154.2	11.2	87.26	85.81	1.03

Appendix B Permission to reuse copyright material

ELSEVIER LICENSE TERMS AND CONDITIONS

Jun 12, 2012

This is a License Agreement between Yiyang Zhu ("You") and Elsevier ("Elsevier") provided by Copyright Clearance Center ("CCC"). The license consists of your order details, the terms and conditions provided by Elsevier, and the payment terms and conditions.

All payments must be made in full to CCC. For payment instructions, please see information listed at the bottom of this form.

Supplier	Elsevier Limited The Boulevard, Langford Lane Kidlington, Oxford, OX5 1GB, UK
Registered Company Number	1982084
Customer name	Yiyang Zhu
Customer address	121 Lafayette road, apartment 518 Syracuse, NY 13205
License number	2901941055362
License date	May 04, 2012
Licensed content publisher	Elsevier
Licensed content publication	The Journal of Supercritical Fluids
Licensed content title	Evidence of thermal decomposition of fatty acid methyl esters during the synthesis of biodiesel with supercritical methanol
Licensed content author	Joaquin Quesada-Medina, Pilar Olivares-Carrillo
Licensed content date	February 2011
Licensed content volume number	56
Licensed content issue number	1
Number of pages	8
Start Page	56
End Page	63
Type of Use	reuse in a thesis/dissertation
Intended publisher of new work	other
Portion	figures/tables/illustrations
Number of figures/tables/illustrations	2
Format	both print and electronic
Are you the author of this Elsevier article?	No
Will you be translating?	No
Order reference number	
Title of your thesis/dissertation	An experimental study on thermal stability of biodiesel fuel
Expected completion date	Jun 2012
Estimated size (number of pages)	100
Elsevier VAT number	GB 494 6272 12
Permissions price	0.00 USD
VAT/Local Sales Tax	0.0 USD / 0.0 GBP

**ELSEVIER LICENSE
TERMS AND CONDITIONS**

Jun 07, 2012

This is a License Agreement between Yiyong Zhu ("You") and Elsevier ("Elsevier") provided by Copyright Clearance Center ("CCC"). The license consists of your order details, the terms and conditions provided by Elsevier, and the payment terms and conditions.

All payments must be made in full to CCC. For payment instructions, please see information listed at the bottom of this form.

Supplier	Elsevier Limited The Boulevard, Langford Lane Kidlington, Oxford, OX5 1GB, UK
Registered Company Number	1982084
Customer name	Yiyong Zhu
Customer address	121 Lafayette road, apartment 518 Syracuse, NY 13205
License number	2923720106759
License date	Jun 07, 2012
Licensed content publisher	Elsevier
Licensed content publication	Journal of Analytical and Applied Pyrolysis
Licensed content title	Thermal decomposition and stability of fatty acid methyl esters in supercritical methanol
Licensed content author	Hee-Yong Shin, Seon-Muk Lim, Seong-Youl Bae, Sea Cheon Oh
Licensed content date	November 2011
Licensed content volume number	92
Licensed content issue number	2
Number of pages	7
Start Page	332
End Page	338
Type of Use	reuse in a thesis/dissertation
Intended publisher of new work	other
Portion	figures/tables/illustrations
Number of figures/tables/illustrations	1
Format	both print and electronic
Are you the author of this Elsevier article?	No
Will you be translating?	No
Order reference number	
Title of your thesis/dissertation	An experimental study on thermal stability of biodiesel fuel
Expected completion date	Jun 2012
Estimated size (number of pages)	100
Elsevier VAT number	GB 494 6272 12
Permissions price	0.00 USD
VAT/Local Sales Tax	0.0 USD / 0.0 GBP
Total	0.00 USD
Terms and Conditions	

References

- Anitescu, G., & Bruno, T. J. (2012). Fluid properties needed in supercritical transesterification of triglyceride feedstocks to biodiesel fuels for efficient and clean combustion – A review. *The Journal of Supercritical Fluids*, 63(0), 133-149.
- Anitescu, G., Deshpande, A., & Tavlarides, L. L. (2008). Integrated technology for supercritical biodiesel production and power cogeneration. *Energy Fuels*, 22(2), 1391-1399.
- Anitescu, G., Tavlarides, L. L., & Geana, D. (2009). Phase transitions and thermal behavior of Fuel-Diluent mixtures. *Energy Fuels*, 23(6), 3068-3077.
- Anitescu, G. (2008). Supercritical fluid technology applied to the production and combustion of diesel and biodiesel fuels. 182.
- Basha, S. A., Gopal, K. R., & Jebaraj, S. (2009). A review on biodiesel production, combustion, emissions and performance. *Renewable and Sustainable Energy Reviews*, 13(6–7), 1628-1634.
- Batts, B. D., & Fathoni, A. Z. (1991). A literature review on fuel stability studies with particular emphasis on diesel oil. *Energy Fuels*, 5(1), 2-21.
- Bridgwater, A. V. (2003). Renewable fuels and chemicals by thermal processing of biomass. *Chemical Engineering Journal*, 91(2–3), 87-102.
- Bunyakiat, K., Makmee, S., Sawangkeaw, R., & Ngamprasertsith, S. (2006). Continuous production of biodiesel via transesterification from vegetable oils in supercritical methanol. *Energy Fuels*, 20(2), 812-817.

- Chisti, Y. (2007). Biodiesel from microalgae. *Biotechnology Advances*, 25(3), 294-306.
- Demirbas, A. (2005). Biodiesel production from vegetable oils via catalytic and non-catalytic supercritical methanol transesterification methods. *Progress in Energy and Combustion Science*, 31(5–6), 466-487.
- Demirbas, A. (2007a). Biodiesel from sunflower oil in supercritical methanol with calcium oxide. *Energy Conversion and Management*, 48(3), 937-941.
- Demirbas, A. (2007b). Importance of biodiesel as transportation fuel. *Energy Policy*, 35(9), 4661-4670.
- Deshpande, A., Anitescu, G., Rice, P. A., & Tavlarides, L. L. (2010). Supercritical biodiesel production and power cogeneration: Technical and economic feasibilities. *Bioresource Technology*, 101(6), 1834-1843.
- Freedman, B., Pryde, E., & Mounts, T. (1984). *Variables affecting the yields of fatty esters from transesterified vegetable oils* Springer Berlin / Heidelberg.
- Glisic, S., & Skala, D. (2009). The problems in design and detailed analyses of energy consumption for biodiesel synthesis at supercritical conditions. *The Journal of Supercritical Fluids*, 49(2), 293-301.
- Gude, M., & Teja, A. S. (1995). Vapor-liquid critical properties of elements and compounds. 4. aliphatic alkanols. *Journal of Chemical & Engineering Data*, 40(5), 1025-1036.

- Gunvachai, K., Hassan, M. G., Shama, G., & Hellgardt, K. (2007). A new solubility model to describe biodiesel formation kinetics. *Process Safety and Environmental Protection*, 85(5), 383-389.
- He, H., Wang, T., & Zhu, S. (2007). Continuous production of biodiesel fuel from vegetable oil using supercritical methanol process. *Fuel*, 86(3), 442-447.
- Imahara, H., Minami, E., Hari, S., & Saka, S. (2008). Thermal stability of biodiesel in supercritical methanol. *Fuel*, 87(1), 1-6.
- Jain, S., & Sharma, M. P. (2010). Prospects of biodiesel from jatropha in india: A review. *Renewable and Sustainable Energy Reviews*, 14(2), 763-771.
- Jain, S., & Sharma, M. P. (2011). Thermal stability of biodiesel and its blends: A review. *Renewable and Sustainable Energy Reviews*, 15(1), 438-448.
- Knothe, G. (2005). Dependence of biodiesel fuel properties on the structure of fatty acid alkyl esters. *Fuel Processing Technology*, 86(10), 1059-1070.
- Kulkarni, M. G., & Dalai, A. K. (2006). Waste cooking Oil An economical source for biodiesel: A review. *Industrial & Engineering Chemistry Research*, 45(9), 2901-2913.
- Kusdiana, D., & Saka, S. (2001). Kinetics of transesterification in rapeseed oil to biodiesel fuel as treated in supercritical methanol. *Fuel*, 80(5), 693-698.
- Kusdiana, D., & Saka, S. (2004). Effects of water on biodiesel fuel production by supercritical methanol treatment. *Bioresource Technology*, 91(3), 289-295.

- Lee, S., Posarac, D., & Ellis, N. (2011). Process simulation and economic analysis of biodiesel production processes using fresh and waste vegetable oil and supercritical methanol. *Chemical Engineering Research and Design*, 89(12), 2626-2642.
- Leung, D. Y. C., Wu, X., & Leung, M. K. H. (2010). A review on biodiesel production using catalyzed transesterification. *Applied Energy*, 87(4), 1083-1095.
- Lim, Y., Lee, H., Lee, Y., & Han, C. (2009). Design and economic analysis of the process for biodiesel fuel production from transesterificated rapeseed oil using supercritical methanol. *Industrial & Engineering Chemistry Research*, 48(11), 5370-5378.
- Lin, R. (2011). Issues on clean diesel combustion technology using supercritical fluids: Thermophysical properties and thermal stability of diesel fuel. (Copyright (C) 2012 American Chemical Society (ACS). All Rights Reserved., , 418.
- Luo, Y., Ahmed, I., Kubátová, A., Št'ávoVá, J., Aulich, T., Sadrameli, S. M., et al. (2010). The thermal cracking of soybean/canola oils and their methyl esters. *Fuel Processing Technology*, 91(6), 613-617.
- Ma, F., & Hanna, M. A. (1999). Biodiesel production: A review. *Bioresource Technology*, 70(1), 1-15.
- Marulanda, V. F., Anitescu, G., & Tavlarides, L. L. (2010a). Biodiesel fuels through a continuous flow process of chicken fat supercritical transesterification. *Energy Fuels*, 24(1), 253-260.

- Marulanda, V. F., Anitescu, G., & Tavlarides, L. L. (2010b). Investigations on supercritical transesterification of chicken fat for biodiesel production from low-cost lipid feedstocks. *The Journal of Supercritical Fluids*, 54(1), 53-60.
- Mohan, D., Pittman, , Charles U., & Steele, P. H. (2006). Pyrolysis of Wood/Biomass for bio-oil: A critical review. *Energy Fuels*, 20(3), 848-889.
- Nicolaou, K. C., Snyder, S. A., Montagnon, T., & Vassilikogiannakis, G. (2002). The diels?alder reaction in total synthesis. *Angewandte Chemie International Edition*, 41(10), 1668-1698.
- Pinnarat, T., & Savage, P. E. (2008). Assessment of noncatalytic biodiesel synthesis using supercritical reaction conditions. *Industrial & Engineering Chemistry Research*, 47(18), 6801-6808.
- Quesada-Medina, J., & Olivares-Carrillo, P. (2011). Evidence of thermal decomposition of fatty acid methyl esters during the synthesis of biodiesel with supercritical methanol. *The Journal of Supercritical Fluids*, 56(1), 56-63.
- Ragonese, C., Tranchida, P. Q., Sciarrone, D., & Mondello, L. (2009). Conventional and fast gas chromatography analysis of biodiesel blends using an ionic liquid stationary phase. *Journal of Chromatography A*, 1216(51), 8992-8997.
- Saka, S., & Kusdiana, D. (2001). Biodiesel fuel from rapeseed oil as prepared in supercritical methanol. *Fuel*, 80(2), 225-231.

- Seames, W., Luo, Y., Ahmed, I., Aulich, T., Kubátová, A., Št'ávoová, J., et al. (2010). The thermal cracking of canola and soybean methyl esters: Improvement of cold flow properties. *Biomass and Bioenergy*, 34(7), 939-946.
- Shay, E. G. (1993). Diesel fuel from vegetable oils: Status and opportunities. *Biomass and Bioenergy*, 4(4), 227-242.
- Shin, H., Lim, S., Bae, S., & Oh, S. C. (2011). Thermal decomposition and stability of fatty acid methyl esters in supercritical methanol. *Journal of Analytical and Applied Pyrolysis*, 92(2), 332-338.
- Vieitez, I., da Silva, C., Borges, G. R., Corazza, F. C., Oliveira, J. V., Grompone, M. A., et al. (2008). Continuous production of soybean biodiesel in supercritical EthanolâWater mixtures. *Energy Fuels*, 22(4), 2805-2809.
- Warabi, Y., Kusdiana, D., & Saka, S. (2004). Reactivity of triglycerides and fatty acids of rapeseed oil in supercritical alcohols. *Bioresource Technology*, 91(3), 283-287.
- West, A. H., Posarac, D., & Ellis, N. (2008). Assessment of four biodiesel production processes using HYSYS.plant. *Bioresource Technology*, 99(14), 6587-6601.
- Widegren, J. A., & Bruno, T. J. (2008). Thermal decomposition kinetics of the aviation turbine fuel jet A. *Industrial & Engineering Chemistry Research*, 47(13), 4342-4348.

Vita

NAME OF THE AUTHOR: Yiyang Zhu

PLACE OF BIRTH: Linhai, Zhejiang, China

DATE OF BIRTH: April 18, 1986

GRADUATE AND UNDERGRADUATE SCHOOLS ATTENDED:

College of Chemical Engineering and Biological Technology, Hebei Polytechnic University,
Tangshan, Hebei, China

PROFESSIONAL EXPERIENCE

Zhejiang Wansheng Chemical Co., Ltd.

Jan. 2006-Feb.2006

Internship in the R&D Laboratory

- Researched into phosphate flame retardant, polyurethane retardants, catalysts and foam rubber retardants.

Linhai Haixing Chemical Plant

Jun. 2007-Sept. 2007

Internship in the Technology Department

- Learned about the plant control system
- Learned about the production process and techniques of cosmetics intermediates

Zhejiang Taizhou Jieneng Chemical Plant

Jun. 2008-Sept. 2008

Internship in the Technology Department

- Experimented with dye intermediates